Effect of Phase-Contacting Patterns and Operating Conditions on Gas Hydrate Formation

By

Sarah Oddy

Thesis submitted to the Faculty of Graduate and Postdoctoral Studies in Partial Fulfillment of the Requirements for the Degree of M.A.Sc. in Chemical Engineering

Department of Chemical and Biological Engineering
University of Ottawa
May 2014

Statement of Contribution of Collaborators

I declare that I the sole author of this thesis. The stirred tank and fixed bed experiments were performed on the equipment of Dr. Phillip Servio (Chemical Engineering Department, McGill University). The stirred tank experiments were performed by me. The bubble column experiments were performed by me on the equipment of my supervisor Dr. Arturo Macchi (Department of Chemical and Biological Engineering, University of Ottawa). A portion of the fixed bed experiments were performed by me, and a portion by Jason Ivall and Jonathan Verrett (Chemical Engineering Department, McGill University). Data analysis and interpretation were performed by me. Elements from discussions with Dr. Phillip Servio were helpful in the interpretation of results in Chapter 2.

My supervisor, Dr. Arturo Macchi of the Department of Chemical and Biological Engineering, University of Ottawa supervised my work during the M.A.Sc. program and provided editorial corrections.

Signature: _____ Date: _____

Abstract

Research into hydrate production technologies has increased in the past years. While many technologies have been presented, there is no consensus on which reactor design is best for each potential application. A direct experimental comparison of hydrate production technologies has been carried out in between a variety of reactor configurations at similar driving force conditions. Three main reactor types were used: a stirred tank, a fixed bed and a bubble column and compared different phase contacting patterns for the stirred tank and bubble column.

In the initial phase of hydrate formation in a stirred tank, formation was mass and heat transfer limited at the lower stirring speed, and heat transfer limited at the higher stirring speed. After more than 10% of the water had been converted to hydrate, formation was mass transfer limited regardless of the other conditions. Neither the use of a gas inducing impeller, nor a 10 wt% particle slurry significantly affected hydrate formation rates; however, the particle slurry did lower the induction time.

Due to the poor scale-up of impeller power consumption in a stirred tank, a semi-batch fixed bed was studied since it does not require any power input for mixing. The significantly slower rates of formation observed in the semi-batch fixed bed, as well as the lost reactor capacity to particles, mean that this type of system would require a much larger reactor.

Faster volume and power normalized rates of hydrate formation were observed in the bubble column than in a stirred tank at similar mass transfer driving force conditions. Higher conversions of water to hydrate were observed in the bubble column because mixing was accomplished by bubbling gas from the bottom rather than by an impeller. The highest conversions of water and gas were achieved during a later stage of accelerated hydrate formation, indicating an optimal hydrate fraction for continuously operated bubble column reactors. The second stage of hydrate formation occurred more frequently at higher gas flowratess. Therefore, the increased water conversion and single-pass gas conversion justify the increased energy input required by the higher gas flowrate. Balancing the rates of mass transfer and heat removal was also critical for optimal bubble column as insufficient mass transfer would

result in a lower rate of formation and insufficient heat transfer would cause previously formed hydrates to dissociate. The addition of 10wt% glass beads to the reactor promoted hydrate formation; however, it did not do so sufficiently to make up for the loss in reactor capacity or the increased energy requirement.

Sommaire

La recherché concernant les technologies pour la production des hydrates a augmenté dans les années passés. Tandis que plusieurs technologies ont été étudié, il n`y a pas d`accord au sujet de la meilleure technologie pour chaque application potentiel. Une comparaison expérimentale des technologies pour la production des hydrates ont été fait entre une variété de configurations de réacteur, aux différentes forces motrices. Cette étude a comparé la performance de trois genres principaux de réacteur : un cuve agitée, un lit fixé et une colonne à bulle, et elle a étudié l`effet des modes de contact entre les phases pour le cuve agitée et la colonne à bulle.

Dans un cuve agitée, la formation des hydrates initial ont été limité par la transfère de matière et chaleur pour les vitesses d`agitation plus basses, et limité par la transfère de chaleur aux les vitesses d`agitation plus élevés. Dans tous les cas, après plus que 10% de l`eau ont été convertir en hydrate, la formation ont été limité par la transfère de matière. L`utilisation d`un rotor gaz provoquant, ni un bouille de particules, n`a pas eu un effet significatif sur le taux de formation, mais le bouille des particules a réduit le temps requis pour nucléation.

Parce que la consommation de l`énergie du rotor augment mal avec l`échelle, un lit fixé semi-continue ont été étudié, car il ne besoin aucune énergie pour l`agitation. Les taux de formation considérablement plus lente dans le lit fixé, et la perde de capacité aux particules, signifient que cette type de réacteur va être considérablement plus grande.

Les taux de formation des hydrates, normaliser pour le volume et la consommation de l`énergie et aux forces motrices similaire, ont été plus élevé dans la colonne à bulle que dans le cuve agitée. À cause de l`agitation dans une colonne à bulle vient de la bouillonnant de gaz au fond du réacteur et non un rotor, les conversions de l`eau en hydrate sont plus grand dans la colonne à bulle que dans le cuve agitée. Les conversions les plus grandes sont eu pendant un période de formation accéléré qui a passé plus tard dans l`expérience. Ceci indique qu`il y a un pourcentage d`hydrates optimal pour une colonne à bulle continue. La période de formation

accéléré s`est produite plus souvent quand le débit de gaz était plus élevé. Donc, la conversion plus grand de l`eau et gaz associé avec le plus grand débit de gaz justifient sa consommation de l`énergie plus grand. Équilibrage des taux de transfère de matière et enlèvement de chaleur sont essentiel pour la performance optimal d`une colonne à bulle. Quand la transfère de matière était insuffisant, la formation des hydrates était plus basses. Quand l`enlèvement de chaleur était insuffisant, les hydrates qui sont déjà créer avait dissocié. Les taux de formation ont étaient plus grand avec un bouille de particules mais ils ne étaient pas asses grand pour justifier l`augmentation de la consommation de l`énergie ou le perde de capacité dans le réacteur.

Acknowledgements

I would like to express my sincere gratitude to Dr. Arturo Macchi for giving me the opportunity to work on this project. I would also like to thank him for his support and guidance during my graduate studies.

I would also like to thank Dr. Phillip Servio from the Department of Chemical Engineering at McGill University for the opportunity to perform experiments on his equipment as well as for his comments on and assistance with the interpretation of the results. I would also like to thank his Ph.D. students Jason Ivall and Jonathan Verrett for their assistance in conducting the experiments.

I would like to thank the staff of the Department of Chemical Engineering at McGill University and the staff of the Department of Chemical and Biological Engineering at the University of Ottawa for their help in accomplishing my laboratory experiments. In particular I would like to thank Frank Caporuscio and Andrew Golsztajn at McGill University and Louis Tremplay, Franco Ziroldo and Gérard Nina at the University of Ottawa.

Finally I would like to thank my family and friends for all of their support during my studies.

Table of Contents

List of Figures

List of Tables

Chapter 1 - Introduction

1.1 – General Background

Gas hydrates are non-stoichiometric ice-like compounds that are members of the class of compounds called clathrates. They are formed when, at the right thermodynamic conditions, gas or guest molecules become trapped within the cavities or cages made by hydrogen bonded water molecules. The repulsive presence of the guest molecule stabilizes the cavity, preventing its collapse. An empty cavity can be stable if a large portion of neighbouring cavities are occupied. (Sloan and Koh 2008)

The lattice structure of water in the hydrate depends on the size of the guest molecule or molecules. The three most common lattice structures are the sI, sII and sH structures. They are illustrated in Figure 1.1 and their characteristics are summarized in Table 1.1. A unit cell of structure sI hydrates consists of two small cages and six large cages. The small cages are pentagonal dodecahedron, 5^{12}, a structure with 12 pentagonal faces with equal edge lengths and equal angles. The larges cages are tetrakaidecahedrons, $5^{12}6^2$, a structure with 12 pentagonal and two hexagonal faces. A unit cell of structure sII hydrate consists of 16 small cages and 8 large cages. The small cages are the same 5^{12} pentagonal dodecahedron seen in sI hydrates and the large cages are $5^{12}6^4$ tetrakaidecahedrons, with 12 pentagonal and 4 hexagonal faces. Lastly, a unit cell of structure sH hydrates consists of three small cages, two medium cages and one large cage. The small cages are 5^{12} pentagonal dodecahedrons, the medium cages are $4^3 5^6 6^3$ irregular dodecahedrons and the large cages are $5^{12}6^8$ tetrakaidecahedrons. (Sloan and Koh 2008)

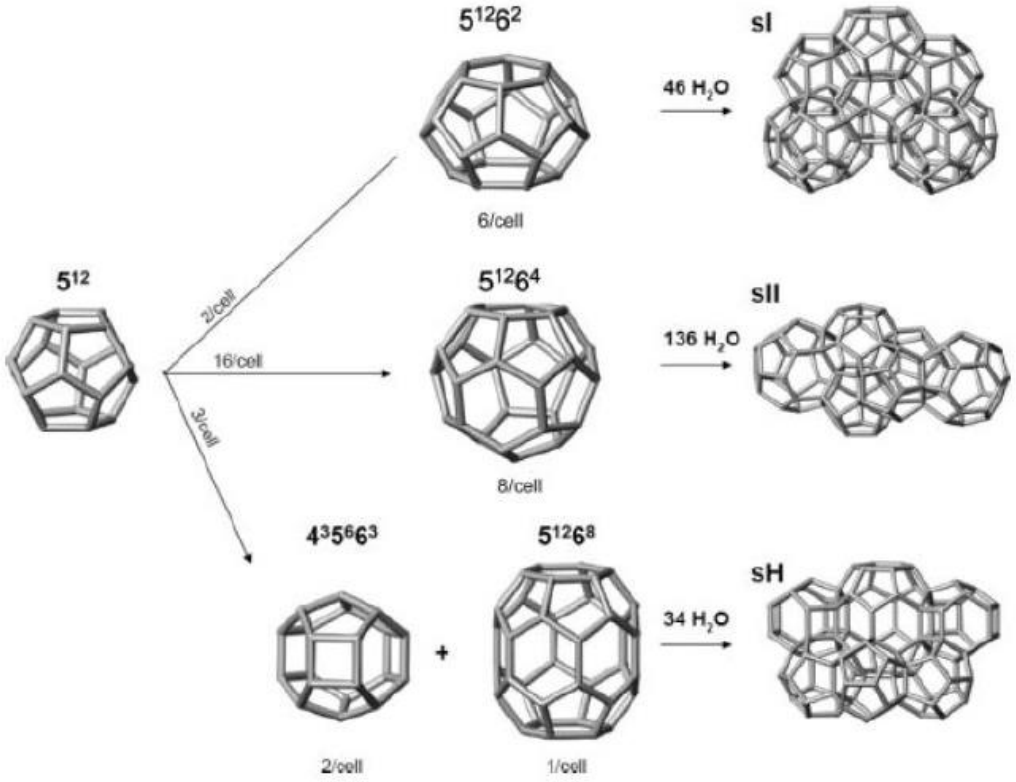

Figure 1.1: sI, sII and sH structure hydrates(Koh and Sloan 2007).

Table 1.1: Structural characteristics and cage types of common hydrate structures (Sloan and Koh 2008).

	sI	sII	sH
Crystal Group	Cubic	Cubic	Hexagonal
Ideal unit cell	$6(5^{12}6^2)\bullet 2(5^{12})\bullet 46H_2O$	$8(5^{12}6^4)\bullet 16(5^{12})\bullet 136H_2O$	$1(5^{12}6^8)\bullet 3(5^{12})\bullet 2(4^35^66^3)$ $34H_2O$
Average cavity radius (Å)	Small cavity = 3.95 Large cavity = 4.33	Small cavity = 3.91 Large cavity = 4.73	Small cavity = 3.94 Medium cavity = 4.04 Large cavity = 5.79

Each cavity in the hydrate will generally be filled with a maximum of one guest molecule. However, it has been observed that multiple guest occupancy can occur for nitrogen, oxygen, argon and hydrogen in a sII structure. The cage filling depends on the thermodynamic conditions and the nature of the guest molecules. It is for this reason that hydrates are non-stoichiometric clathrate compounds. The relative water to guest ratio is known as the hydration

number, the actual hydration number is always smaller than the ideal hydration number since the cages are rarely all occupied. (Sloan and Koh 2008)

It should be noted that mixtures of gases can form hydrates in the presence of water. The larger guest molecules will be contained in the larger hydrate cages while the smaller guest molecules will primarily fill the smaller cages, though they may also stabilize a portion of the larger cages. Predicting the structure of a mixed hydrate must be done prudently; for example, methane and ethane will usually form a sI structure hydrate when on their own but a mixture of methane and ethane will form sII structure hydrates. (Sloan and Koh 2008)

1.2 - Hydrate Formation

Hydrate formation is analogous to crystallization and consists of two main steps: nucleation and hydrate growth (Sloan and Koh 2008). The carbon dioxide – water system will be used as an example to illustrate hydrate formation. In order to produce hydrates, the pressure and temperature conditions have to be above the L_w-H-V equilibrium line of the system. The P-T diagram of this system is shown in Figure 1.2 (Hashemi, Macchi et al. 2009). Before the L_w-H-V is crossed, the solubility of CO_2 in liquid water increases with decreasing temperature as illustrated in Figure 1.3. After the system has entered the hydrate forming region, the solubility of CO_2 in water continues to increase but the system becomes metastable as hydrate formation is favoured (Myre, Macchi et al. 2010). Once nucleation has occurred, dissolved gas is used primarily for hydrate growth (Hashemi, Macchi et al. 2009). Since nucleation is a stochastic process and thus difficult to control (Sloan and Koh 2008), only the growth phase will be studied in this work.

Hydrate growth occurs through the mass transfer of guest molecules from the gas phase to the liquid phase and into the hydrate phase. Gas molecules diffuse into the liquid phase in order to saturate what is seen as an unsaturated solution. At the same time, the hydrate phase incorporates more CO_2 to lower the bulk CO_2 concentration and restore the system to the hydrate-liquid water (H-L_w) equilibrium. If this transfer across phase boundaries does not occur

quickly enough relative to the kinetics of enclathration, then hydrate growth will be mass transfer limited.(Hashemi, Macchi et al. 2009)

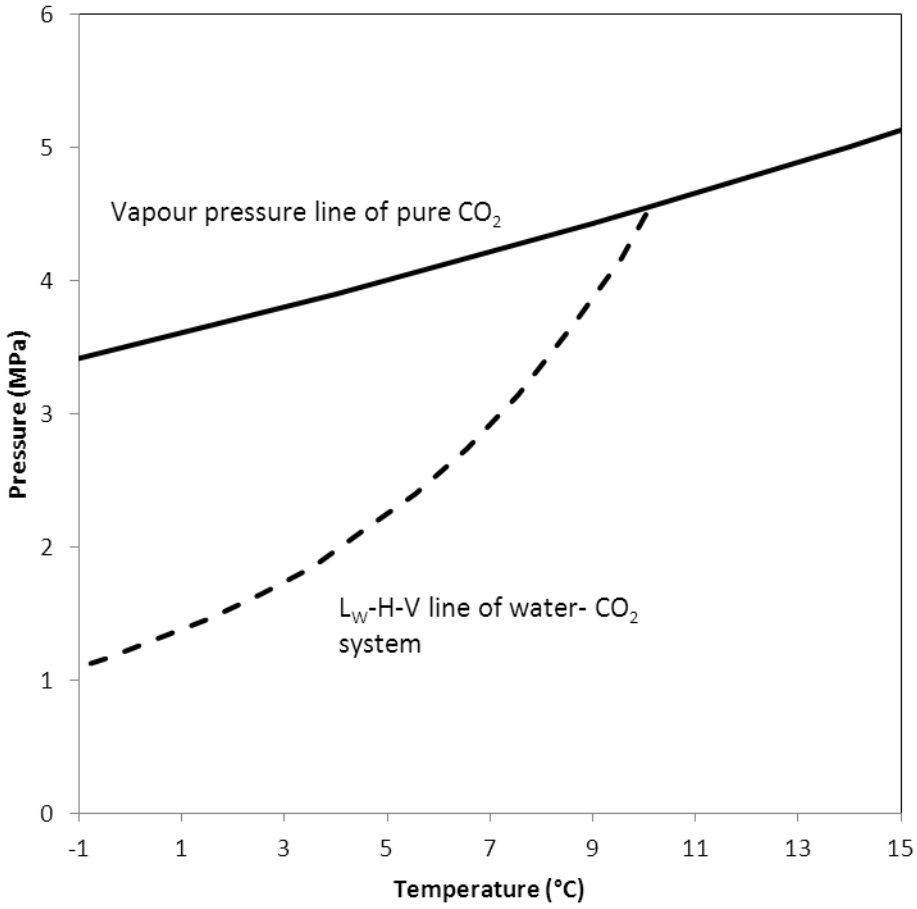

Figure 1.2: P-T diagram showing the vapour pressure line of pure CO_2 and the L_w-H-V line of water –CO_2 system(Sloan and Koh 2008), (Vahakis, Chen et al. 1972).

Hydrate growth can also be controlled by the rate of heat transfer. Hydrate growth is exothermic and thus heat must be removed from the reacting system to maintain isothermal operation. If the temperature increases, the concentration driving force for mass transfer will decrease until eventually the system will exit the thermodynamic region for hydrate formation. It should be noted that heat and mass transfer limitations generally affect the rate of hydrate formation more than the intrinsic enclathration kinetics (Sloan and Koh 2008).

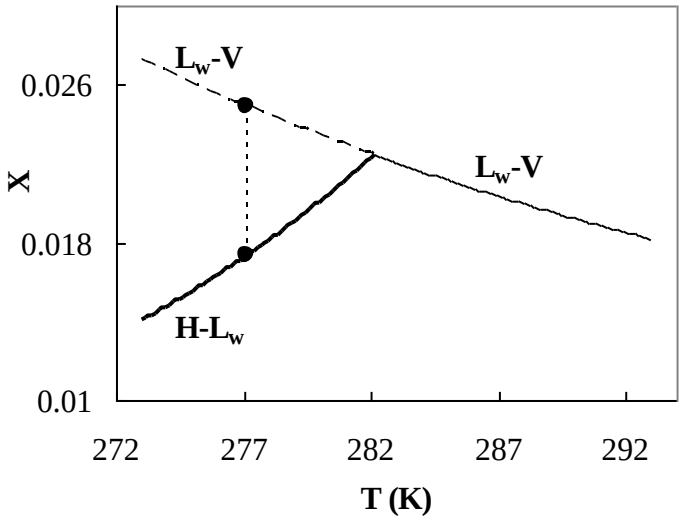

Figure 1.3: Carbon dioxide solubility (X) in terms of mole fraction in water under liquid water-vapour and liquid water-hydrate equilibrium at P = 3.5 MPa (Hashemi, Macchi et al. 2009).

Hydrate growth can also be controlled by the rate of heat transfer. Hydrate growth is exothermic and thus heat must be removed from the reacting system to maintain isothermal operation. If the temperature increases, the concentration driving force for mass transfer will decrease until eventually the system will exit the thermodynamic region for hydrate formation. It should be noted that heat and mass transfer limitations generally affect the rate of hydrate formation more than the intrinsic enclathration kinetics (Sloan and Koh 2008).

1.3 - Potential Applications

Hydrate research had traditionally been focussed on inhibiting hydrate formation. Hydrates are problematic in gas and oil production and transportation, particularly in subsea flow lines where temperature and pressure are favourable to hydrate formation (Koh and Sloan 2007). Hydrates forming in flow lines can lead to blockages which are a safety risk. Kinetics and thermodynamic inhibitors have been successfully used to prevent hydrate formation; however, research into inhibitors continues since the current inhibitors are uneconomical for certain applications. (Sloan and Koh 2008)

More recently, interest in hydrate for other applications has increased. Natural gas hydrates found in the permafrost and deep water deposits represent a source of alternative energy. It is estimated that these deposits hold 10 000 Gton or 53% of the world's total combustible carbon(Wegrzyn, Mahajan et al. 1999). Furthermore, the methane in these hydrates may be released into the atmosphere as a result of global warming, perpetuating the effect as methane is a potent greenhouse gas. It might then be beneficial to transform the methane into CO_2, a greenhouse gas that is 20 times less effective at trapping heat (Koh and Sloan 2007).

Another research field is the capture of CO_2 in hydrate form and sequestering it in the deep ocean or underground. Various promoters have been researched for this application to allow for CO_2 hydrates to be formed at lower pressures and higher temperatures, reducing operating costs. However, most promoters become enclathrated in the hydrate with CO_2 which may significantly reduce its overall capacity. (Myre, 2010)

Hydrates are also being investigated for the purpose of transportation and storage of natural gas. The current methods that are used include pipelines, liquefied natural gas (LNG) and compressed natural gas (CNG). The required conditions, storage capacity as well the advantages and disadvantages of these methods as well as natural gas hydrate transportation (NGH) are given in Table 1.2.

Table 1.2: Summary of natural gas transportation options

Method	Pipeline	LNG	CNG	NGH
Temperature (° C)	Ambient	-162	20	2-10
Pressure (atm)	45-76	1	120-250	80-100
Storage capacity (Sm^3 gas/m^3)	N/A	637	200	160
Advantages/ Disadvantages	• Very convenient once in place. • Limited to one destination. • Requires high pressure • Pipe installation is expensive ($1-5 million/mile) and demands compressor stations.	• Does not require pipeline installation. • Low pressure • Requires large scale refrigeration units. • Not economically attractive for locations where the resource is far from demand and where the reserve is small.	• Less expensive than a LNG liquefier. • Large capital and operating costs due to the high pressure required.	• Storage and transportation conditions are less intensive. • Dissociation rate is potentially limited by self-preservation. • Optimal hydrate reactor technology is unknown.

1.4 - Literature Review

Research into different hydrate reactors has been performed by a variety of researchers. The different reactor types will be compared based on their ability to provide sufficient heat and mass transfer as well as any post-production processing required. For the purposes of natural gas transportation as well as CO_2 sequestration, the hydrates would have to have a low liquid water fraction to eliminate unnecessary transportation costs.

The different reactor designs can be classified into two main groups, liquid-dispersed and gas dispersed as well as being semi-batch and continuous. In liquid dispersed reactors, liquid water is sprayed into a reactor vessel that is filled with the desired guest gas. In a gas dispersed reactors, liquid water is present in the reactor vessel and gas is introduced into the liquid phase

either by using mechanical stirring to mix-in gas from the head space, bubbling it from the bottom or through some other mechanism. In semi-batch mode hydrates accumulate in the system while the dispersed phase is circulated through the system. In a continuous reactor, hydrates slurry is being continuously removed. Figure 1.4 illustrates these systems in semi-batch mode.

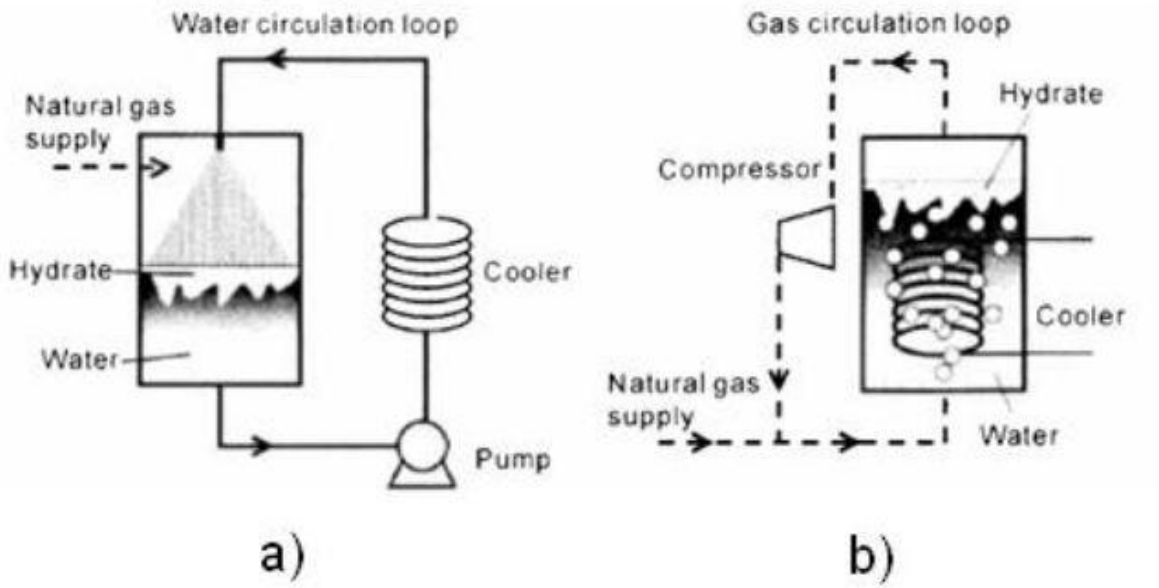

Figure 1.4: Illustration of hydrate forming systems operating in semi-batch mode. Figure 1.4 a) shows a liquid-dispersed reactor while Figure 1.4 b) shows a gas-dispersed reactor. (Mori 2003)

1.4.1 - Liquid-Dispersed Reactors

There are two main advantages to liquid-dispersed reactors. First, a large gas/water interfacial area can be achieved by atomizing the liquid water by using atomizing nozzles. Second, the high translational velocity of the water droplets eliminates the need for mechanical agitation. However, liquid-dispersed reactors are poor at removing the heat of hydrate formation and heat transfer limitations have already been observed in multiple liquid dispersed reactors (Matsuda, Tsuda et al. 2006; Fujita, Watanabe et al. 2009; Li, Liu et al. 2010). Heat removal through the wall is difficult because of the low heat capacity of gas and the low convective transport of heat. Some heat removal can be achieved by cooling the re-circulating water but the

amount is limited to avoid hydrates formation and resulting blockages within the loop. For the same reason the resulting hydrates must be in the form of a slurry solution. (Mori 2003)

A number of alternate heat removal methods have been proposed. Two of these will be discussed. In the first alternative, proposed in Matsuda, Tsuda and Mori, 2006, the system is cooled by a brass block placed within the reactor. Coolant flows on one side of the block while hydrate formation occurs on the other. The schematic of the system is shown in Figure 1.5. The brass block was effective for cooling; however, it was observed that hydrates tend to build up on the brass block and periodically fall off. This results in a fluctuating rate of heat transfer. Additionally, it was observed that a portion of the water sprayed onto the brass block was reflected. This resulted in hydrate build-up on the spray nozzle which would eventually plug the nozzle. (Matsuda, Tsuda et al. 2006).

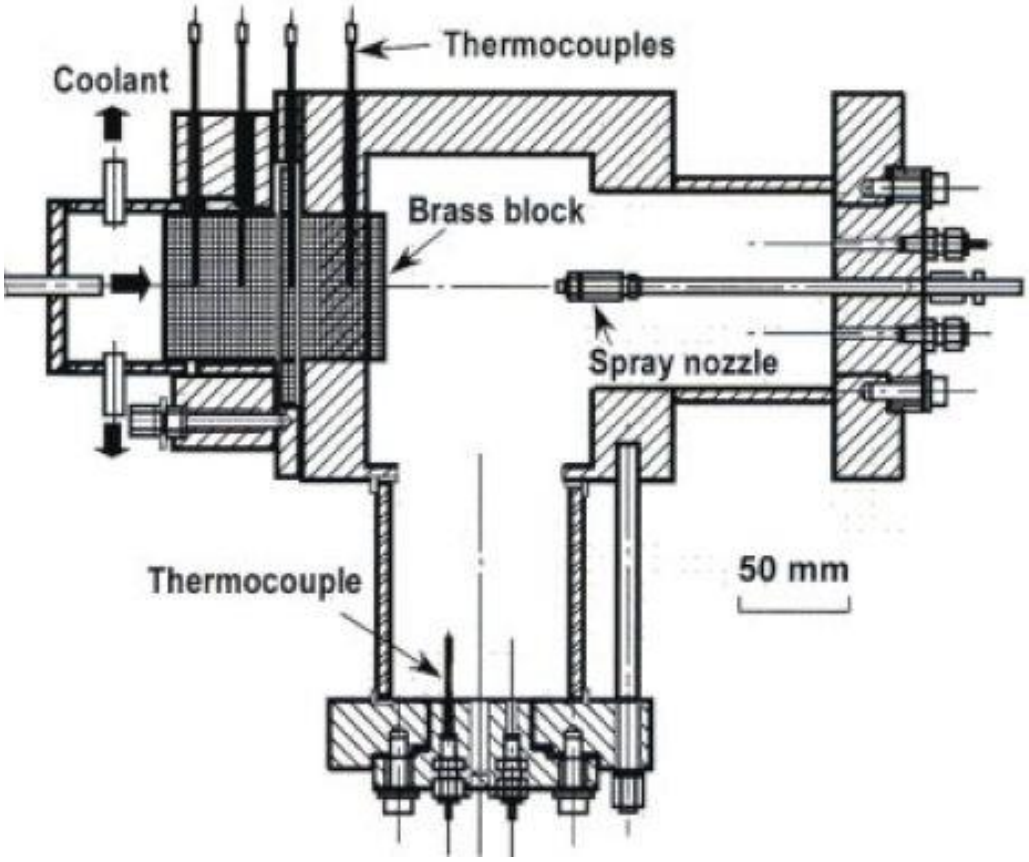

Figure 1.5: Liquid-dispersed reactor with brass block cooling mechanism. (Matsuda, Tsuda et al. 2006)

To overcome the issues present in the Matsuda, Tsuda and Mori reactor, Fujiat, Watanabe and Mori proposed and alternative design. A schematic of this system is shown in Figure 1.6. As illustrated in Figure 1.6, the system is cooled by a stream of hydrophobic liquid (decane) flowing across a porous plate. Any hydrates formed are caught in the decane and removed from the reactor, ensuring a constant rate of heat removal. Additionally, the use of a liquid flowing over a porous plate significantly reduced the amount of hydrate formation on the nozzle. The reactor design, however, does require an additional separation step to remove decane from the hydrate phase. This could be partly avoided by using a hydrophobic liquid that could be incorporated into the hydrate with the gas but this would change the equilibrium conditions and reduced the gas capacity of the resulting hydrate. (Fujiat, Watanabe et al. 2009)

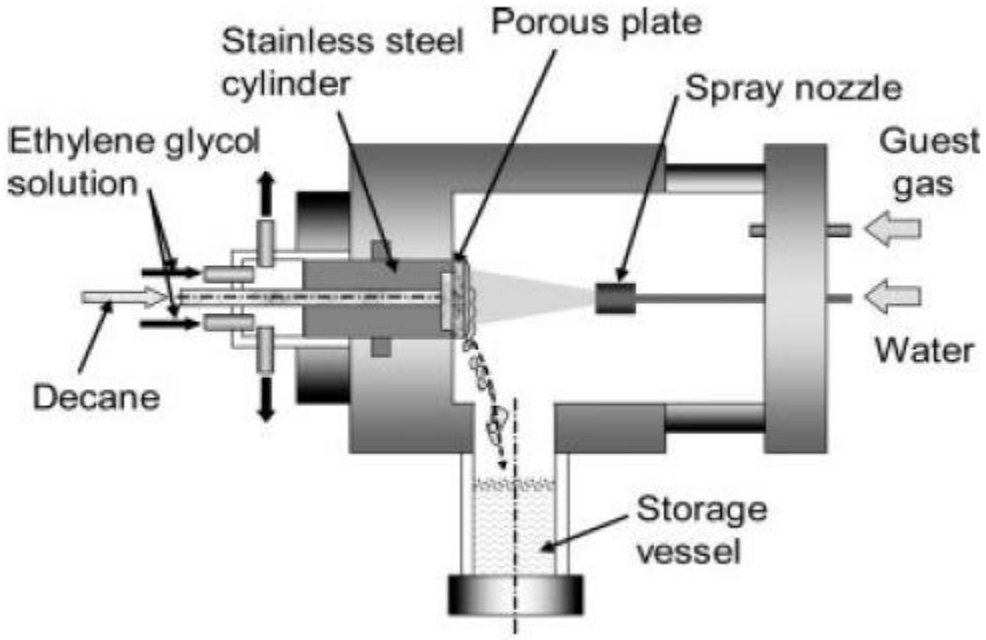

Figure 1.6: Liquid-dispersed reactor with porous plate cooling mechanism. (Fujiat, Watanabe et al. 2009)

1.4.2 - Gas-Dispersed Reactors

Gas dispersed reactors have less effective mass transfer but the heat transfer is greatly improved compared to liquid dispersed reactors, with heat being removed through a cooling jacket or cooling coil. Gas-dispersed reactors can also completely convert the water into a dry hydrate solid if operated in semi-batch mode since the water phase does not need to be recirculated. (Mori, 2003)

The disadvantages of gas-dispersed reactors are the increased energy costs associated with re-circulating the gas and mechanical agitation to increase the water/gas interfacial area (Mori, 2003). If all of the gas can be enclathrated in one pass through the reactor then the cost of re-circulating the gas can be avoided (Mori, 2003). Various methods have been proposed to reduce the cost of mechanical agitation, three of which will be discussed here. In lab scale experiments, typically an impeller was used to provide agitation (Bergeron, Beltran, & Servio, 2010; Mork & Gudmundsson, 2002; Lee, Susilo, & Englezos, 2005; Linga, Kumar, Lee, Ripmeester, & Englezos, 2010). Improvement on the impeller design has been attempted by Lee, Ripmeester &Englezos, a schematic is shown in Figure 1.7. In this design, the low pressure at the impeller tip causes gas to be pulled through the holes in the impeller shaft above the water line. This allows more efficient phase mixing compared to a traditional impeller(Linga, Kumar et al. 2010). However, on scale up, the viscosity of hydrate solution and the sealing required for the shaft insertion assembly significantly increases the capital cost; furthermore, the power requirements for stirring increase with 5^{th} power of the impeller size which scales linearly with reactor diameter (Mori 2003), (McCabe, 1993).

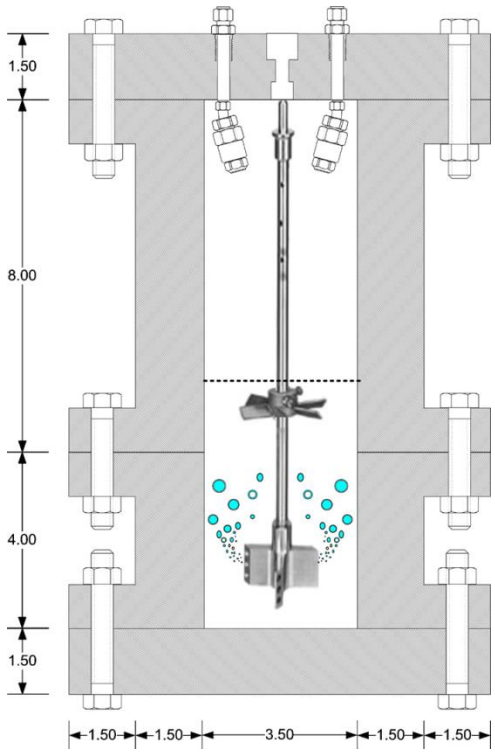

Figure 1.7: Impeller design used by Lee, Ripmeester & Englezos, 2010.

A proposed way to avoid the need for mechanical agitation is using a fixed bed reactor (Linga, Haligva, Nam, Ripmeester, & Englezos, 2009; Kang & Lee, 2010). Gas hydrates form in between the particles in the fixed bed and a heat is removed through wall cooling. Particulates have been used to achieve a higher conversion rate in a shorter period of time than mechanical agitation(Linga, Haligva et al. 2009). In particular, 82.4% water conversion was achieved over a period of 95.4 hours using silica sand(Kang and Lee 2010). This degree of conversion would significantly decrease the amount of post-production de-watering required. This reactor design does have the disadvantage of poor mass transfer capabilities. As shown in Figure 1.8, it is difficult for the gas to reach the water located at the bottom of the reactor and as the amount of hydrates increase, any convection within the water will decrease. For this reason, all reported production periods for fixed beds are long, usually in tens of hours. Additionally, if a porous material is used for the particulates in the fixed bed the capillary effect will inhibit hydrate formation(Kang and Lee 2010).

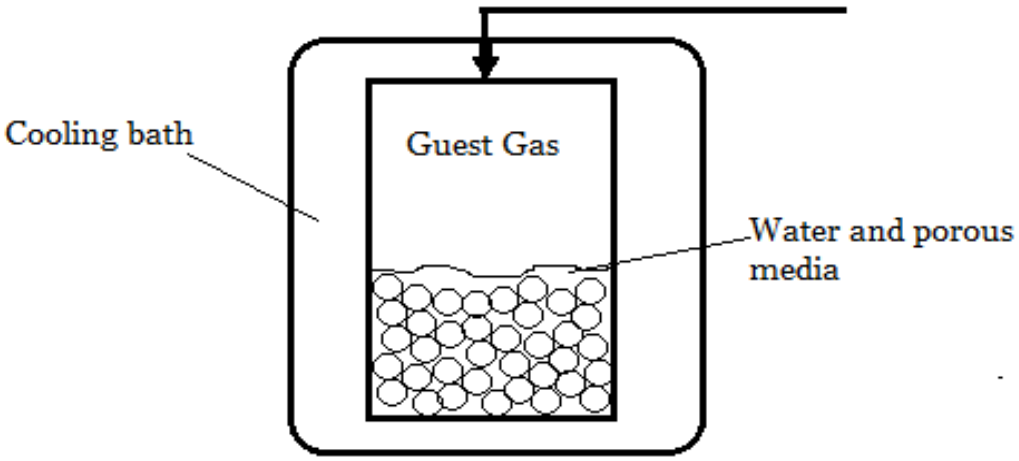

Figure 1.8: Approximate schematic of the typical fixed bed hydrate reactors.

A slurry bubble column has also been proposed as an alternative (Myre, 2010), (Luo, 2007). Rising gas bubbles provide interfacial area for mass transfer and the convection caused by them provides mixing. Heat from hydrate formation is then removed through a cooling jacket. Low fluid turbulence in a bubble column was observed to lead to the formation of a hydrate shell on the surface of the bubble, leading to reduced hydrate formation (Luo, 2007). Increasing the gas velocity, and thereby increasing fluid turbulence, was able to prevent the significant formation of a shell (Myre, 2010). The energy requirements of bubble columns scale linearly with reactor size since the mixing is provided by the bubbling gases instead of by a mechanical agitator and therefore can be more economically scaled up than stirred tanks.

1.5 - Research Objectives

As mentioned above, the requirements of a hydrate producing reactor vary depending on the application. While the differences between the various reactor designs are known qualitatively, this study aims to directly compare different configurations at similar mass transfer driving force conditions to compare transport phenomena between different designs. Stirred tank reactors are frequently used in literature due to their applicability for determining reaction intrinsic kinetics. The performance of a basic impeller within will be compared with that of a gas inducing impeller, another proposed reactor design (Linga, Kumar et al. 2010), in order to study the effect of improved mass transfer within a stirred tank. The effect of adding a small

amount of glass beads will also be studied. The glass beads will provide sites for heterogeneous nucleation as well as have an abrasive effect on hydrates that have formed on the walls of the reactor when used in the form of stirred slurry. The use of the particles in a fixed bed was also studied since there is no mechanical agitation in these reactors and therefore, their energy costs are considerably lower than other designs. This work is entitled "The effect of phase contacting patters on gas hydrate formation" and is presented in Chapter 2.

The formation of gas hydrates in a bubble column is a potential avenue for large scale production. The energy requirements of bubble columns scale more favourably than stirred tanks and they are also able to remove heat more efficiently based on energy input. Therefore a bubble column was selected for additional study at different conditions as well as with the addition of a particle slurry. This work is entitled "The Effect of Bubble Column Operating Conditions on Gas Hydrate Formation" and is presented in Chapter 3.

1.6 - References

Bergeron, S., Beltran, J., & Servio, P. (2010). Reaction rate constant of methane clathrate formation . *Fuel* , 294-301.

Fujiat, S., Watanabe, K., & Morie, Y. H. (2009). Clathrate-Hydrate Formation by Water Spraying onto a Porous Metal Plate Exuding a Hydrophobic Liquid Coolant. *AIChE Journal* , 1056-1064.

Hashmeni, S., Macchi, A., & Servio, P. (2009). Dynamic simulation of gas hydrate formation in a three-phase slurry reactor. *Industrial and Engineering Chemistry Research* , 6983-6991.

Kang, S., & Lee, J. (2010). Formation characteristics of Synthesized Natural Gas Hydrates in Meso- and Macroporous Silica Gels. *Journal of Physical Chemistry B* , 6973-6978.

Koh, C., & Sloan, D. (2007). Natural gas hydrates: Recent advances and challenges in energy and environmental applications. *American Institute of Chemical Engineering* , 1636-1643.

Lee, J., Susilo, R., & Englezos, P. (2005). Kinetics of structure H gas hydrate. *Energy and Fuels* , 1008-1015.

Lin, W., Delahay, A., & Fournaison, L. (2007). Phase Equilibrium and Dissociation Enthalpy for Semi-Clathrate Hydrate of CO2 + TBAB. *Fluid Phase Equilibria* , 220-227.

Linga, P., Haligva, C., Nam, S., Ripmeester, J., & Englezos, P. (2009). Gas Hydrate Formation in a Variable Volumn Bed of Silica Sand Particles. *Energy and Fuels* , 5496-5507.

Linga, P., Kumar, R., Lee, J., Ripmeester, J., & Englezos, P. (2010). A new apparatus to enhance the rate of gas hydrate formation: Application to capture of carbon dioxide. *International Journal of Greenhouse Gas Control* , 630-637.

Matsuda, S., Tsuda, H., & Mori, Y. H. (2006). Hydrate Formation Using Water Spraying onto a Cooled Solid Surface in a Guest Gas. *AIChE Journal* , 2978-2987.

Mori, Y. H. (2003). Recent Advances in Hydrate-Based Technologies for Natural Gas Storage - A Review. *Journal of Chemical Industry and Engineering (China)* , Vol. 54 Supplemental.

Mork, M., & Gudmundsson, J. (2002). Hydrate formation rate in a continuous stirred tank reactor. *Proceeding of the 4th International Conference on Gas Hydrates.* Yokohama.

Myre, D. (2011). *Sythesis of Carbon Dioxide Hydrates in a Slurry Bubble Column.* Ottawa: University of Ottawa.

Myre, D., Macchi, A., & Servio, P. (2010). Synthesis of CO2 hydrates in a slurry bubble column. *Proceedins of the 7th Internation Conference on Gas Hydrates* .

Sloan, E. D., & Koh, C. A. (2008). *Clathrate Hydrates of Natural Gas. 3rd ed.* Boca Raton, Florida: CRC Press.

Wegrzyn, J., Mahajan, D., & Gurevich, M. (1999). Catalyitic routes to transportation fuels utilizing natural gas hydrates. *Catalysis Today* , 97-108.

Chapter 2 – Effect of Phase Contacting Patterns on Gas Hydrate Formation

2.1 - Introduction

Gas hydrates are non-stoichiometric ice-like compounds that are members of the class of compounds called clathrates. They are formed when, at the appropriate thermodynamic conditions, gas or guest molecules become trapped within the cavities or cages made by hydrogen bonded water molecules. The repulsive presence of the guest molecule stabilizes the cavity, preventing its collapse. Gas hydrates are non-stoichiometric since an empty cavity can be stable if a large percentage of neighbouring cavities are occupied. The hydration number itself will vary as the relative size of the cavity and guest molecule, and as a result the stability of an empty cavity, will vary with changes in temperature and pressure (Sloan and Koh 2008).

Hydrate research had traditionally been focussed on inhibiting hydrate formation. Recently gas hydrates have been considered for natural gas storage and transportation (Gudmundsson, Hveding et al. 1995), secondary refrigeration (Marinhas, Delahaye et al. 2006) and gas separation (Kang and Lee 2010, Linga, Kumar et al. 2010). All three of these applications require an effective hydrate production reactor; however, the requirements for each application vary. In a natural gas storage and transportation application, maximizing storage capacity is the most important design consideration, while the rate of formation needs to be compatible with the general production rate of natural gas at a particular facility. Hydrate stability is important but not crucial for this application as the gas is expected to be released eventually. Secondary refrigeration uses hydrate slurry that needs to be transported from the primary refrigeration unit to the location where the cooling is required. Therefore, there is a maximum acceptable hydrate concentration in order to pump the slurry from one location to another, as well as a minimum acceptable hydrate concentration to make the slurry an effective coolant. Additionally, the rate of hydrate formation should be maximized to make the heat

transfer from the primary coolant to the forming hydrate slurry as efficient as possible. When hydrate formation is used for gas separation, the conditions are set so that one component will preferentially enclathrate. The enclathrated gas can be obtained later by dissociating the hydrate. This technology could be used to separate CO_2 from flue gas. For this application the rate of hydrate formation should be maximized and the hydrate should be easily dissociable to facilitate the recovery of the enclathrated gas.

Hydrate formation is analogous to crystallization and consists of two main steps: nucleation and hydrate growth (Sloan and Koh 2008). The carbon dioxide – water system will be used as an example to illustrate hydrate formation. In order to produce hydrates, the pressure and temperature conditions have to be above the L_w-H-V equilibrium line of the system. The P-T diagram of this system is shown in Figure 2.1. Before the L_w-H-V is crossed, the solubility of CO_2 in liquid water increases with decreasing temperature as illustrated in Figure 2.2. After the system has entered the hydrate forming region, the solubility of CO_2 in water continues to increase but the system becomes metastable as hydrate formation is favoured (Myre, Macchi et al. 2010). Once nucleation has occurred, dissolved gas is used primarily for hydrate growth (Hashemi, Macchi et al. 2009). Since nucleation is a stochastic process and thus difficult to control (Sloan and Koh 2008), only the growth phase will be studied in this work.

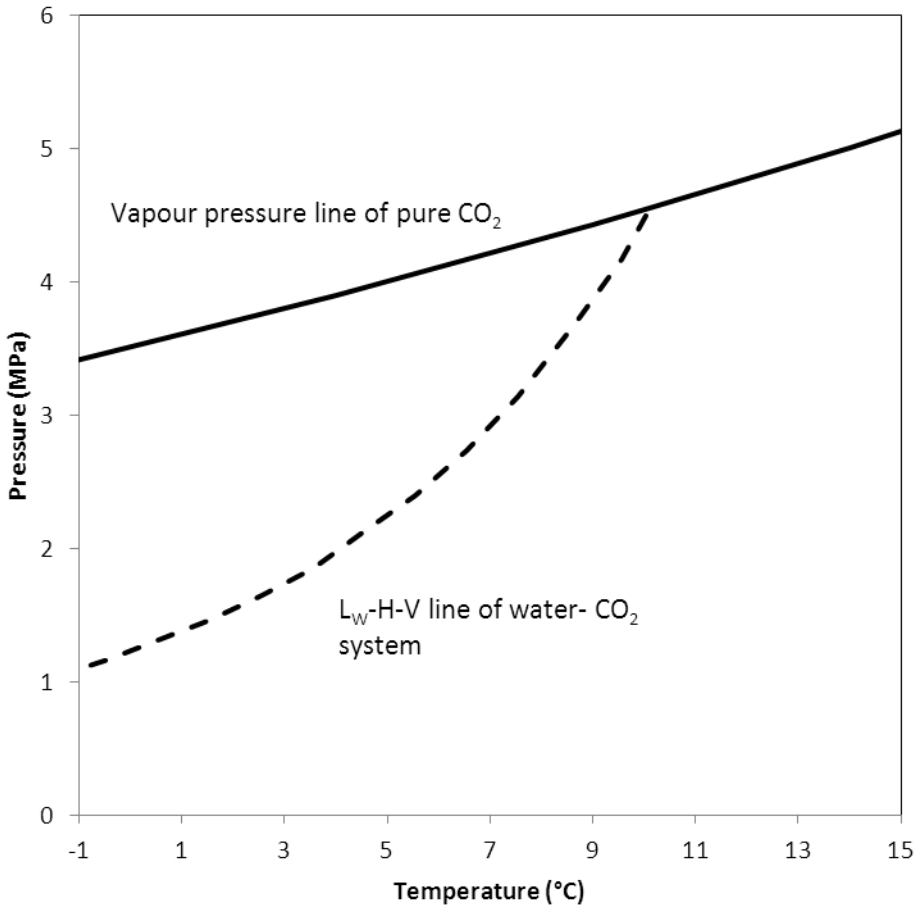

Figure 2.1: P-T diagram showing the vapour pressure line of pure CO_2 (solid line) and the L_w-H-V line of water – CO_2 system (dashed line) (Sloan and Koh 2008), (Vahakis, Chen et al. 1972).

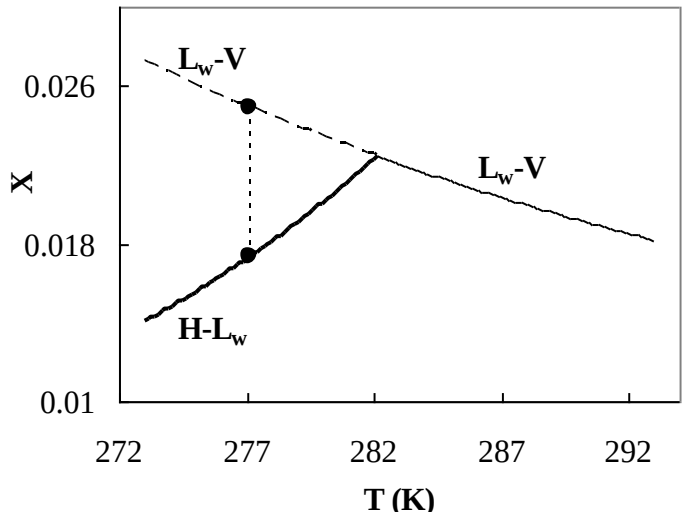

Figure 2.2: Carbon dioxide solubility (X) in terms of mole fraction in water under liquid water-vapour and liquid water-hydrate equilibrium at P = 3.5 MPa (Hashemi, Macchi et al. 2009).

Hydrate growth occurs through the mass transfer of guest molecules from the gas phase to the liquid phase and into the hydrate phase. Gas molecules diffuse into the liquid phase in order to saturate what is seen as an unsaturated solution. At the same time, the hydrate phase incorporates more CO_2 to lower the bulk CO_2 concentration and restore the system to the hydrate-liquid water ($H\text{-}L_w$) equilibrium. If this transfer across phase boundaries does not occur quickly enough relative to the kinetics of enclathration, then hydrate growth will be mass transfer limited.(Hashemi, Macchi et al. 2009)

Hydrate growth can also be controlled by the rate of heat transfer. Hydrate growth is exothermic and thus heat must be removed from the reacting system to maintain isothermal operation. If the temperature increases, the concentration driving force for mass transfer will decrease until eventually the system will exit the thermodynamic region for hydrate formation. It should be noted that heat and mass transfer limitations generally affect the rate of hydrate formation more than the intrinsic enclathration kinetics (Sloan and Koh 2008).

The reactor designs for gas hydrate synthesis fall into two main categories, ones where gas is the dispersed phase and ones where liquid is the dispersed phase (Mori 2003). In a liquid dispersed reactor, liquid water is sprayed into a reactor vessel that is filled with the desired guest gas. In a gas dispersed reactors, liquid water is present in the reactor vessel and gas is introduced into the liquid phase either by using mechanical stirring to mix-in gas from the head space, bubbling it from the bottom or through some other mechanism. Liquid dispersed reactors have good mass transfer since a very large interfacial area can be achieved using atomizing nozzles, but suffer from poor heat transfer due to the low heat capacity of gases relative to liquid water (Mori 2003). Gas dispersed reactors have less effective mass transfer but the heat transfer is greatly improved compared to liquid dispersed reactors (Mori 2003). Since heat transfer limitations have already been observed in multiple liquid dispersed reactors (Matsuda, Tsuda et al. 2006; Fujita, Watanabe et al. 2009; Li, Liu et al. 2010), liquid dispersed reactor designs will not be studied in this work.

As mentioned above, the requirements of a hydrate producing reactor vary depending on the application. While the differences between the various reactor designs are known qualitatively,

this study aims to directly compare different configurations within the same overall piece of equipment and thus the same external heat removal capacity in order to compare transport phenomena within the reactor itself. Stirred tank reactors are frequently used in literature due to their applicability for determining reaction intrinsic kinetics and are thus the basis for this study. The stirred tank with a basic impeller will be used to generate a baseline performance and then compare the effects of changing the driving force, the guest gas and different phase contacting patterns. The performance of the basic impeller will be compared with that of a gas inducing impeller, another proposed reactor design (Linga, Kumar et al. 2010). The effect of adding a small amount of glass beads will also be studied. The glass beads will provide sites for heterogeneous nucleation as well as have an abrasive effect on hydrates that have formed on the walls of the reactor when used in the form of a stirred slurry. It has also been proposed to use solid particles to create a fixed bed with hydrates forming within the bed itself (Linga, Daraboina et al. 2012, Babu, Kumar et al. 2013). Fixed bed reactors have been shown in the literature to achieve very high conversions of water, in particular, 82.4% water conversion was obtained over a period of 95.4 hours using silica sand (Kang and Lee 2010). Since there is no mechanical agitation in these reactors, their energy costs are considerably lower than other designs. This study will also investigate the performance of a fixed bed design and compare it with that of the stirred systems.

2.2 - Experimental Methods

2.2.1 – Materials

Experiments were performed using reverse-osmosis de-ionized water. The methane and carbon dioxide used in the experiments were purchased from MEGS Specialty Gases with research-grade purity specifications of > 99.995%. The glass beads (P-0060) are from Potters Industries and have a diameter of 0.1 to 0.15 mm.

2.2.2 – Apparatus

Hydrates are formed in a 316 stainless steel crystallizer with a 20-MPa pressure rating and an internal volume of 6×10^{-4} m^3. A schematic diagram of the apparatus is shown in Figure 2.3. The crystallizer has two sapphire glass windows for visual inspection and is equipped with a MM-D06 magnetic stirrer from Pressure Product Industries. The impeller used on the magnetic stirrer is a Gaspersator^{TM} impeller from Pressure Products Industries, with a maximum power requirement and rotational speed of 50W and 2500rpm, respectively. It can be used as a gas inducing impeller, when the holes in the impeller are aligned with the holes in the impeller shaft, or as a regular flat blade impeller when the holes are offset. A schematic of the impeller and the shaft of the mixer are shown in Figure 2.4. A temperature probe extends from the inner wall to the centre of the crystallizer to measure the liquid temperature. The temperature probe is equidistant from the crystallizer bottom and the liquid-interface when the system is unmixed.

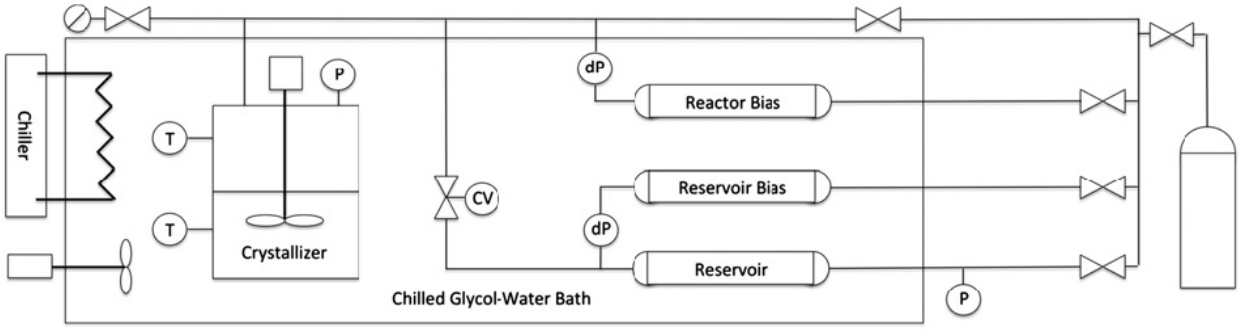

Figure 2.3: Simplified schematic of the experimental setup (Verrett, Posteraro et al. 2012)

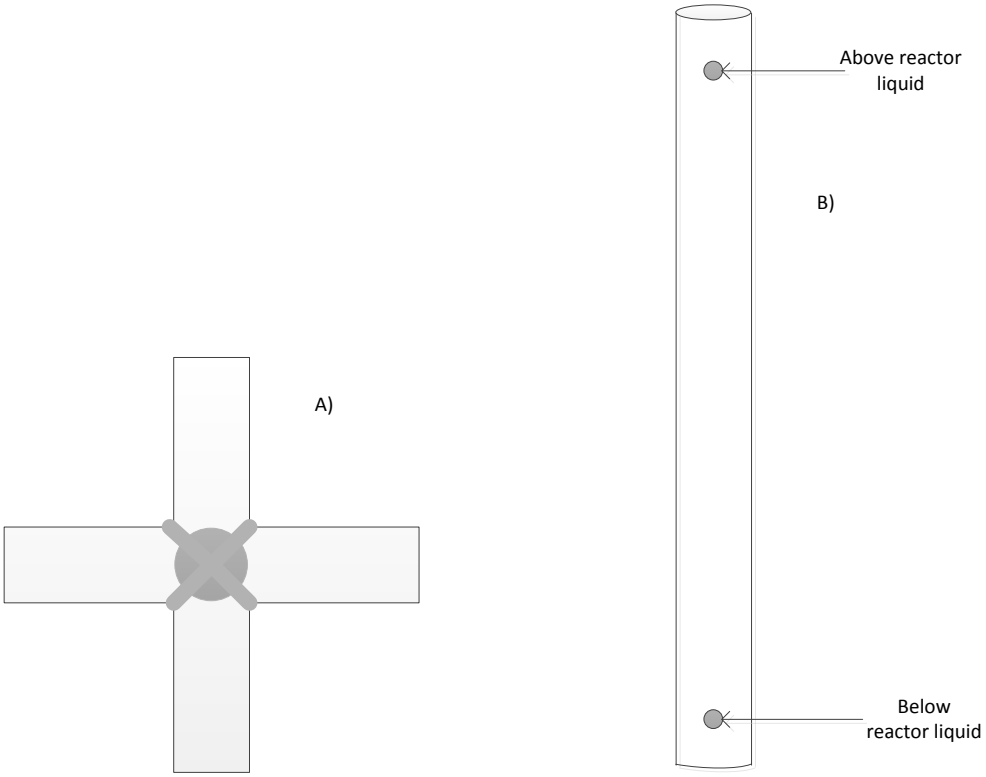

Figure 2.4: Schematic of the mixer impeller (A) and mixer shaft (B). The impeller is lined up with the holes below the liquid level on the shaft.

2.2.3 - Experimental Conditions

A variety of system configurations and thermodynamic conditions were studied in this work. The justification is presented below and the conditions summarized in Table 2.1. Six runs

at condition 2.b were performed to determine the variance of the system while two runs were performed at all other conditions.

Table 2.1: Experimental Conditions

Modified Numbers	Particle Level	Driving Force	Impeller Type	Impeller Speed	Gas	# of Runs
1.a	No Particles	Low	Basic	Low	CO_2	2
1.b	No Particles	Low	Basic	High	CO_2	2
2.a	No Particles	High	Basic	Low	CO_2	2
2.b	No Particles	High	Basic	High	CO_2	6
3.a	No Particles	Low	Basic	Low	CH_4	2
3.b	No Particles	Low	Basic	High	CH_4	2
4.a	Slurry	Low	Basic	Low	CO_2	2
4.b	Slurry	Low	Basic	High	CO_2	2
5.a	Slurry	High	Basic	Low	CO_2	2
5.b	Slurry	High	Basic	High	CO_2	2
6	Slurry	Low	Basic	High	CH_4	2
7.a	No Particles	Low	Gas Inducing	Low	CO_2	2
7.b	No Particles	Low	Gas Inducing	High	CO_2	2
8.a	No Particles	High	Gas Inducing	Low	CO_2	2
8.b	No Particles	High	Gas Inducing	High	CO_2	2
9	No Particles	Low	Gas Inducing	High	CH_4	2
10	Fixed Bed	Low	N/A	N/A	CO_2	2
11	Fixed Bed	High	N/A	N/A	CO_2	2
12	Fixed Bed	Low	N/A	N/A	CH_4	2

2.2.3.1 - Internal Geometry

Four different internal geometries were studied in this work. The first geometry is a basic semi-batch stirred tank. The reactor is filled with 300mL of water and a flat blade impeller is used. This geometry serves as a baseline comparison for the other geometries and is illustrated in Figure 2.5A. In the second configuration, the impeller is adjusted to draw gas from the reactor head space into the liquid phase through the hollow impeller shaft yielding an increased mass transfer rate from the gas to the liquid phase and ultimately to the hydrate phase. If gas conversion is low, this type of system would also be more energy efficient than a continuous net flow through of gas that must be recompressed before recycled to the reactor inlet. The geometry of the system is the same as for the basic stirred tank and is shown in Figure 2.5A. In the third configuration, shown in Figure 2.5B, the reactor liquid contains 10 wt% glass beads.

Relative to water, the apparent density of the slurry increases by approximately 6% while the apparent viscosity increases by up to 25% based on the correlation from (Springman, Steiff et al. 1991). This change in density and rheology due to the glass beads is acceptable since the slurry physical properties will also change upon the formation of hydrates. The volume of water is reduced to 280 mL to maintain a constant reactor volume of 300mL so that the impact on overall hydrodynamics is minimised. The fourth configuration is a fixed bed of glass beads and is illustrated in Figure 2.5C. The reactor was filled with 300mL or 428g of particles with sufficient water, 125 mL, to fill the void space between particles. A stationary impeller was left in the reactor to keep consistent heat transfer conditions. Since the fixed bed is not mixed, the temperature probe measures the local bed temperature instead of the average liquid temperature.

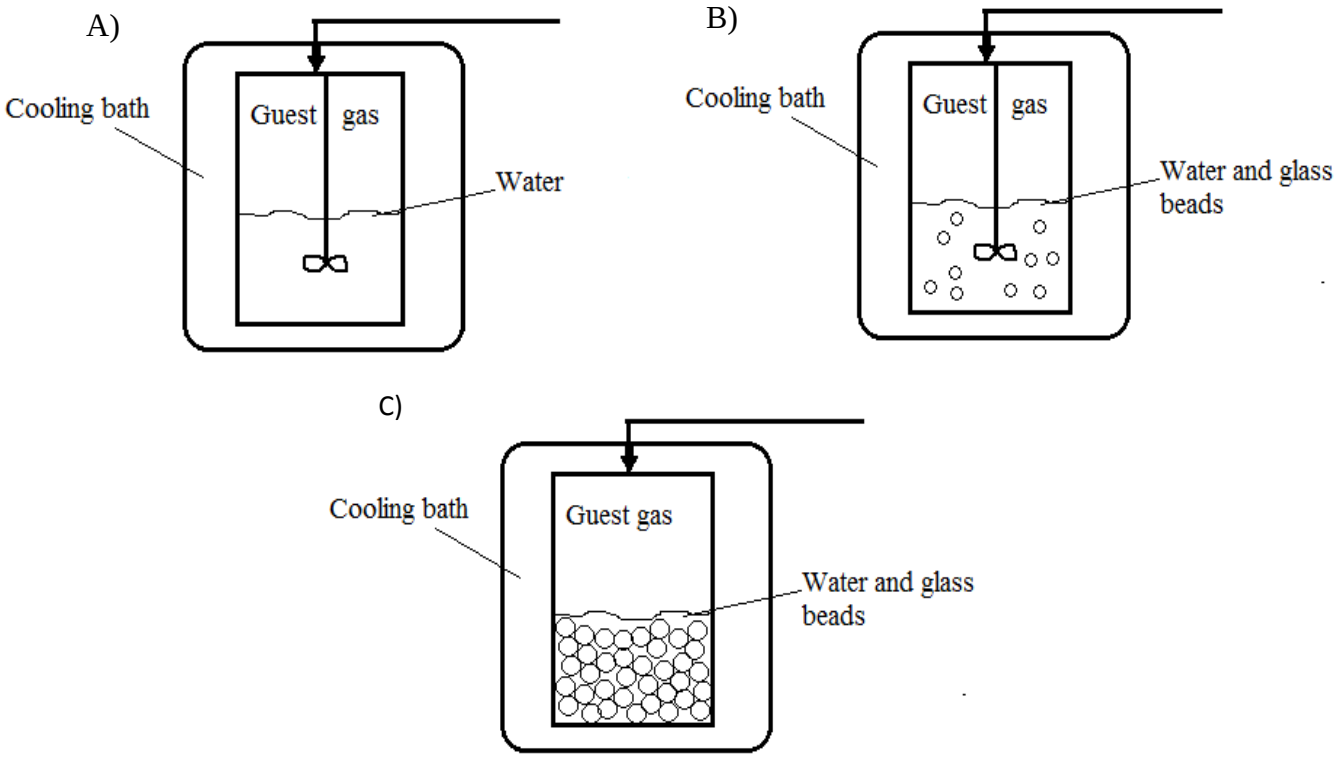

Figure 2.5: Reactor geometry for A) basic stirred tank and stirred tank with Gaspersator™ impeller; B) glass bead slurry in stirred tank; C) fixed bed.

2.2.3.2 - Guest Gas

Two different guest gases were used in these experiments, CO_2 and CH_4, which respectively have heat of hydrate formation of 81 and 57 kJ/mol, both of which can be considered constant for the range of temperature and pressure studied (Sloan and Koh 2008). Due to the lower heat of hydrate formation for CH_4 hydrates, a higher rate of hydrate growth can be sustained while the system is heat transfer limited. So, using CH_4 is the equivalent of using CO_2 with a higher rate of heat removal. This allows the simulation of better heat transfer without changing the system since the heat removal rate is independent of the guest gas. To simulate a worst case scenario in terms of heat transfer, the majority of the experiments used CO_2.

2.2.3.3 - Stirring Speed

Since the stirring speed affects both the maximum heat and mass transfer rates for a given set of conditions, for those experiments where it was applicable, a high and a low stirring speed was used. Specifically, 750rpm for the low stirring speed and 1750rpm for the high stirring speed. These speeds corresponded to 30% and 70% of the maximum speed of the motor. Documentation from the manufacturer indicates that the relationship between rotational speed and power required by motor can be approximated as linear. Therefore, the power consumption of the low and high impeller speed runs are 34W and 15W respectively. The formation of hydrates during a run will increase the power consumption due to the increase in the viscosity and slight increase in the density (for CO_2 hydrates) of the stirred fluid. As the fluid is in the turbulent flow regime, it is not expected that the power consumption will increase significantly for the amount of hydrates being produced.

2.2.3.4 - Thermodynamic Conditions

The driving force for mass transfer between the gas phase and hydrate phase is also influenced by the thermodynamic conditions as shown in Figure 2.2. Therefore, consistent driving force conditions must be used for both CO_2 and CH_4 to ensure comparable results. In this work, driving force is measured as the difference between the concentration of the guest

molecule in water according to the L_W-H equilibrium and the L_W-V equilibrium. The experimental conditions are shown in Table 2.2. Since heat transfer limitations were observed at both the low and high driving force CO_2 runs, to increase the likelihood that the CH_4 runs would not be heat transfer limited, the CH_4 runs were performed at an equivalent of the low driving force CO_2.

Since heat transfer limitations were not negligible in all runs, maintaining a constant reactor temperature was not possible. Therefore, the driving force for mass transfer is not constant, and the driving force for the thermodynamic conditions given in Table 2.2 is an initial driving force. Since pressure was used to change the mass transfer driving force, mass transfer driving force for the high driving force conditions, is still greater than that of the low driving force runs even if the temperature increases.

Table 2.2: Thermodynamic Conditions

	$T_{experimental}$ (°C)	$P_{experimental}$ (MPa)
Methane		
Low Driving Force	3.69	5.00
Carbon Dioxide		
Low Driving Force	3.00	2.75
High Driving Force	3.00	3.10

2.2.4 - Experimental Procedure

The reactor was filled with the appropriate amount of water and glass beads and the system was filled with the experiment gas to ~0.5MPa. The system was then allowed to reach the experiment temperature. Once this had been achieved, the reservoir, reservoir bias and reactor bias were filled with gas until the pressure was 2 MPa above the experiment pressure or the maximum that could be achieved without exceeding the vapour pressure. The gas was

allowed to equilibrate before the reactor was pressurized to the experiment pressure. Once again the gas was allowed to cool down and small amounts of gas were added as required to raise the reactor pressure to the experiment pressure. The control valve was set, the recording software initiated and then the mixer switched on. The experiments were allowed to proceed for 2 hours after nucleation. At the end of the experiment, the hydrates were allowed to dissociate by reducing the reactor pressure to ~0.5MPa and stirring. When required, the pressure generated by dissociating hydrates was again reduced.

2.2.5 – Calculations

As hydrates are formed, gas is fed from the reservoir through the control valve to maintain a constant reactor pressure. At the beginning of the experiment, the reservoir and reservoir bias are at the same pressure; therefore, the quantity of enclathrated gas can be measured using the differential pressure between the reservoir and reservoir bias. Hence, at any time the number of moles of gas that have been consumed in hydrate growth is calculated using equation 2.1. From this, the number of moles of water converted to hydrate can be determined using equation 2.2. Since the amount of water in the reactor varies depending on the internal geometry, reactor performance will be evaluated based on the fraction of water converted. This is calculated using equation 2.3.

$$\Delta n_{gas} = Z\frac{\Delta P_{reservoir} V_{reservoir}}{R\, T_{reservoir}} \tag{2.1}$$

$$\Delta n_{H_2O} = \Delta n_{gas} \times hydration\ number \tag{2.2}$$

$$fraction\ H_2O\ converted = \frac{\Delta n_{H_2O}}{V_{water}\rho_{water} MW_{H_2O}} \tag{2.3}$$

2.2.5 - Hydration Number

Literature values for the hydration number of CO_2 hydrates span from 5.3 to 7.7 (Yang, Le et al. 2011), and from 5.8 to 7.2 for CH_4 (Sloan and Koh 2008). As there is considerable variation in the reported values, in this work the hydration numbers were set at constant values of 6.2 and 5.8 for CO_2 and CH_4, respectively. These values were determined using the relationships based on the Clapeyron equation developed in (Anderson 2003) and (Anderson 2004) for CO_2 and CH_4, respectively. Both were calculated at the set experimental temperature for each gas. The hydration number does not vary significantly between the pressures studied for each gas (Anderson 2003, Anderson 2004).

2.3 - Results and Discussion

The experiments were monitored for two hours after nucleation. The progress of each run after 15min of hydrate growth is presented in Figure 2.6. The progress of the run is represented by the amount of water that has been converted in hydrate during that time period, i.e. for a given time the greatest mole fraction converted corresponds with the greatest average production rate during that time period. Runs where a higher impeller speed was used clearly have a greater amount of water converted into hydrate than either the low impeller speed runs or the fixed bed runs, which were comparable. At this point in the hydrate formation, there is no clear difference between runs using the gas inducing impeller and the standard impeller, between particle slurry runs and water runs, between high and low driving force runs, or between the CO_2 and CH_4 runs in terms of the average result. The CH_4 runs are more tightly grouped than the CO_2 runs particularly at high impeller speed. This difference in conversion is due to the lower heat of hydrate formation of CH_4 hydrates which gives the system a better rate of heat transfer per mol of hydrate. It is therefore able to sustain a more consistent rate of hydrate formation before mass transfer limitations dominate, since greater heat transfer limitations will magnify any minor variations in the conditions at the start of hydrate formation.

The hydrate formation after 30min is shown in Figure 2.7. At this point, the difference in hydrate formation due to impeller speed is still present. The conversions of the methane runs

are, again, more tightly grouped than the CO_2 runs, particularly at high impeller speed. The difference between the gas inducing impeller and the standard impeller, as well as between the slurry runs and the non-slurry runs remains insignificant. For the stirred runs there is no apparent effect of driving force on hydrate formation; however, driving force does seem to have an effect on the fixed bed runs.

After 60min of formation, shown in Figure 2.8, many of the differences in hydrate formation have begun to disappear. This behaviour is due to the decreased rate of formation in the high impeller speed runs as well as in the CH_4 runs. The difference between the fixed bed and the stirred tank runs, however, has continued to increase. The rate of hydrate formation in the fixed beds remains significantly lower than that of the stirred systems. The effect of driving force on the fixed bed runs remains and the difference in hydrate formation between the high and low driving force runs has increased.

After 120min of formation, shown in Figure 2.9, the differences between the various stirred runs have become negligible given the inherent variation in the stirred system. The stirred systems have produced significantly more gas hydrate than the fixed bed runs. The effect of driving force remains apparent only for the fixed bed runs.

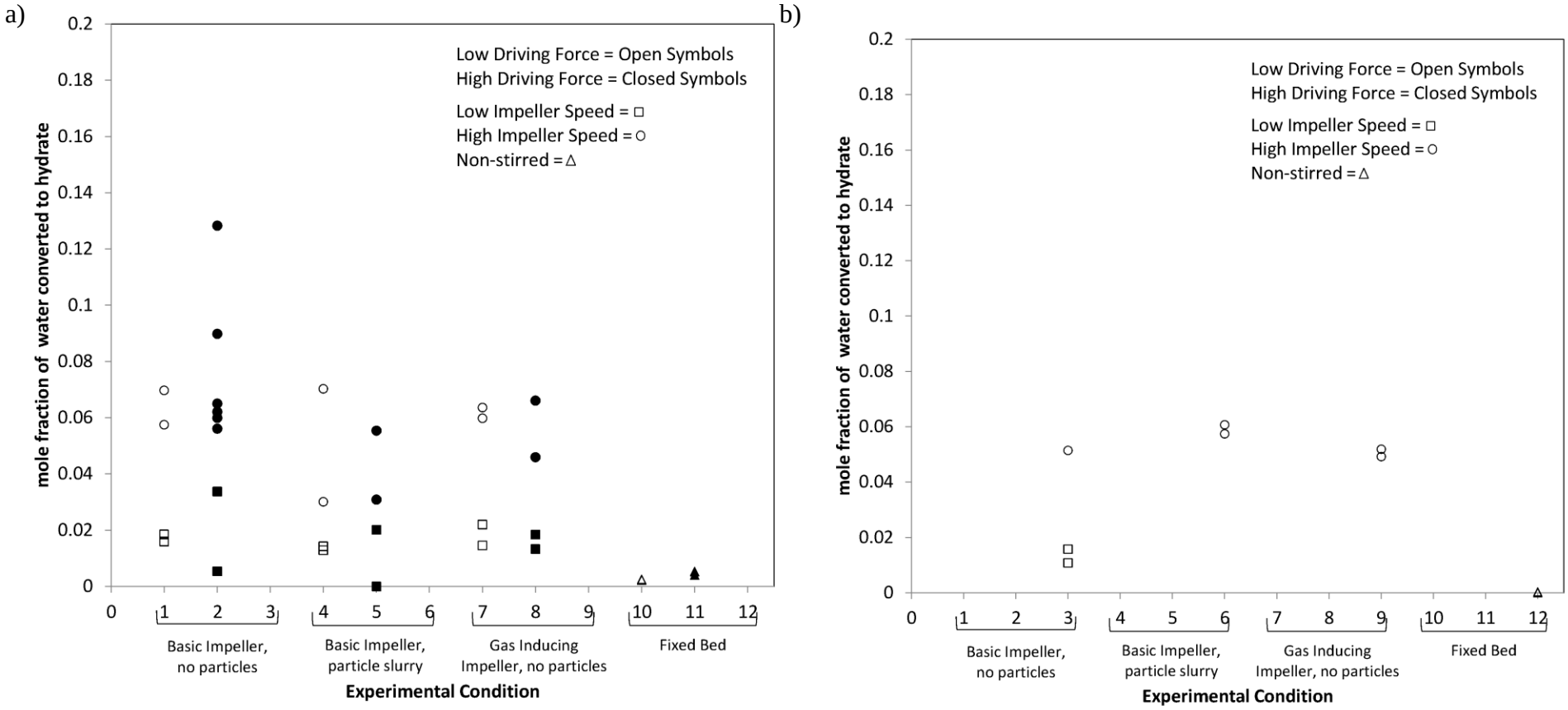

Figure 2.6: Fraction of water converted to hydrate 15min after nucleation for A) CO_2 and B) CH_4.

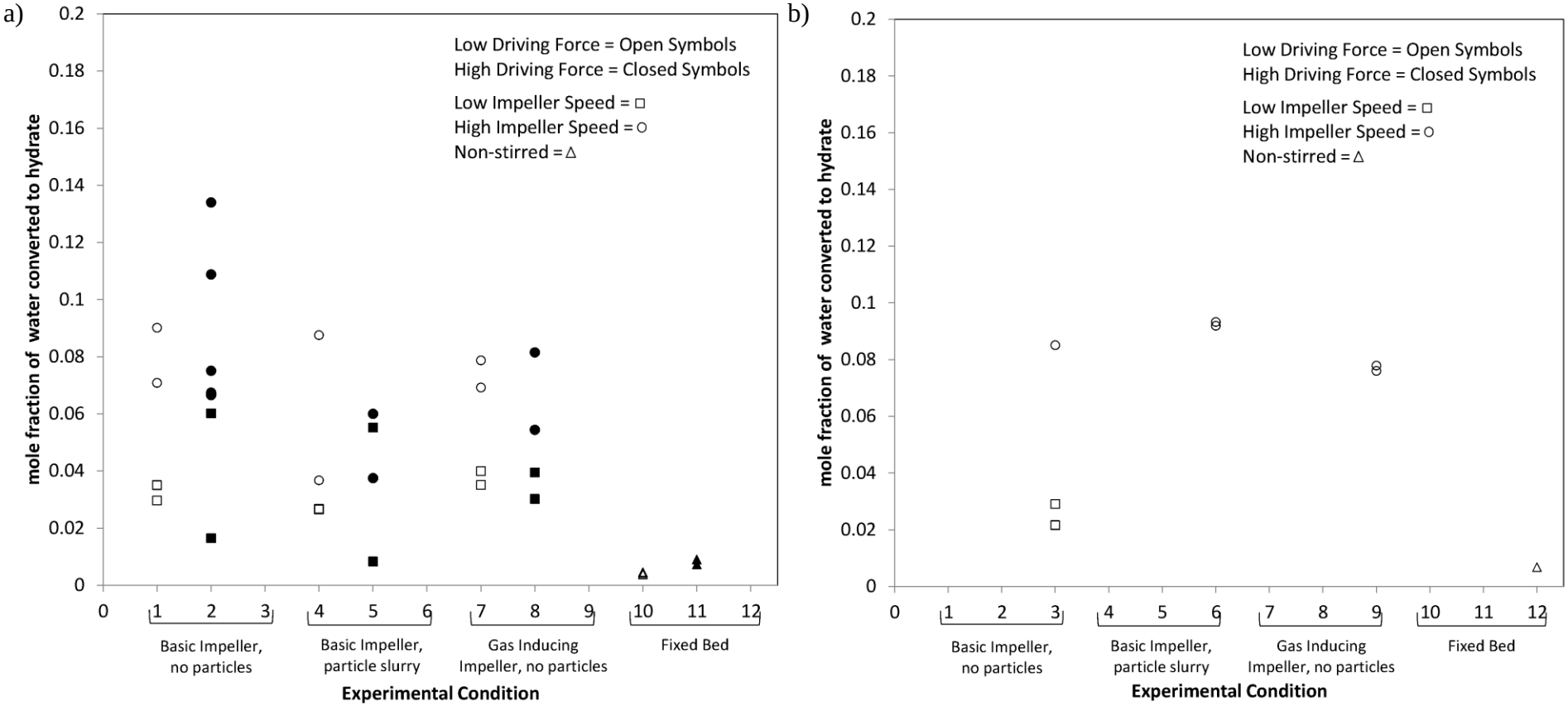

Figure 2.7: Fraction of water converted to hydrate 30min after nucleation for A) CO_2 and B) CH_4.

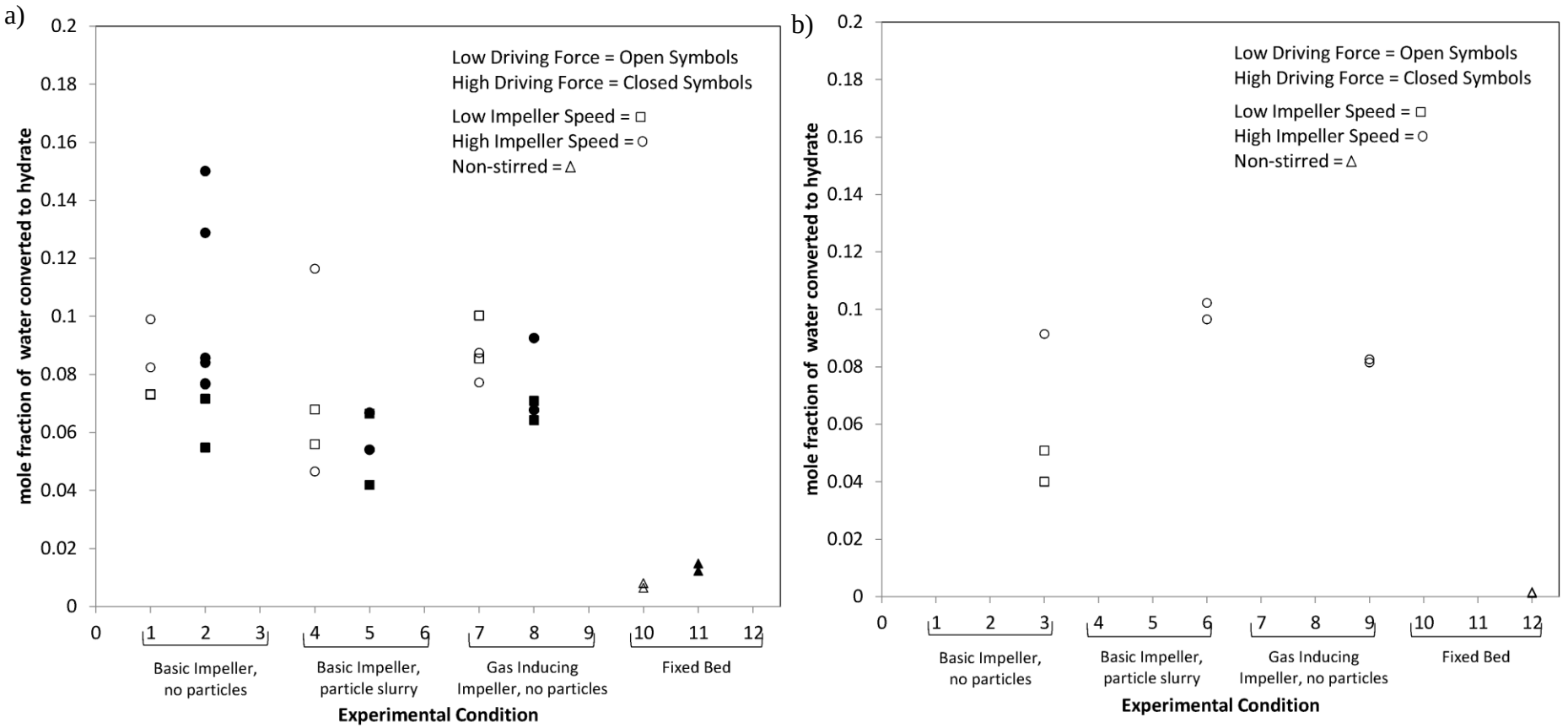

Figure 2.8: Fraction of water converted to hydrate 60min after nucleation for A) CO_2 and B) CH_4.

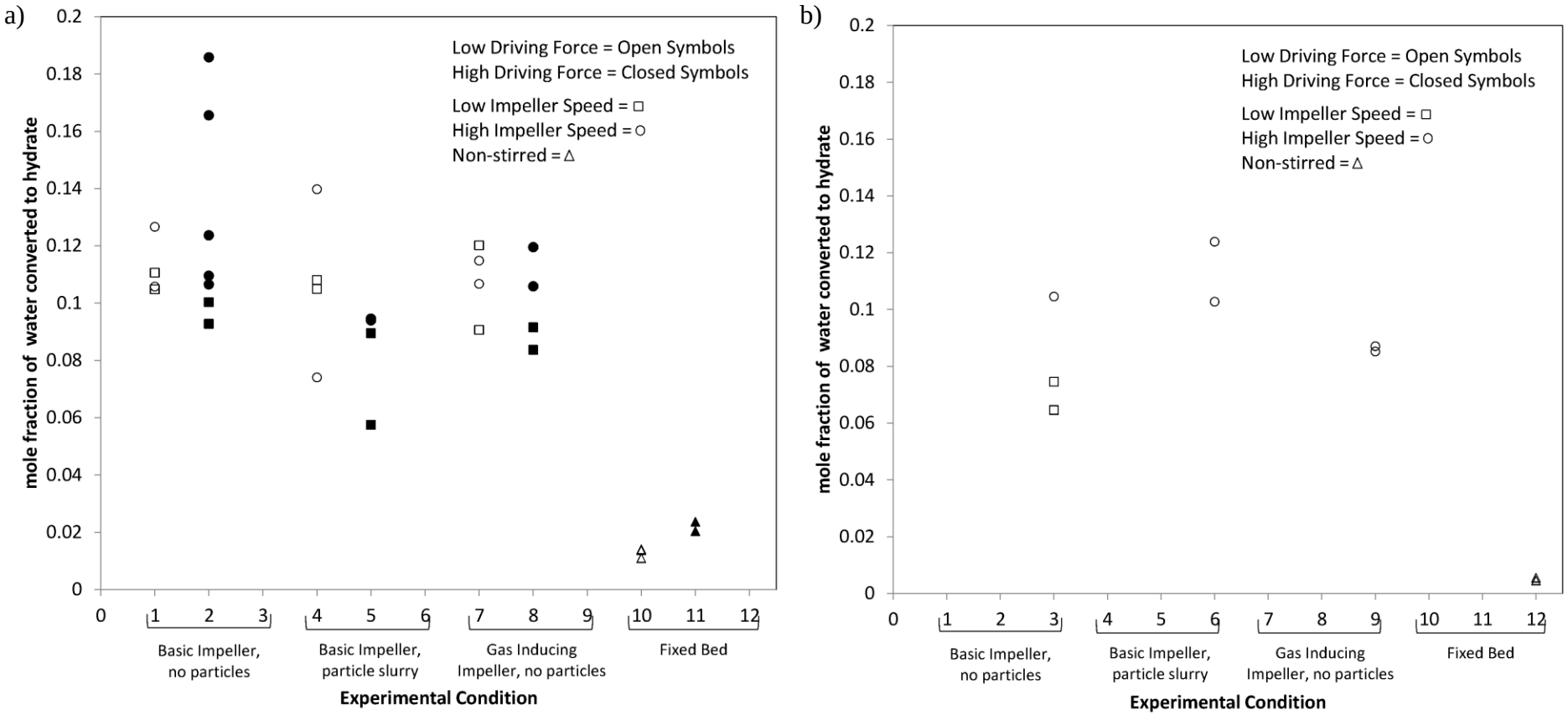

Figure 2.9: Fraction of water converted to hydrate 120min after nucleation for A) CO_2 and B) CH_4.

The reasons for this behaviour are seen in greater detail in the individual temperature and hydrate formation profiles. The profiles for low driving force, basic impeller CO_2 runs at high impeller speed and low impeller speed are shown in Figure 2.10 and Figure 2.11, respectively. Condition 1b, showed an initial fast rate of hydrate formation that quickly became heat transfer limited. As the run goes on, the rate of hydrate formation continues to slow and eventually becomes mass transfer limited after a critical amount of water has been converted into hydrate. This behaviour is seen in all high impeller speed runs. The impeller speed affects both the mass and heat transfer rates in the stirred tank, and as a result a distinctly different profile is seen when the lower impeller speed is used. When a lower impeller speed is used, the same fast initial rate of hydrate formation is not achieved; however, as a result the system does not become as heat transfer limited and the systems sustains a relatively fast rate of hydrate formation. After 120min, condition 1a also becomes mass transfer limited and 1a and 1b achieve similar final hydrate fractions. Therefore, if the goal of a stirred system was to produce a hydrate slurry with a high hydrate fraction, i.e. high enough that mass transfer would be the limiting factor, an optimum impeller speed exists that would minimize both the total residence time as well as the power requirements of the impeller.

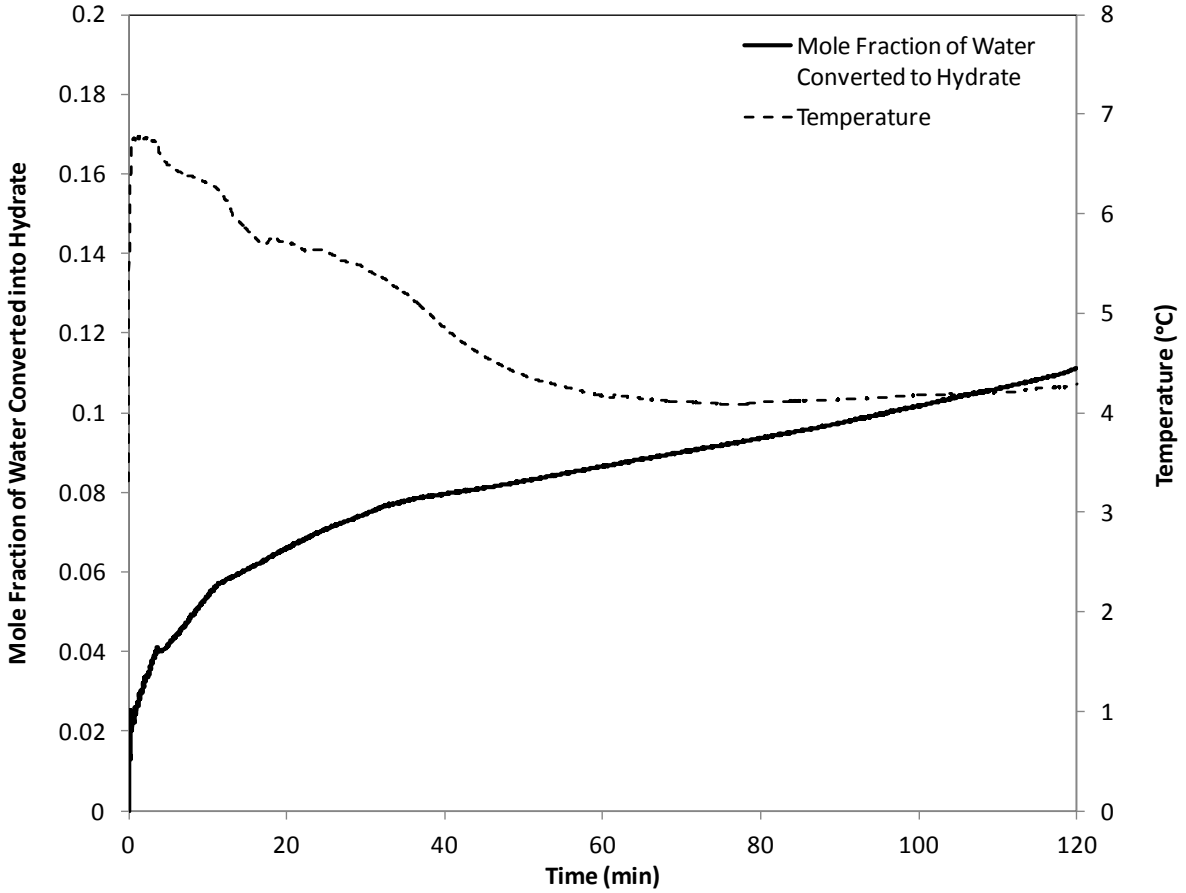

Figure 2.10: Temperature and hydrate formation profiles for condition 1b, run 2.

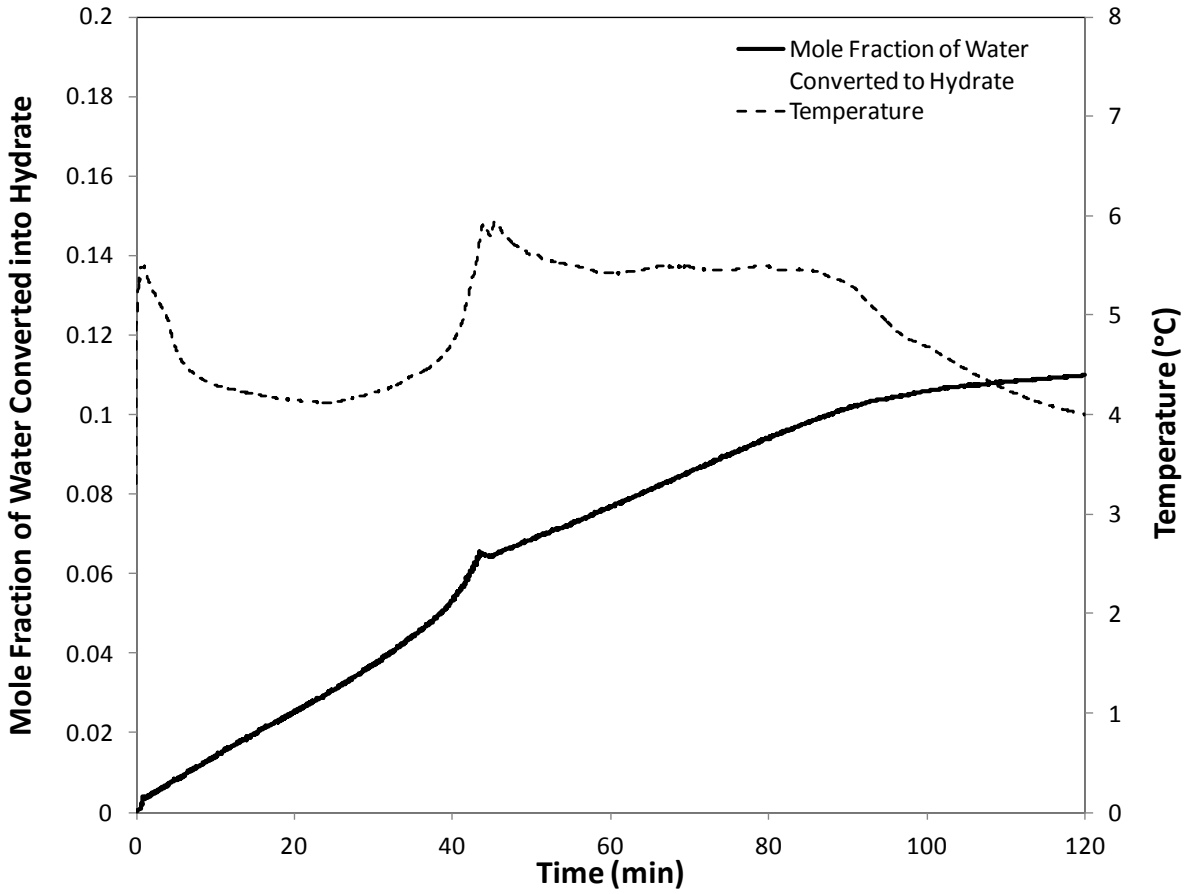

Figure 2.11: Temperature and hydrate formation profiles for condition 1a, run 1.

The heat transfer and the later mass transfer limitations are further supported by the profiles from the CH_4 runs presented in Figure 2.12 when they are compared with the corresponding CO_2 run presented in Figure 2.10. Due to the lower heat of hydrate formation for CH_4 hydrates, a higher rate of hydrate formation can be sustained while the system is heat transfer limited. Once the system becomes mass transfer limited there is a clear transition to a slower rate of formation and the reactor temperature drops. As hydrates are still being formed and producing heat in the process, the reactor temperature remains elevated relative to the initial temperature.

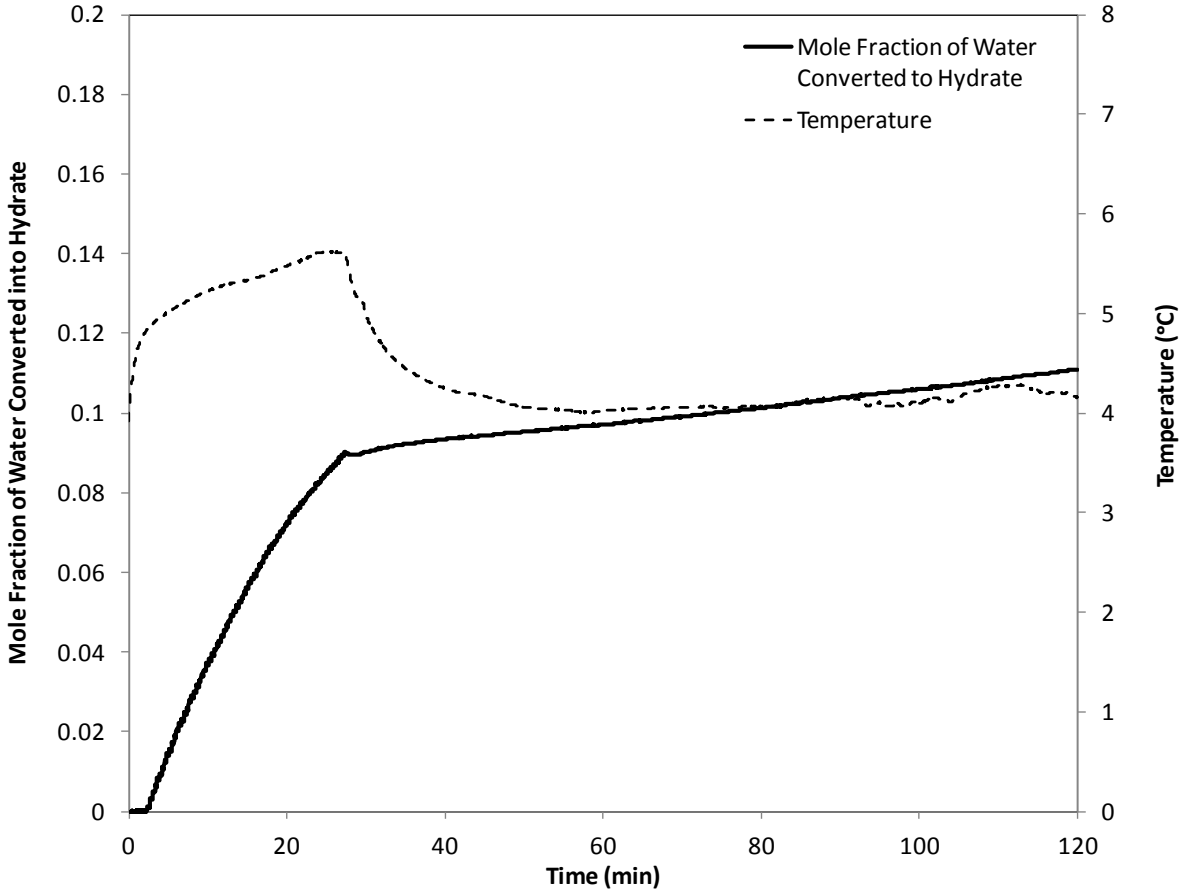

Figure 2.12: Temperature and hydrate formation profiles for condition 3b, run 1.

Additionally, when CO_2 hydrate formation profiles from condition 1 (low driving force) in Figure 2.10 and Figure 2.11 are compared with those from condition 2 (high driving force), in Figure 2.13 and Figure 2.14, it can be seen that higher maximum temperatures are reached during condition 2. The high driving force conditions had the same temperature, but a higher pressure. Therefore higher temperatures can be reached before hydrate growth becomes thermodynamically impossible. However, since the system becomes quickly heat transfer limited and later becomes mass transfer limited, there is no significant difference in the overall formation of hydrate due to driving force.

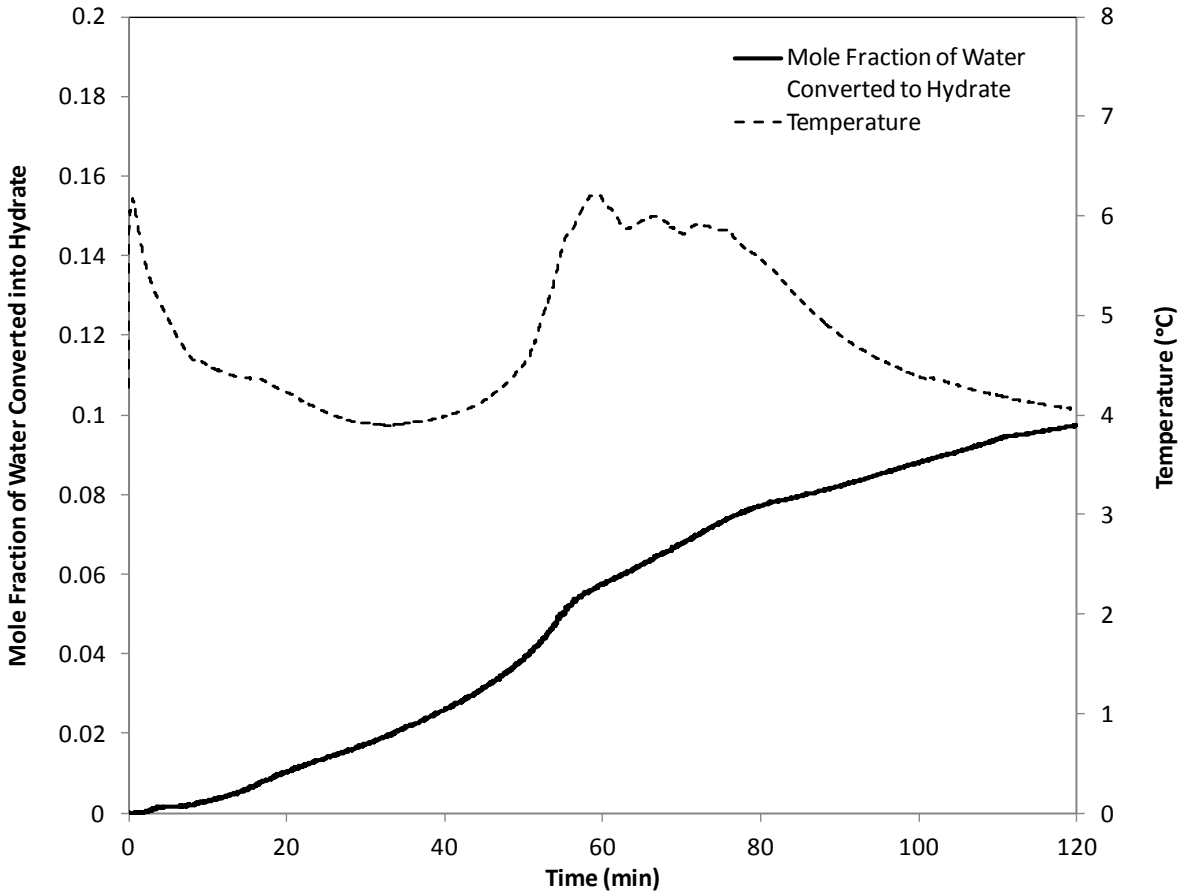

Figure 2.13: Temperature and hydrate formation profiles for condition 2a, run 1.

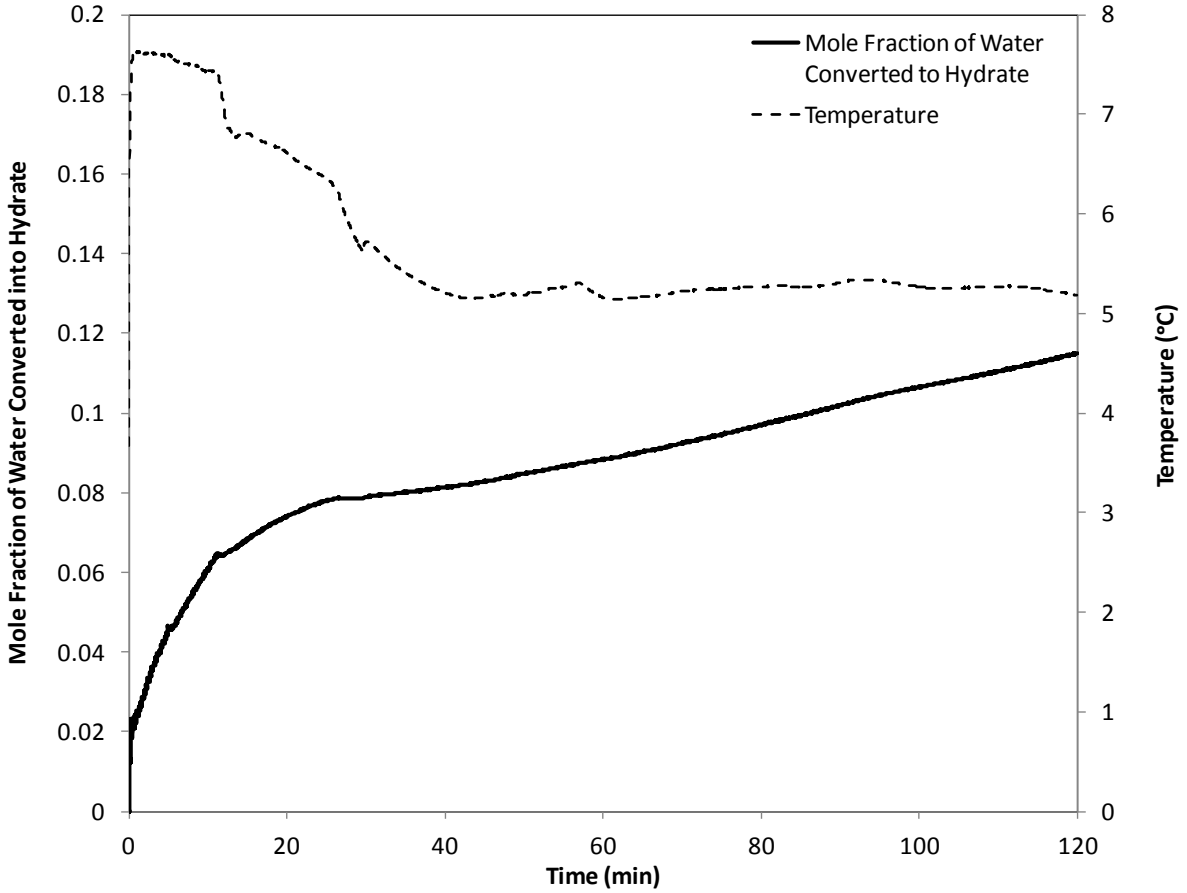

Figure 2.14: Temperature and hydrate formation profiles for condition 2b, run 1.

Figure 2.15 shows the profiles from a particle slurry run, with high driving force and high impeller speed. While there was no significant difference in the amount of hydrate formed, what was affected by the presence of the particles was the induction time, the time between the start of the experiment and observable nucleation. In all of the particle slurry runs, the induction times were less than 5min, while they could be up to several hours long for other conditions. This result is expected since the surface of the particles provides additional sites for heterogeneous nucleation. As a result, much of the heat from gas dissolution at the start of the experiment (not shown) had not yet dissipated before hydrate growth started. This can be observed when Figure 2.15 is compared to the equivalent profiles without particles, Figure 2.14. The temperature at 0min after nucleation 6.4°C in condition 5b, run 2, while in condition 2b, run 1 it is 3.7°C. As a result, less hydrate is produced during the initial fast rate of formation. Therefore, in a system that is less heat transfer limited, the particle slurry could be used to ensure faster nucleation without affecting hydrate growth.

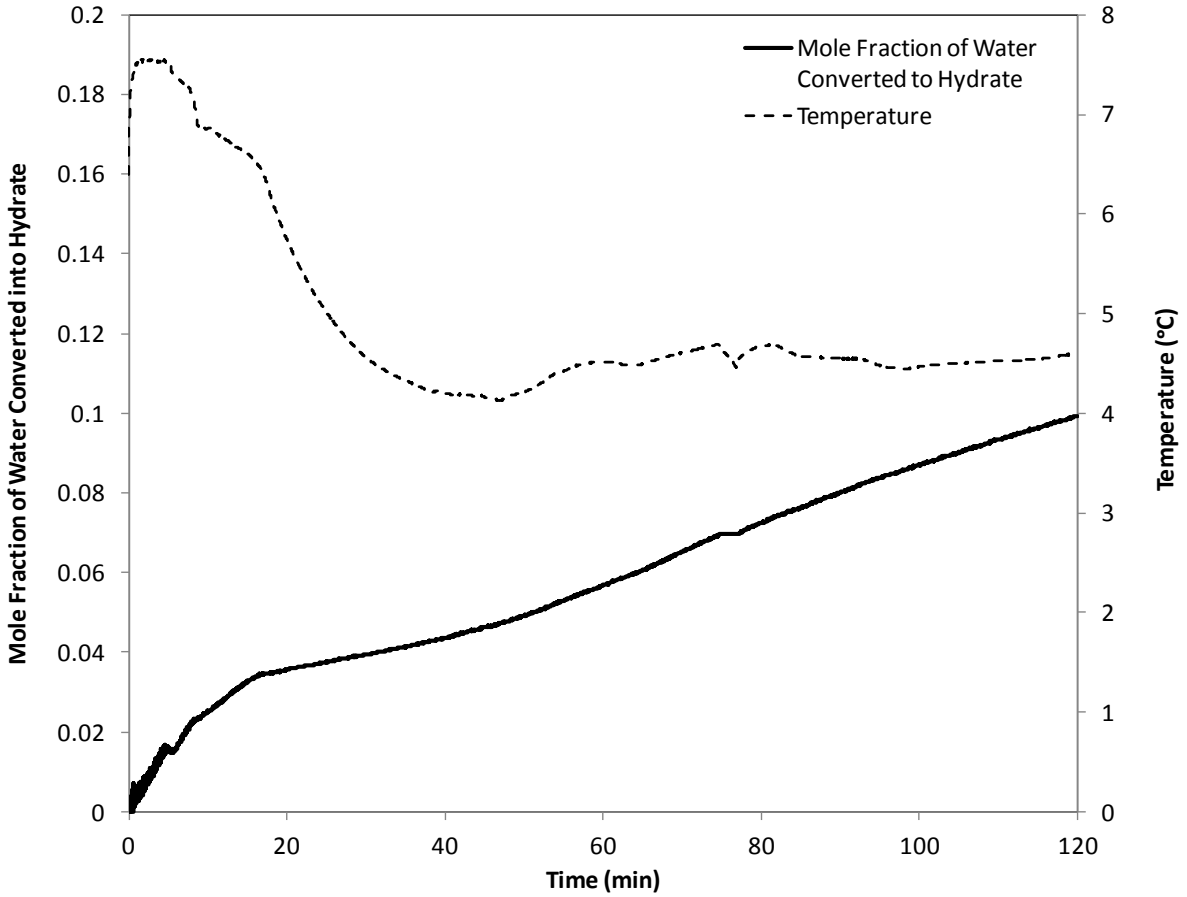

Figure 2.15: Temperature and hydrate formation profiles for condition 5b, run 2.

Figure 2.16, relative to Figure 2.12, further illustrates the lack of effect of the Gaspersator gas inducing impeller on the formation of hydrates. Unfortunately, the design of the Gaspersator, a commercially purchased gas inducing impeller, could have been improved by changing the location of the holes in the impeller blade. If the holes had been located on the tips of the impeller blades rather than in the valleys between the blades, then the greater radial displacement of the hole in the impeller blades would have resulted in a greater difference in velocity between the holes in the impeller shaft above the water line in the head space and the holes in the impeller blade below the water line. This difference in velocity would have led to greater pressure drop between the two locations and provided a higher driving force for gas transport. Due to the already heat transfer limited nature of the high impeller speed runs, it is unlikely that these modifications would have changed the outcome at this condition. However, at the lower impeller speed it is possible that the hydrate formation behaviour could have been impacted.

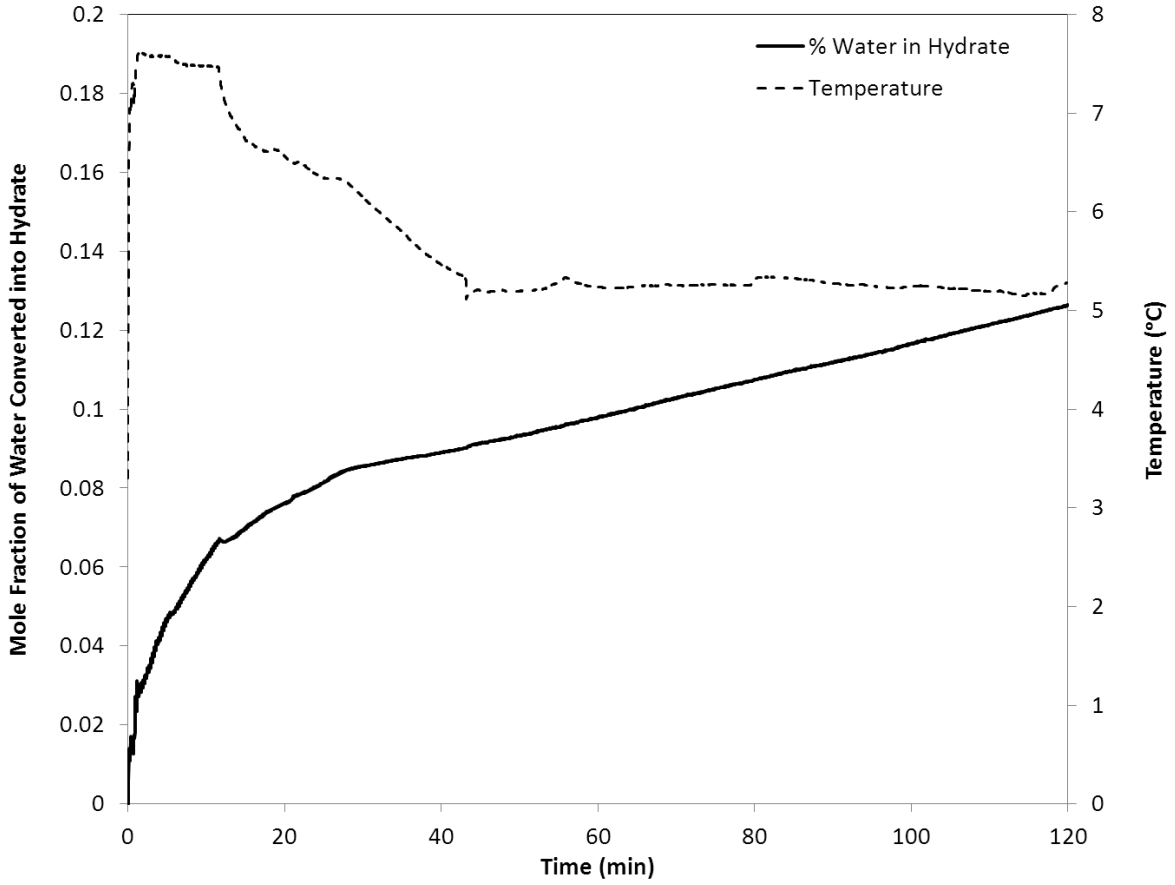

Figure 2.16: Temperature and consumption profiles for condition 8a, run 1.

As can be seen in the example profiles from the fixed bed runs in Figure 2.17 and Figure 2.18, these runs were mass transfer limited from the start unlike the stirred runs. Moreover, the driving force will now have a significant effect. Since there was no stirring, the temperature in the bed was not uniform and the small increases in temperature indicate hydrate formation near the temperature probe rather than increases in hydrate formation.

Due to the mass transfer limited nature of the fixed bed system, the rate of hydrate formation is much lower in these systems relative to the stirred systems. Specifically, the average rate of hydrate formation in terms of mole fraction of water over the full 120min run time was a factor of 10 slower for the fixed bed systems than for the stirred systems. The fixed bed system does not show the initial rapid growth seen in the stirred systems and the slow growth shown is still less than the slowest rate seen in stirred systems. To reach a similar fraction of hydrate, a fixed bed system would have to be left for considerably longer than a

stirred system. To reach the average mole fraction of hydrate observed in 120min in the stirred systems, 0.105, at the average rate of hydrate formation, calculated using Simpson's rule over the full 120min period, from condition 11, it would take 572min. While a fixed bed has lower energy demands due to the lack of agitation, a larger set of reactors would have to be maintained in order to keep up with the production rate; leading to a higher capital cost.

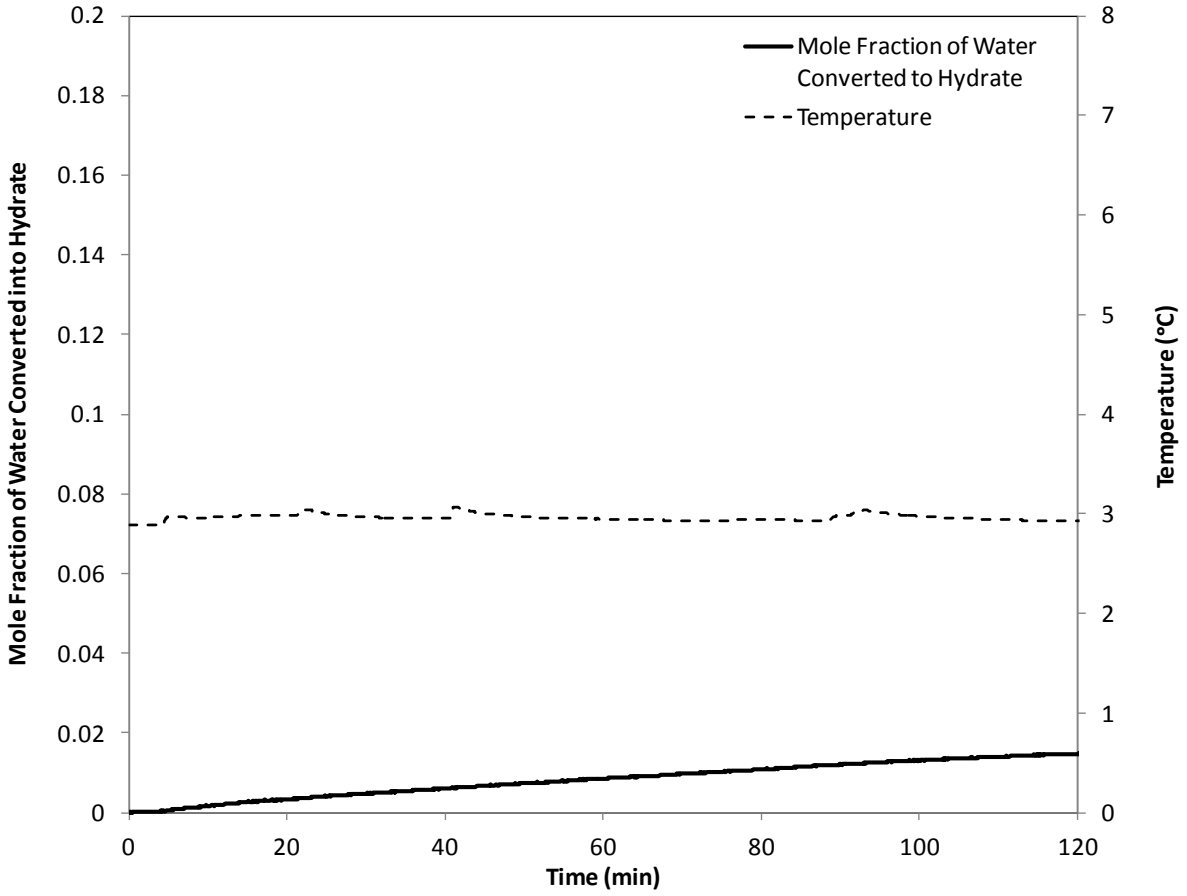

Figure 2.17: Temperature and hydrate formation profiles for condition 10, run 2.

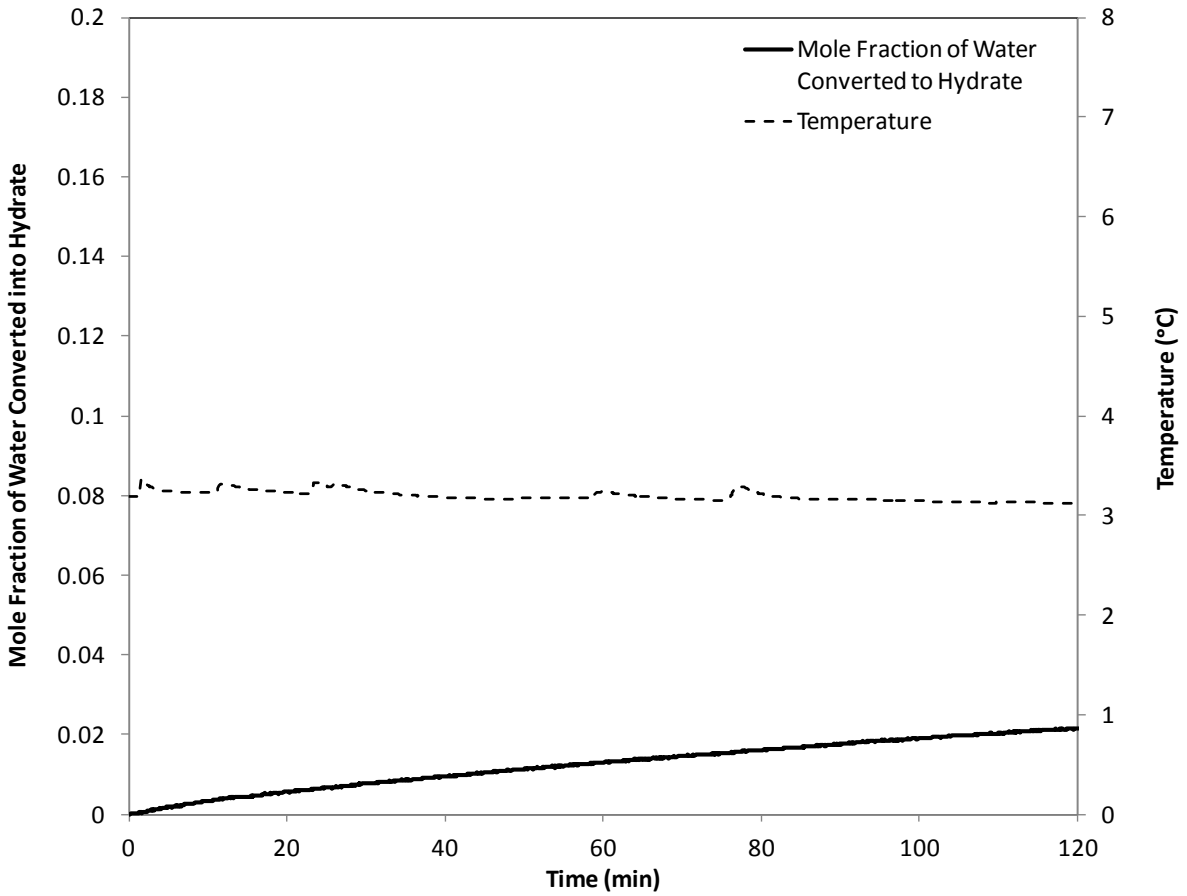

Figure 2.18: Temperature and hydrate formation profiles for condition 11, run 2.

In order to consider these reactor designs for an industrial level application, two more pieces of information are required: the rate of hydrate formation per unit volume of reactor and the amount of power required for hydrate formation. Since the performance of the various configurations has already been compared in detail on the basis of fraction of water converted, only the maximum rates achieved will be discussed in relation to volume and power requirement. The average rate of formation was calculated from 0-15min, 15-30min and then for every subsequent 30min period. The maximum of those rates for each configuration was selected for comparison and it is assumed that a continuous reactor could be designed to operate in that regime. The results are shown in Figure 2.19. What can be observed is that there is no significant difference between any of the stirred runs. This is particularly expected between the basic impeller and gas inducing impeller since they both allow for the full 300mL of reactor volume to be filled with water. As for the slurry runs, the volume that the particles occupy

(20mL) is not large enough to affect the performance significantly. Also of note is that the fixed bed configuration falls further behind the stirred configuration. In the fixed bed, the particles occupy the majority of the reactor volume (175mL) and this leaves much less room for the water that could turn into hydrates.

The energy required by each configuration was based on the power requirement on the mixer. The energy required for heat removal was not considered as it will be consistent across all the configurations studied. The results are shown in Figure 2.20. Since the fixed bed does not require any mixing, and thus no power for mixing results are not included in the figure. It should be noted that one of the major advantages of the fixed bed is this lack of power required for mixing. One of the main differences between Figure 2.19 and Figure 2.20 is the much tighter grouping of the high and low impeller speed runs. In particular, some of the low impeller speed runs, for all stirred configurations, show a better power normalized rate than some high impeller speed runs. This further reinforces the point that there is an optimal impeller speed that will balance power consumption and hydrate production.

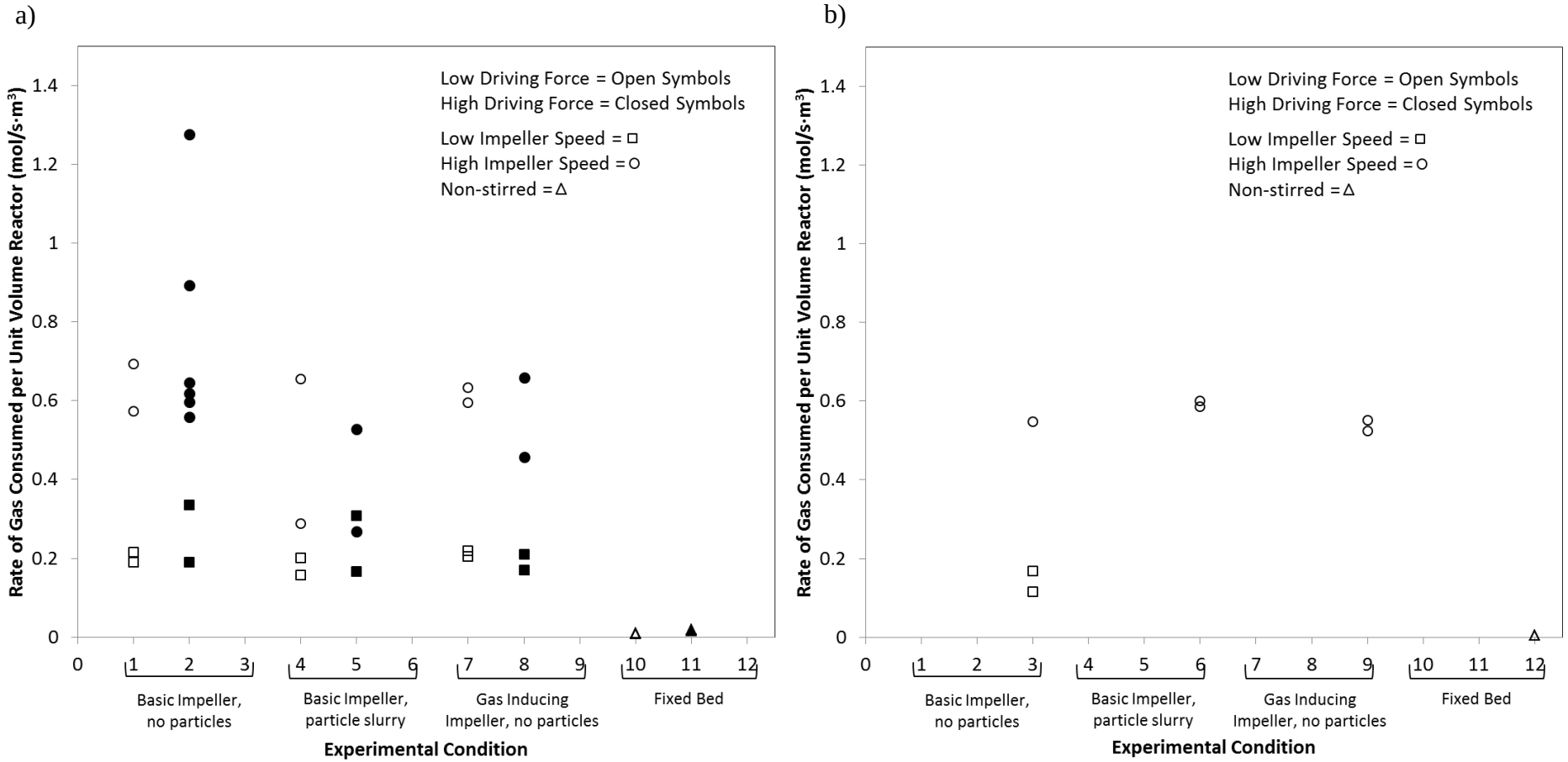

Figure 2.19: Maximum rate of gas consumption per unit volume of reactor for A) CO_2 and B) CH_4.

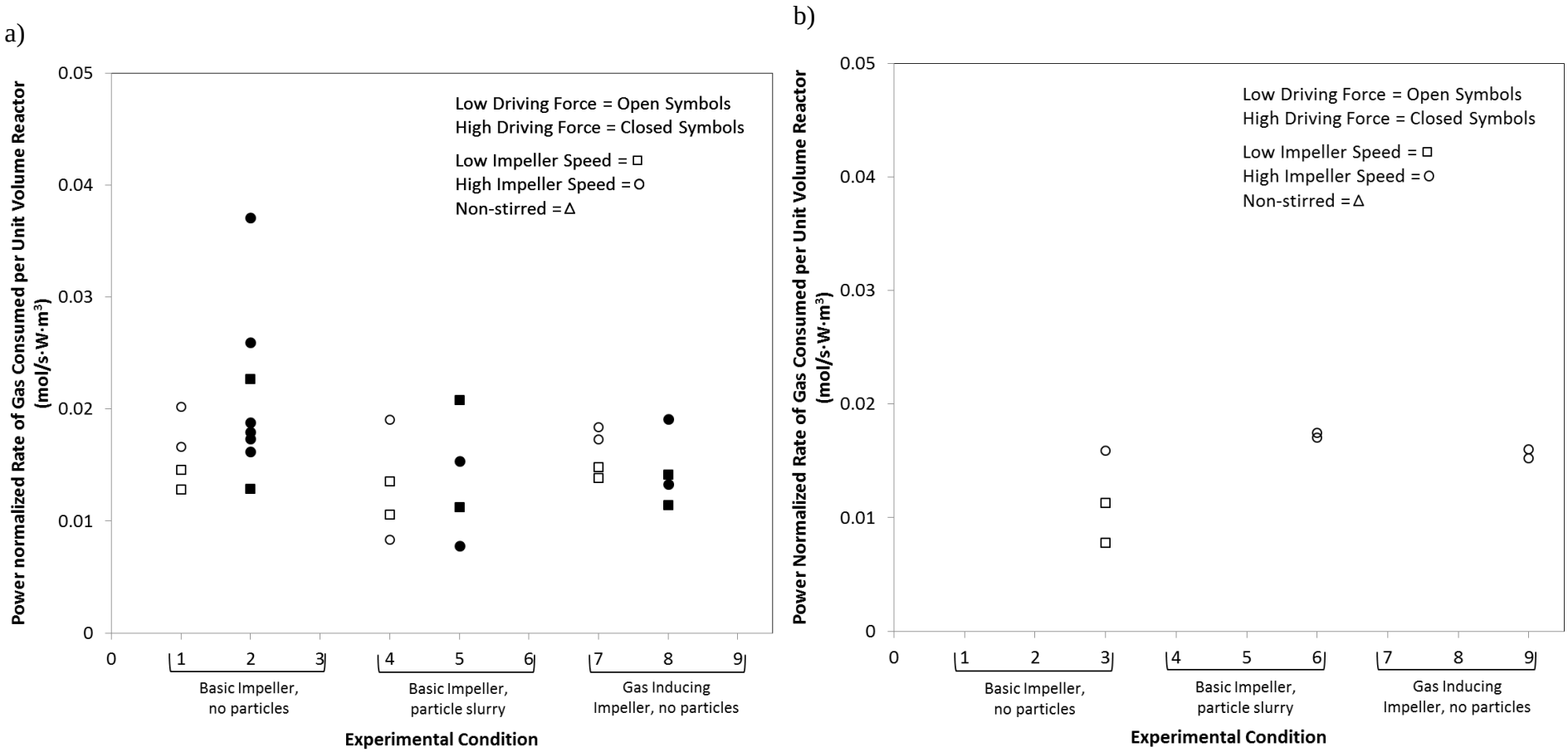

Figure 2.20: Maximum rate of gas consumption per unit volume of reactor, normalized for power consumption for A) CO_2 and B) CH_4.

2.4 – Conclusions

Increased stirring intensifies both heat and mass transfer within the reactor, but the initial rapid rate of hydrate formation leads to heat transfer limited conditions. As the rate of hydrate formation slows and more hydrates are present in the reactor, the impact of interphase mass transfer becomes significant. Operating conditions that only influence the interphase mass transfer, i.e. increased pressure and use of a gas-inducing impeller, were not significant and further suggest the heat transfer limited nature of the stirred tank system studied. Greater stirring rates require more energy and thus any application involving a stirred tank should include an effective heat removal heat in order to maximize hydrate formation per power input. Alternatively, a bubble column with similar heat removal capacity and lower intrinsic power consumption could be used to produce gas hydrates, and this type of system will be studied in future work. Using a particle slurry decreased the induction time but otherwise had a negligible effect on hydrate formation: indicating an effective way to stimulate nucleation without negatively affecting hydrate formation. The particles would also be easily recoverable from the process water after the hydrates have been dissociated, unlike chemical promoters. For the conditions investigated, fixed bed systems are mass transfer limited and show much slower rates of hydrate formation than the stirred systems. As a result, driving force has a significant effect on hydrate formation. Fixed bed systems will require a much larger reactor volume to have a comparable performance, not just because of the slower rates of hydrate formation, but also because of the low water fraction within the reactor. Therefore, a fixed bed simulates the conditions where gas hydrates are found naturally, e.g., in the sand at the bottom of the ocean, in both pressure and long residence times, and would only be viable in applications with these requirements.

2.5 – Nomenclature

MW	Molecular Mass
n	Number of moles
P	Pressure
R	Gas constant
T	Temperature
V	Volume
X	Mole fraction in liquid phase
Z	Compressibility Factor
ρ	Density

2.6 – Acknowledgements

The authors are grateful to Jason Ivall and Jonathan Verrett (McGill University) for their valuable insights. The authors would like to acknowledge the Natural Sciences and Engineering Research Council of Canada, the Canadian Foundation for Innovation, the Ontario Innovation Trust and Ontario Graduate Scholarship Program for financial assistance.

2.7 – References

Anderson, G. K. (2003). "Enthalpy of dissociation and hydration number of carbon dioxide hydrate from the Clapeyron equation." Journal of Chemical Thermodynamics **35**(7): 1171-1183.

Anderson, G. K. (2004). "Enthalpy of dissociation and hydration number of methane hydrate from the Clapeyron equation." Journal of Chemical Thermodynamics **36**(12): 1119-1127.

Babu, P., R. Kumar and P. Linga (2013). "Pre-combustion capture of carbon dioxide in a fixed bed reactor using the clathrate hydrate process." Energy **50**(1): 364-373.

Fujita, S., K. Watanabe and Y. H. Mori (2009). "Clathrate-Hydrate Formation by Water Spraying onto a Porous Metal Plate Exuding a Hydrophobic Liquid Coolant." AIChE Journal **55**(4): 1056-1064.

Gudmundsson, J. S., F. Hveding and A. Borrehaug (1995). Transport of Natural Gas as Frozen Hydrate. Fifth International Offshore & Polar Engineering Conference, The Hague.

Hashemi, S. M. R., A. Macchi and P. Servio (2009). "Dynamic simulation of gas hydrate formation in a three-phase slurry reactor." Industrial and Engineering Chemistry Research **48**(15): 6983-6991.

Kang, S.-P. and J.-W. Lee (2010). "Formation characteristics of synthesized natural gas hydrates in meso- and macroporous silica gels." Journal of Physical Chemistry B **144**: 6973-6978.

Li, G., D. Liu, Y. Xie and Y. Xiao (2010). "Study on effect factors for CO2 hydrate rapid formation in a water-spraying apparatus." Energy and Fuels **24**(8): 4590-4597.

Linga, P., N. Daraboina, J. A. Ripmeester and P. Englezos (2012). "Enhanced rate of gas hydrate formation in a fixed bed column filled with sand compared to a stirred vessel." Chemical Engineering Science **68**(1): 617-623.

Linga, P., R. Kumar, J. D. Lee, J. Ripmeester and P. Englezos (2010). "A new apparatus to enhance the rate of gas hydrate formation: Application to capture of carbon dioxide." International Journal of Greenhouse Gas Control **4**(4): 630-637.

Marinhas, S., A. Delahaye, L. Fournaison, D. Dalmazzone, W. Fürst and J. P. Petitet (2006). "Modelling of the available latent heat of a CO2 hydrate slurry in an experimental loop applied to secondary refrigeration." Chemical Engineering and Processing: Process Intensification **45**(3): 184-192.

Matsuda, S., H. Tsuda and Y. H. Mori (2006). "Hydrate formation using water spraying onto a cooled solid surface in a guest gas." AIChE Journal **52**(8): 2978-2987.

Mori, Y. H. (2003). "Recent Advances in Hydrate-Based Technologies for Natural Gas Storage - A Review." Journal of Chemical Industry and Engineering (China) **54**.

Myre, D., A. Macchi and P. Servio (2010). Sythesis of CO2 Hydrates in a Slurry Bubble Column. 7th International Conference for Gas Hydrates. Edinburg, Scotland.

Sloan, E. D. and C. A. Koh (2008). Clathrate Hydrates of Natural Gas. 3rd ed. Boca Raton, Florida, CRC Press.

Springman, H. G., A. Steiff and P. M. Weinspach (1991). "Feststoffeinfluß auf den Stofftransport in Suspensionblasensäulen." Chem. Ing. Tech. **63**: 512-513.

Vahakis, J. G., H.-S. Chen, M. S. Suwandi and A. J. Barduhn (1972). "Research and Development Report 830." Prepared for the US DOE of the Interior.

Verrett, J., D. Posteraro and P. Servio (2012). "Surfactant effects on methane solubility and mole fraction during hydrate growth." Chemical Engineering Science **84**(0): 80-84.

Yang, D., L. A. Le, R. J. Martinez, R. P. Currier and D. F. Spencer (2011). "Kinetics of CO2 hydrate formation in a continuous flow reactor." Chemical Engineering Journal **172**(1): 144-157.

Chapter 3 – Effect of Bubble Column Operating Conditions on Gas Hydrate Formation

3.1 – Introduction

Gas hydrates are non-stoichiometric ice-like compounds that are members of the class of compounds called clathrates. They are formed when, at the appropriate thermodynamic conditions, gas or guest molecules become trapped within the cavities or cages made by hydrogen bonded water molecules. The collapse of the cavity is prevented by the repulsive presence of the guest molecule stabilizes the cavity. Since an empty cavity can be stable if a large percentage of neighbouring cavities are occupied, gas hydrates are non-stoichiometric. The hydration number itself will vary as the relative size of the cavity and guest molecule, and as a result the stability of an empty cavity, will vary with changes in temperature and pressure (Sloan and Koh 2008).

While hydrate research had traditionally been focussed on inhibiting hydrate formation, recently gas hydrates have been considered for natural gas storage and transportation (Gudmundsson, Hveding et al. 1995), secondary refrigeration (Marinhas, Delahaye et al. 2006) and gas separation (Kang and Lee 2010, Linga, Kumar et al. 2010). All three of these applications require an effective hydrate production reactor; however, the requirements for each application vary. Maximizing storage capacity is the most important design consideration in a natural gas storage and transportation application, while the rate of formation needs to be compatible with the general production rate of natural gas at a particular facility. As the gas is expected to be released eventually, hydrate stability is important, but not crucial for this application. Secondary refrigeration uses a hydrate slurry that needs to be transported from the primary refrigeration unit to the location where the cooling is required. Therefore, there a minimum acceptable hydrate concentration to make the slurry an effective coolant as well as a maximum acceptable hydrate concentration in order to pump the slurry from one location to another. Additionally, to make the heat transfer from the primary coolant to the forming hydrate slurry as efficient as possible, the rate of hydrate formation should be maximized. When hydrate

formation is used for gas separation, the conditions are set so that one component will preferentially enclathrate. The enclathrated gas can be obtained later by dissociating the hydrate. For example, this technology could be used to separate CO_2 from flue gas. For this application, the hydrate should be easily dissociable to facilitate the recovery of the enclathrated gas and the rate of hydrate formation should be maximized.

Hydrate formation is analogous to crystallization and consists of two main steps: nucleation followed by hydrate growth (Sloan and Koh 2008). To help illustrate hydrate formation, the carbon dioxide – water system is used as an example. For hydrates to form, the pressure and temperature conditions have to be above the L_w-H-V equilibrium line of the system. The P-T diagram of this system is shown in Figure 3.1. As illustrated in Figure 3.2**,** before the L_w-H-V is crossed, the solubility of CO_2 in liquid water increases with decreasing temperature. In the hydrate forming region, the solubility of CO_2 in water continues to increase but the system becomes metastable as hydrate formation is favoured (Myre, Macchi et al. 2010). Dissolved gas is used primarily for hydrate growth after nucleation has occurred (Hashemi, Macchi et al. 2009). Only the growth phase will be studied in this work because nucleation is a stochastic process and thus difficult to control (Sloan and Koh 2008).

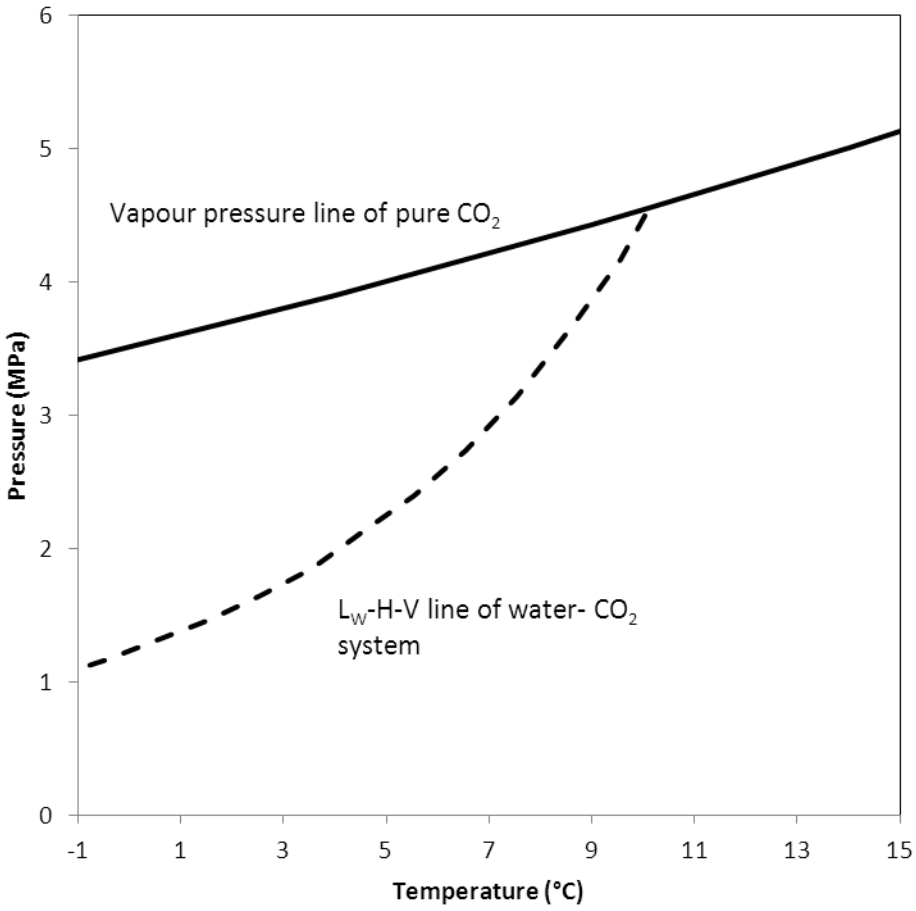

Figure 3.1: P-T diagram showing the vapour pressure line of pure CO_2 (solid line) and the L_w-H-V line of water – CO_2 system (dashed line) (Sloan and Koh 2008), (Vahakis, Chen et al. 1972).

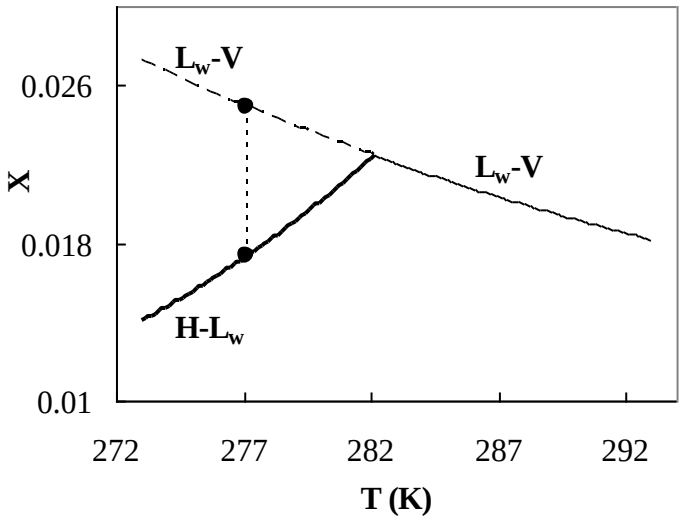

Figure 3.2: Carbon dioxide solubility (X) in terms of mole fraction in water under liquid water-vapour and liquid water-hydrate equilibrium at P = 3.5 MPa (Hashemi, Macchi et al. 2009).

Hydrate growth occurs through the mass transfer of guest molecules from the gas phase to the liquid phase and into the hydrate phase. In order to saturate what is seen as an unsaturated solution, gas molecules diffuse into the liquid phase. Simultaneously, the hydrate phase incorporates more CO_2 to lower the bulk CO_2 concentration and restore the hydrate-liquid water ($H\text{-}L_w$) equilibrium. Hydrate growth will be mass transfer limited if this transfer across phase boundaries does not occur quickly enough relative to the kinetics of enclathration. (Hashemi, Macchi et al. 2009)

Hydrate growth can also be controlled by the rate of heat transfer. Hydrate growth is exothermic and therefore heat must be removed from the reacting system to maintain isothermal operation. If the temperature increases, the concentration driving force for mass transfer will decrease until eventually the system will exit the thermodynamic region for hydrate formation. It should be noted that heat and mass transfer limitations generally affect the rate of hydrate formation more than the intrinsic enclathration kinetics (Sloan and Koh 2008).

The reactor designs for gas hydrate synthesis fall into two main categories, ones where liquid is the dispersed phase and ones where gas is the dispersed phase (Mori 2003). In a gas dispersed reactors, liquid water is present in the reactor vessel and gas is introduced into the liquid phase either by using mechanical stirring to mix-in gas from the head space, bubbling it from the bottom or through some other mechanism. In a liquid dispersed reactor, liquid water is sprayed into a reactor vessel that is filled with the desired guest gas. Liquid dispersed reactors have good mass transfer since a very large interfacial area can be achieved using atomizing nozzles, but suffer from poor heat transfer due to the low heat capacity of gases relative to liquid water (Mori 2003). Gas dispersed reactors have less effective mass transfer but the heat transfer is greatly improved compared to liquid dispersed reactors (Mori 2003). Liquid dispersed reactor designs will not be studied in this work since heat transfer limitations have already been observed in multiple liquid dispersed reactors (Matsuda, Tsuda et al. 2006);(Fujita, Watanabe et al. 2009, Li, Liu et al. 2010).

As mentioned above, the requirements of a hydrate producing reactor vary depending on the application. While the differences between the various reactor designs are known qualitatively, this study aims to investigate the performance of a bubble column at various operating conditions, which will provide insight into the impact of transport phenomena at rapid hydrate growth rates. The results will also be compared with that of a semi-batch stirred tank reactor from a previous study, discussed in Chapter 2, where heat transfer limitations were observed in the initial phases of hydrate. In the later phases of hydrate growth, mass transfer limitations were observed as the hydrate slurry thickened. The bubble column reactor will likely improve the performance on both of these fronts. Bubble columns have more efficient heat transfer for the same energy input. Additionally, since the gas is bubbled in from the bottom it will be easier to maintain good mass transfer between the gas, liquid and hydrate phases even as the slurry thickens.

The bubble column operating at lower gas flowrate, driving force for hydrate growth and driving force for heat removal will serve as the baseline performance. Then the effects of independently increasing the gas flowrate, the driving force for hydrate growth and the driving force for heat removal will be observed. The driving force for hydrate growth will be increased by increasing the set experimental pressure rather than changing the experimental temperature, since the latter would also alter the heat transfer characteristics of the system. The driving force for heat removal is altered by lowering the temperature of the cooling jacket on the bubble column. The effect of adding a small amount of glass beads will also be studied. The glass beads will provide sites for heterogeneous nucleation as well as have an abrasive effect on any hydrates or ice that form on the walls of the reactor.

3.2 - Experimental Methods

3.2.1 - Materials

Experiments were performed using distilled water. The carbon dioxide used in the experiments were purchased from Linde Canada Industrial Gases has a purity of 99.8%. The glass beads (P-0060) are from Potters Industries and have a diameter of 0.1 to 0.15 mm.

3.2.2 - Apparatus

Hydrates were formed in a SS316 column with an inner diameter of 0.1 m and a maximum liquid level of 1.22 m. A schematic diagram of the set-up is shown in Figure 3.3. Two glass windows of 118.8 mm x 15.6 mm are located on the front and rear sides of the column to allow visual observation. Due to the location of the gas inlet and the drainage valves, there is a volume of 1.6L that will contain water but will not have any direct contact with introduced gas. A distributor plate located below the gas inlet prevents any hydrates or other particles from becoming trapped in the non-gas-contacting region. When filled with a total volume of 8.5L, the remaining column volume and piping give a volume of 50.2L that is filled with gas. The column wall is jacketed and the coolant temperature can be reduced to 263K. The temperature of the column contents is controlled by adjusting the flowrate of coolant through the jacket. National Instruments hardware and software was used for data acquisition.

The system allows a single pass of the gas through the column. A cylinder of carbon dioxide feeds the gas at either the bottom of the column or at the top, above the liquid level. When gas enters at the bottom of the column it passes through a sparger and into the water. The inlet and outlet flow rates are both measured using orifice plates (Rosemount, Model: 1195S010P1S0345CS4J3J1) and pressure transducers (Rosemount, Model: 8732CT12N0). At the column outlet, an automated control valve maintains the system at the desired pressure. At the end, the gas is collected in two empty cylinders. Gas consumption due to hydrate formation is calculated from temperature, pressure and flow rate measurements before and after the reactor. The pressure drop from the gas inlet to a point 72cm above the inlet was measured by a differential pressure transducer (Rosemount, Model 1195S010P1S0345CS4J3J1). This was used to estimate the changes in gas hold-up as hydrates formed.

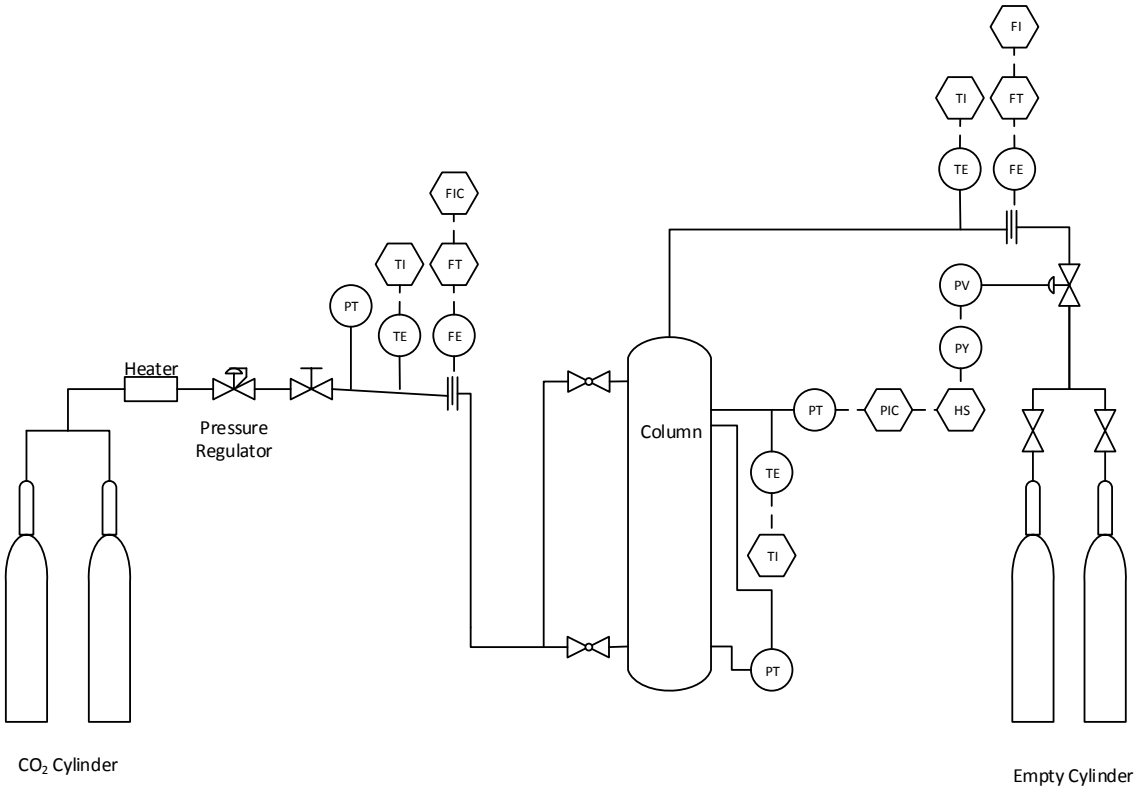

Figure 3.3: Simplified schematic of the experimental set-up

3.2.3 - Experimental Conditions

A variety of thermodynamic conditions and phase contacting conditions were studied in this work. The justification is presented below and the conditions summarized in Table 3.1. Two runs were conducted at each condition.

Table 3.1: Experimental Conditions

Modified Numbers	Particle Level (wt%)	Column Temperature (°C)	Column Pressure (kPa)	Coolant Temperature (°C)	Gas Velocity (mm/s)
1.a	0	3	3100	0	20
1.b	0	3	3100	0	50
2.a	0	3	2750	0	20
2.b	0	3	2750	0	50
3.a	0	3	3100	-5	20
3.b	0	3	3100	-5	50
4.a	0	3	2750	-5	20
4.b	0	3	2750	-5	50
5.a	10	3	3100	-5	20
5.b	10	3	3100	-5	50
6.a	10	3	2750	-5	20
6.b	10	3	2750	-5	50

3.2.3.1 - Gas Flowrate

The inlet gas superficial velocity was studied at two conditions, a low point of 20mm/s and a high point of 50mm/s. Changing the gas flowrate affects several parameters of the bubble column operation. Firstly, increasing it increases the amount of gas being introduced to the column (i.e., holdup) and therefore provides more gas molecules with which hydrates can be formed. Secondly, it increases the mixing within the column, which affects both the interphase mass/heat transfer as well as the wall-to-bed heat transfer within the system. The high point of 50mm/s was selected as it is the maximum that the experimental system can sustain over the run time, and the low point was set to be sufficiently lower to provide a good contrast while not being so low as to approach the operable minimums of the experimental system.

3.2.3.2 - Coolant Temperature

Coolant temperature is a parameter that almost exclusively affects the heat transfer out of the column. Given the heat transfer limited nature of hydrate formation observed in previous semi-batch stirred tank study, the coolant temperature should be as low as possible before the resistance to heat transfer caused by ice formation on the column wall becomes greater than the effect of increasing the temperature driving force by lowering the coolant temperature. For this work a coolant temperature of 0°C was selected as the higher temperature since it is the lowest temperature that can be sustained without risking ice formation. The lower coolant temperature of -5°C was selected to study the effect of potential ice formation.

3.2.3.3 - Thermodynamic Conditions

The driving force for mass transfer between the gas phase and hydrate phase is also influenced by the thermodynamic conditions as shown in Figure 3.2. Therefore, consistent driving force conditions must be used to ensure comparable results. In this work, driving force is measured as the difference between the concentration of the guest molecule in water according to the L_W-H equilibrium and the L_W-V equilibrium. Driving force for mass was varied by changing the pressure while maintaining a constant temperature so that only the driving force for mass transfer was altered and the driving force for heat transfer was kept constant.

Heat transfer limitations were not negligible in all runs; therefore, maintaining a constant reactor temperature was not possible. Since, the driving force for mass transfer is not constant, and the driving force for the thermodynamic conditions given in Table 3.1 is an initial driving force. Since pressure was used to change the mass transfer driving force, mass transfer driving force for the high driving force conditions, is still greater than that of the low driving force runs even if the temperature increases.

3.2.3.4 - Particle Level

Two different particle levels were studied. First the performance without any particles was measured to serve as a baseline and then the performance of a 10 wt% slurry was measured to study the effect of particles. In both cases, the total volume was maintained at 8.5L. In the case of the slurry this meant that 8.16L of water and 906g or 0.34L of particles were added. Relative to water, the apparent density of a 10 wt% slurry increases by approximately 6% while the apparent viscosity increases by up to 25% based on the correlation from (Springman, Steiff et al. 1991). This change in density and rheology due to the glass beads is acceptable since the slurry physical properties will also change upon the formation of hydrates.

3.2.4 - Experimental Procedure

The reactor was filled with the appropriate amount of water and glass beads and the orifice meters were calibrated appropriately before the start of each run. The orifice meters were calibrated to a smaller range for the low flowrate experiments to more accurately capture data when the larger range was not required. Prior to the start of the experiment, the manual valves to the empty cylinders were closed and the control valve was placed on manual and fully closed. The system was then cooled down to the experimental temperature while slowly pressurizing through the lower gas inlet. To prevent premature ice formation, a coolant temperature of 0°C was always used for this portion. Once the experimental temperature had been reached, the column continued to be pressured through the lower gas inlet until the minimum pressure for hydrate formation was reached. At this point, the upper gas inlet was used to prevent nucleation from occurring before the desired experimental pressure was reached. If applicable, the coolant temperature was reduced to -5°C at this point. This final pressurization phase was also used to adjust the inlet flowrate to that required by the experiment. Once the experimental pressure was reached the valve to the upper gas inlet was closed.

For the start of the run, the control valve was taken off manual and the inlet valve to one of the empty cylinders was opened. Then the valve to the lower gas inlet was opened and the run started. Over the course of the run, the gas flowrate was monitored and valve position was

adjusted to maintain it at the desired level as the driving force for gas flow decreased due to the collecting cylinders filling up. This was done by first switching the collecting cylinder, then when the pressure increase again affected gas flow both collecting cylinders were opened and the pressure of the inlet gas was increased. The runs were ended after 10 minutes by stopping the flow of inlet gas.

Hydrates were dissociated by venting all the gas from the system and turning off the coolant system. Dissociation was considered complete when the system pressure was at atmospheric pressure, there was no visual evidence of hydrates and the temperature of the column contents had risen by 1°C.

3.2.5 - Calculations

Hydrates are formed using the gas passing through the column. The velocity of the entering and exiting gas flows was measured using a pair of orifice meters and calculated using equation 3.1. This can then be converted into a volumetric flowrates using equation 3.2. The temperature and pressure of the entering and exiting gas flows were also measured. These were used to covert the volumetric flowrates into a molar flowrates using equation 3.3.

$$v_{2,in/out,i} = C_v \left(\frac{\left(2\Delta P_{orifice,in/out,i}\right)}{\rho\left(1 - \frac{D_2^4}{D_1^4}\right)} \right)^{\frac{1}{2}} \tag{3.1}$$

$$Q_{in/out,i} = \frac{\pi D_2^2 v_{2,in/out,i}}{4} \tag{3.2}$$

$$n_{in/out,i} = Z \frac{P_i Q_i}{R T_i} \tag{3.3}$$

With the inlet and outlet molar flowrates, the number of moles of gas converted into hydrate can be calculated using a mass balance. To complete the mass balance, the distinction must be made between gas molecules consummed by hydrate formation and gas that has accumulated in/left the headspace of the column as increased/decreased pressure. This is represented by the n_{acc} term in the mass balance and is calculated using equation 3.4. Combined with the measurement of the entering and exiting gas flows, the change in the number of hydrates in the hydrate phase is calculated using the mass balance shown in equation 3.5. The total amount of gas in the hydrate phase at any given moment is calculated using equation 3.6 through a summation of the changes up to that point.

$$n_{acc,i} = \frac{\left(P_{column,i} - P_{column,i-1}\right)V_{head\ space}}{RT_{column,i}} \tag{3.4}$$

$$\Delta n_{hydrates,gas,i} = n_{in,i} - n_{out,i} - n_{acc,i} \tag{3.5}$$

$$n_{hydrates,gas,i} = \sum_{j=0}^{j=i} \Delta n_{hydrates,gas,j} \tag{3.6}$$

The amount of water that has been converted into hydrate is estimated using the hydration number for the conditions of the experiment, as shown in equation 3.7. This can then be converted into the fraction of water converted using equation 3.8.

$$\Delta n_{hydrates,H_2O} = \Delta n_{hydrates,gas} \times hydration\ number \tag{3.7}$$

$$fraction\ H_2O\ converted = \frac{\Delta n_{H_2O}}{V_{water}\rho_{water}MW_{H_2O}} \tag{3.8}$$

A further parameter that was monitored during the experiments was the gas hold-up. The pressure drop at a set vertical position was measured. The gas hold-up was then calculated using equation 3.9.

$$\varepsilon_g = \frac{\Delta P_D}{g\Delta z(\rho_L - \rho_G)} \tag{3.9}$$

The power consumption of the bubble column reactor was also estimated to further compare it with the stirred tank reactor in the previous work. The power consumption of the bubble column was calculated using equation 3.10.

$$\frac{p_G}{V_L} = (\rho_L - \rho_G) g v_G \tag{3.10}$$

3.2.6 - Hydration Number

Literature values for the hydration number of CO_2 hydrates span from 5.3 to 7.7 (Yang, Le et al. 2011). As there is considerable variation in the reported values, in this work the hydration numbers were set at constant values of 6.2 for CO_2. These values were determined using the relationships based on the Clapeyron equation developed by for CO_2(Anderson 2003). The hydration number is calculated at the set experimental temperature, and does not vary significantly between the pressures studied for each gas (Anderson 2003).

3.3 - Results and Discussion

Each configuration was allowed to run for 10min, and it is at this point that the overall performance of each reactor was compared. The mole fraction of the water in the reactor that was converted into gas hydrate after 10 min is shown in Figure 3.4. At this point in the operation of the reactor, all configurations had reached the three-phase equilibrium temperature for the given experimental pressure. Condition 2a is selected as the base case for comparison, since it does not contain particles, has the lower gas flowrate and has the lower driving force for both heat and mass transfer. When the gas flowrate is increase for condition 2b, the increase in heat transfer, mass transfer and available gas causes a large increase in the amount of hydrates formed. When the driving force for mass transfer is increased in condition 1, the net amount of

hydrates formed decreases since the system becomes heat transfer limited. Due to the significant heat transfer limitations, there is no noticeable effect of changing the gas flowrate in condition 1.

The heat transfer limited nature of the reactor at condition 1 is confirmed by the improved performance of condition 3 relative to it. In condition 3, the coolant temperature was lowered to -5°C, increasing the driving force for heat removal. However, there is still no discernable effect of gas flowrate in condition 3 due to the large spread in the data. This is consistent with previous results in that when the reactor is heat transfer limited the performance varies greatly, since variations in starting temperatures will be magnified.

Increasing the driving force for heat removal did not have an observable effect on the performance of the conditions with low mass transfer driving force: conditions 2 and 4. This is due to two factors. Firstly, condition 2 was less affected by heat transfer limitations compared to condition 1 and therefore increasing the driving force for heat transfer will have less of an effect. Secondly, in practical terms the driving force for heat removal was increased less between conditions 2 and 4 than between conditions 1 and 3. Since in all cases the reactor final temperature was effectively the equilibrium temperature for the experimental pressure, the lower pressure of conditions 2 and 4 resulted in an equilibrium temperature, and therefore an average experimental temperature, that was approximately 2°C lower than that of conditions 1 and 3. As a result the driving force for heat transfer was effectively 2°C lower in condition 4 than in condition 3. The increased hydrate formation with increased gas flow rate seen in condition 2 is also seen in condition 4.

With the addition of particles, the same effect of increasing gas flowrate was observed in conditions 5 vs 6 as was observed in conditions 1 vs 2 and 3 vs 4. The addition of particles also caused a slight increase in hydrate formation between all the comparable conditions.

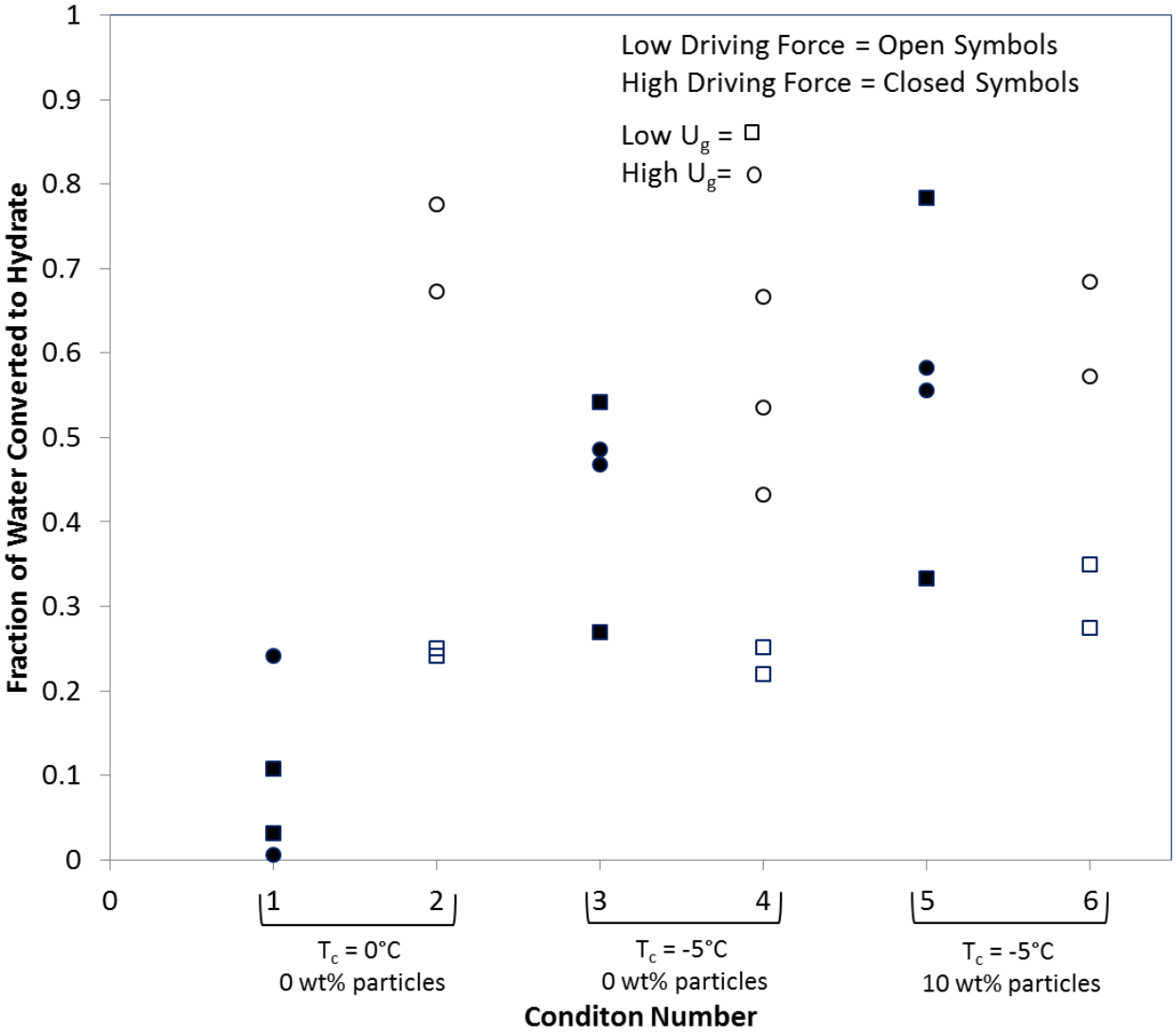

Figure 3.4: Gas consumed by hydrate formation after 10min.

The reasons for the differences in performance between the different conditions are further explained by looking at the individual temperature and hydrate formation profiles. As illustrated in Figure 3.5, in condition 1b, hydrates form very quickly initially; however, the corresponding heat that results from their formation quickly overwhelms the heat removal capacity of the cooling jacket. The temperature rise that results from this heat production is sufficient to cause the dissociation of hydrates that have already formed. As the run progresses, the temperature is maintained at a level above the equilibrium temperature (7 ^{o}C), indicating that hydrates continue to form in localized regions of the reactor vessel. However, the hydrates then

dissociate in another region of the bed and the net amount of hydrates decreases. It is likely that hydrates are forming closer to the walls where the cooling jacket is able to lower the local temperature, and dissociating closer to the middle of the column where the local temperature will be higher.

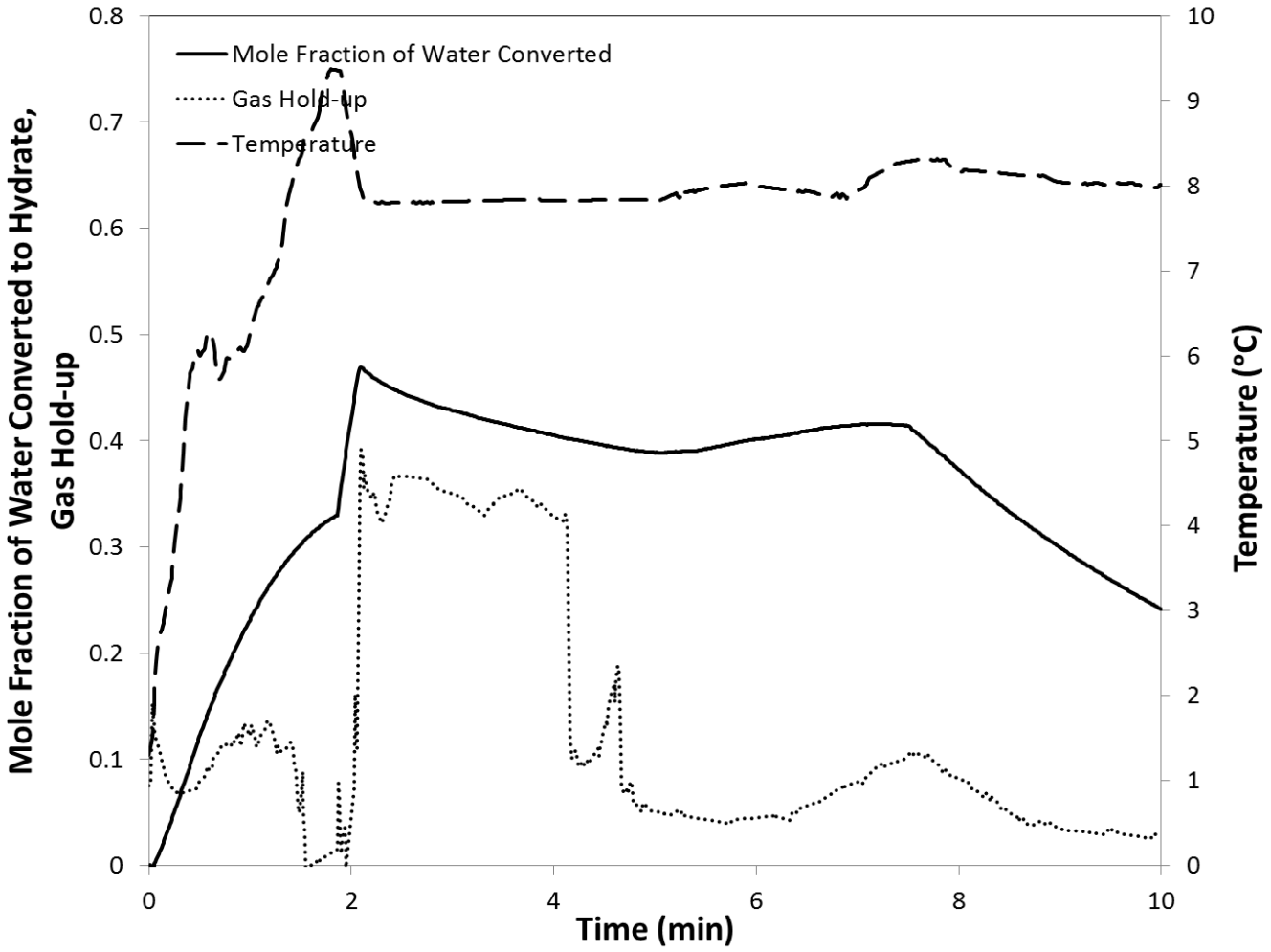

Figure 3.5: Temperature, hydrate formation and gas hold-up profiles for condition 1b, run 2.

When the reactor is subject to the same conditions but with a lower coolant temperature this behaviour is eliminated, shown in Figure 3.6. Initial hydrate formation, again causes a rise in temperature, but due to the lower coolant temperature it is able to remain below the equilibrium temperature for the duration of the run. Therefore, the hydrates in the reactor do not dissociate and the amount can grow over the course of the run.

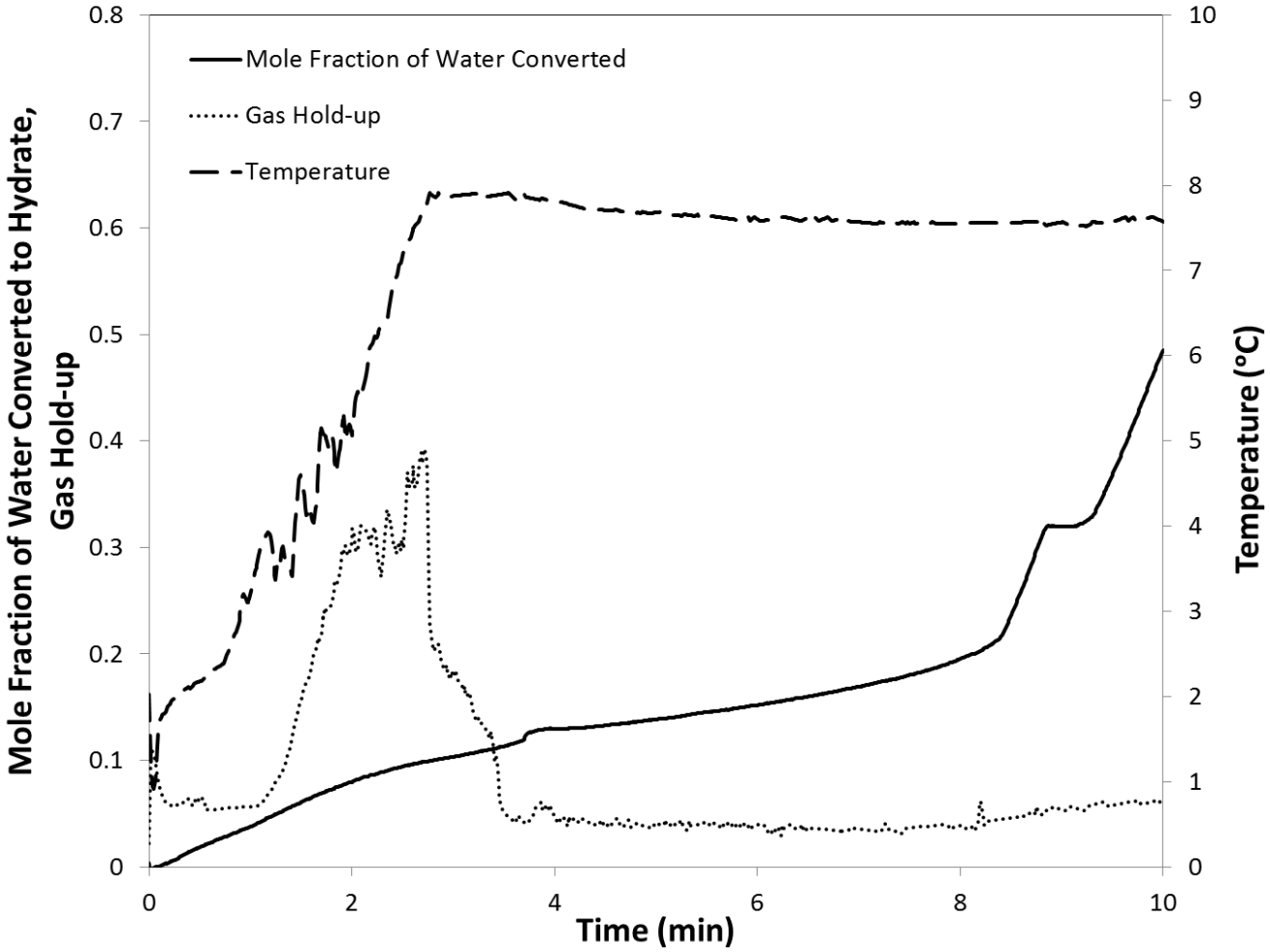

Figure 3.6: Temperature, hydrate formation and gas hold-up profiles for condition 3b, run 1.

The effect of increasing the gas flowrate is illustrated in the profiles for condition 4. In Figure 3.7, at the lower gas flowrate a smaller amount of hydrates are formed than at the higher gas flowrate shown in Figure 3.8. Additionally, the temperature profile for the lower gas flowrate is not constantly maintained at the equilibrium temperature (6°C), but instead dips below it for a significant portion of the run. This indicates that for this portion of the run, mass transfer was limiting enough to allow the cooling system to lower the temperature of the reactor. However, since the temperature did not drop back to the set-point of 3°C, heat transfer was still an important factor in hydrate formation. At the higher gas flowrate, the additional mixing provided by the greater flowrate caused an increase in mass and heat transfer. Mass transfer was increased sufficiently that the system became entirely heat transfer limited and the reactor

temperature was held constant at the equilibrium temperature. As a result faster rates of hydrate formation were achieved.

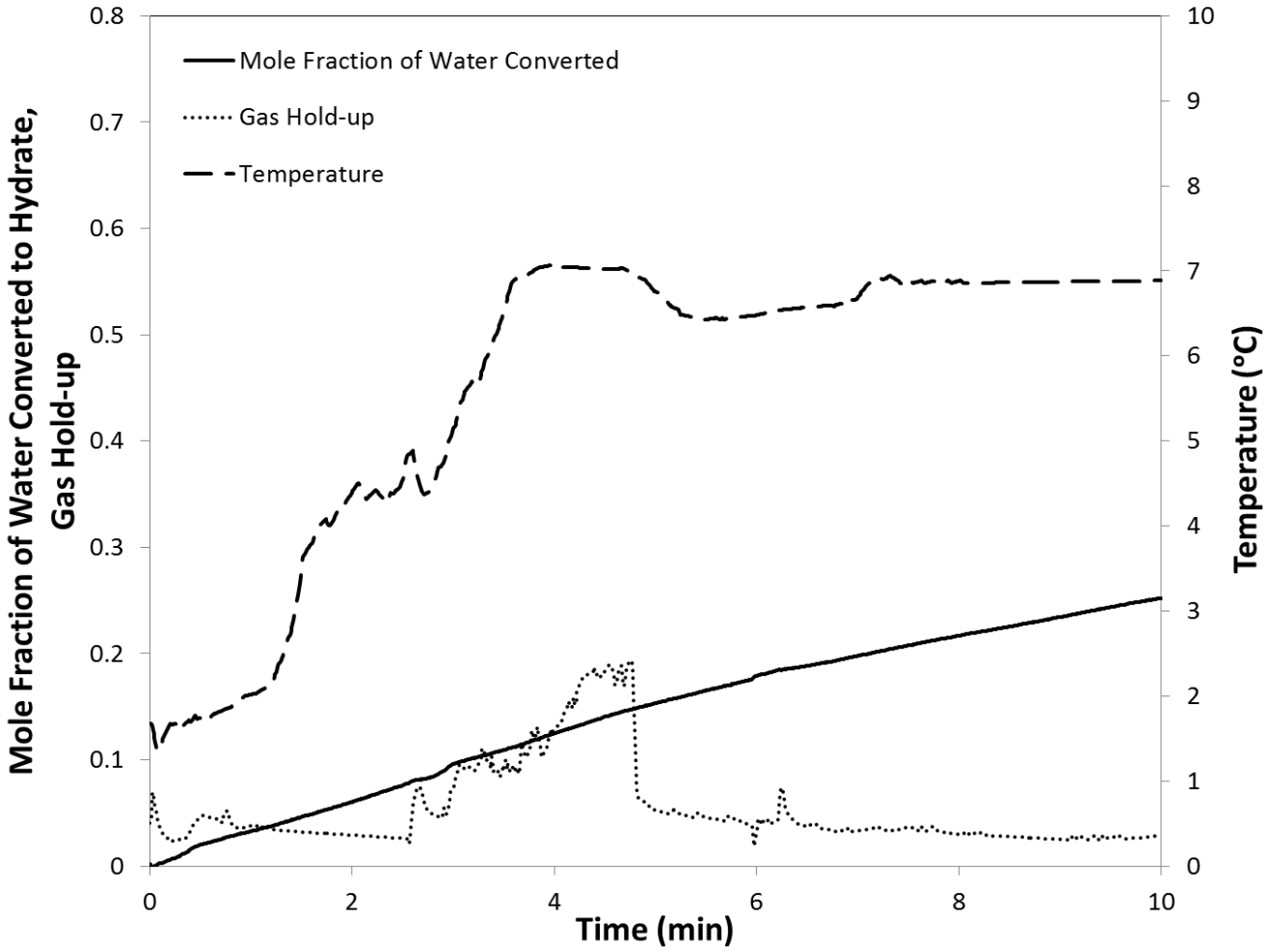

Figure 3.7: Temperature, hydrate formation and gas hold-up profiles for condition 4a, run 2.

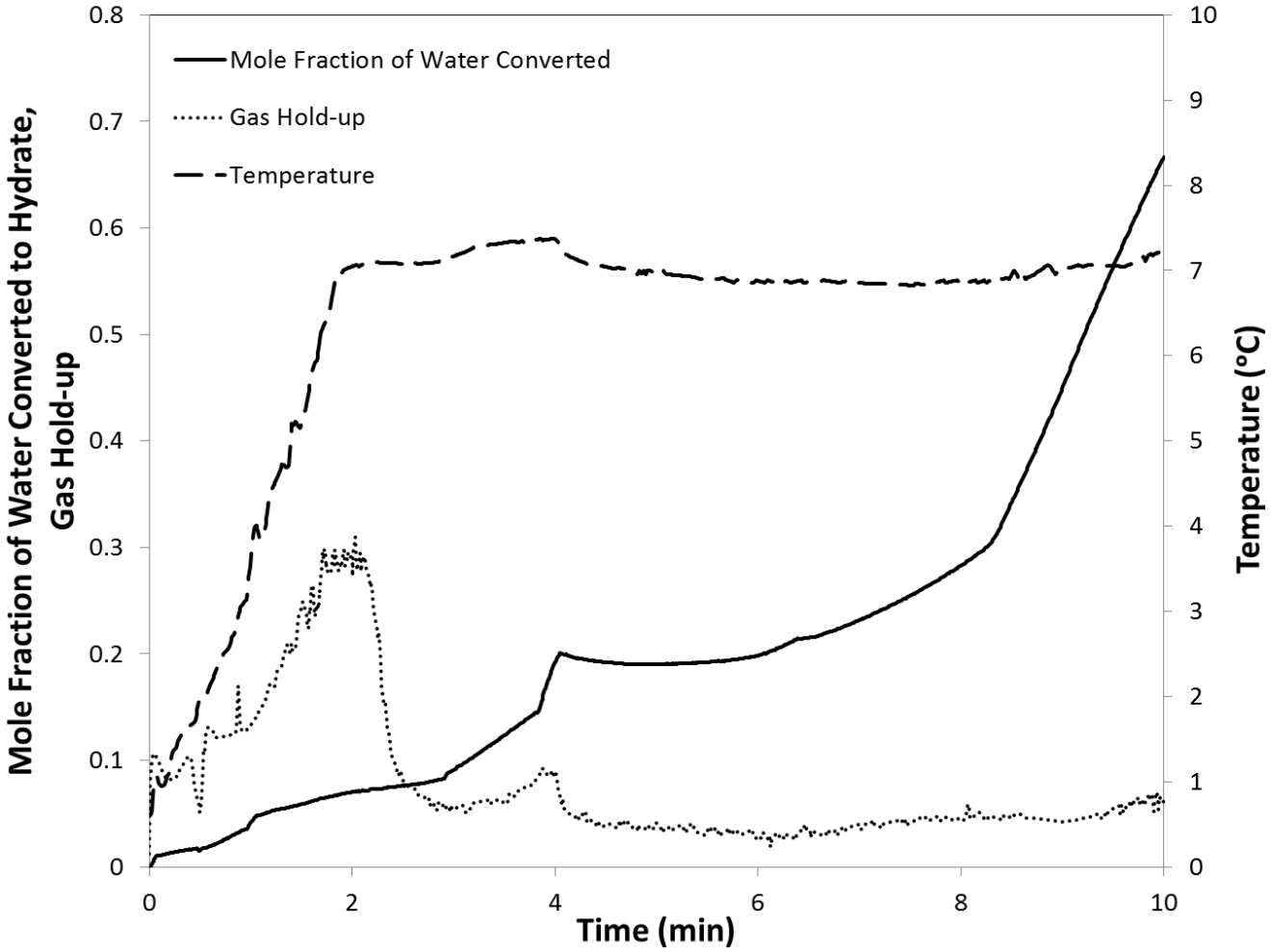

Figure 3.8: Temperature, hydrate formation and gas hold-up profiles for condition 4b, run 1.

At the higher driving force for mass transfer, with the lower coolant temperature to prevent severe heat transfer limitations, condition 3a, growth is heat transfer limited even at lower gas flowrates. This is shown in Figure 3.9. Hydrate growth is steady but the temperature rises to the equilibrium temperature and stays at that value for the rest of the run. Since heat transfer is already dominant, the increase in mass transfer provided by increasing the gas flowrate does not significantly affect the amount of hydrates formed. The increase in heat transfer associated with increasing gas flowrate is not large enough to significantly affect hydrate formation.

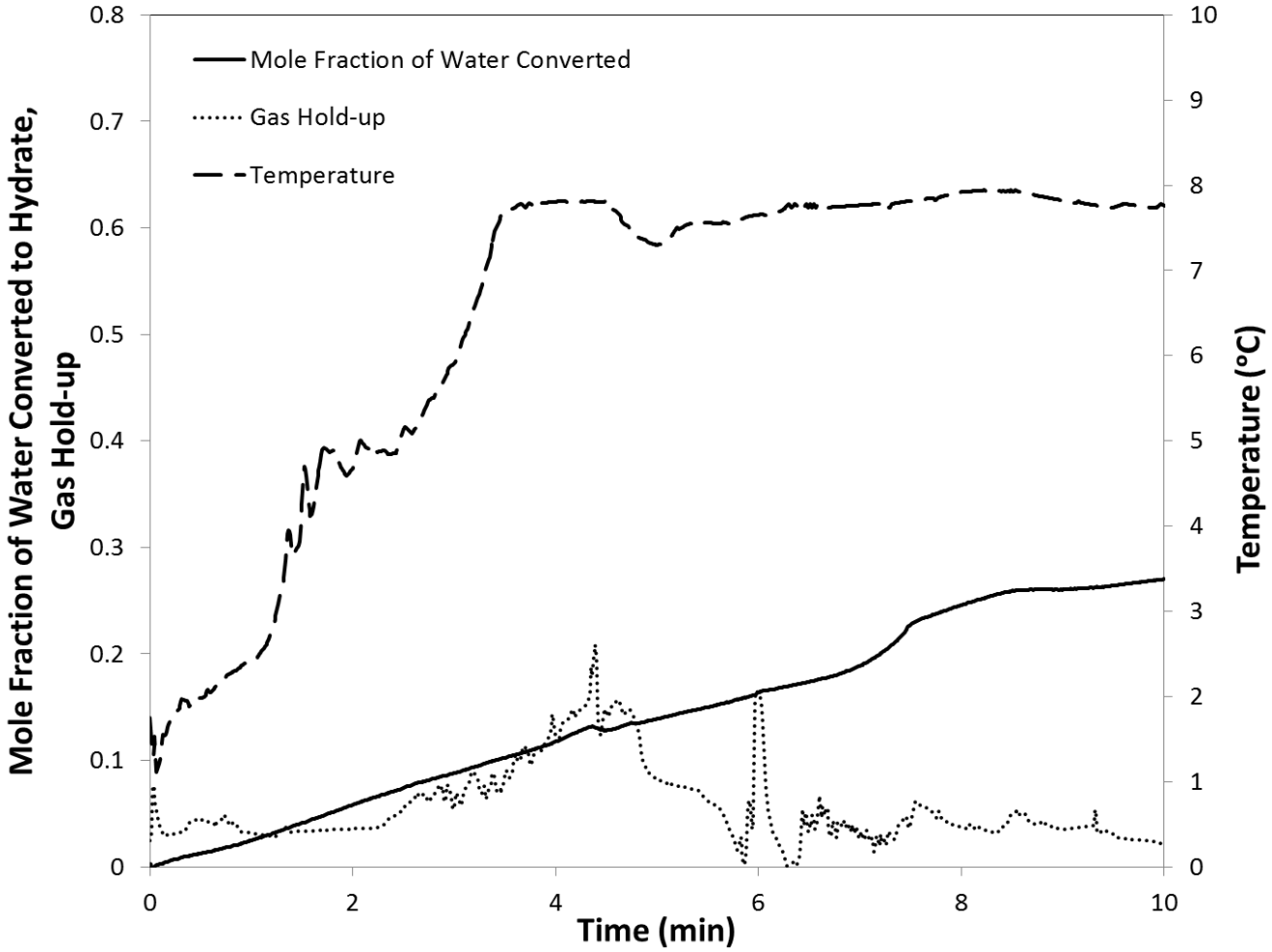

Figure 3.9: Temperature, hydrate formation and gas hold-up profiles for condition 3a, run 1.

The effect of adding particles to the reactor can be further studied by comparing condition 4a and 6a, shown in Figure 3.7 and Figure 3.10. The shapes of the two sets of profiles are similar but the slope on the line of hydrate formation is steeper for condition 6a. This indicates that adding particles to reactor increases overall interphase mass transfer rates and since the temperature profile does not change it also increases the heat transfer rate. This is supported by the fact that adding particles increases performance for all conditions studied. Therefore, adding 10 wt% particles changes the flow patterns of the gas and liquid in the system in a way that is beneficial for hydrate growth. Since the particles can be easily separate from water after the hydrates have been dissociated they could be used to promote hydrate growth without causing the concerns about water contamination that chemical promoters would.

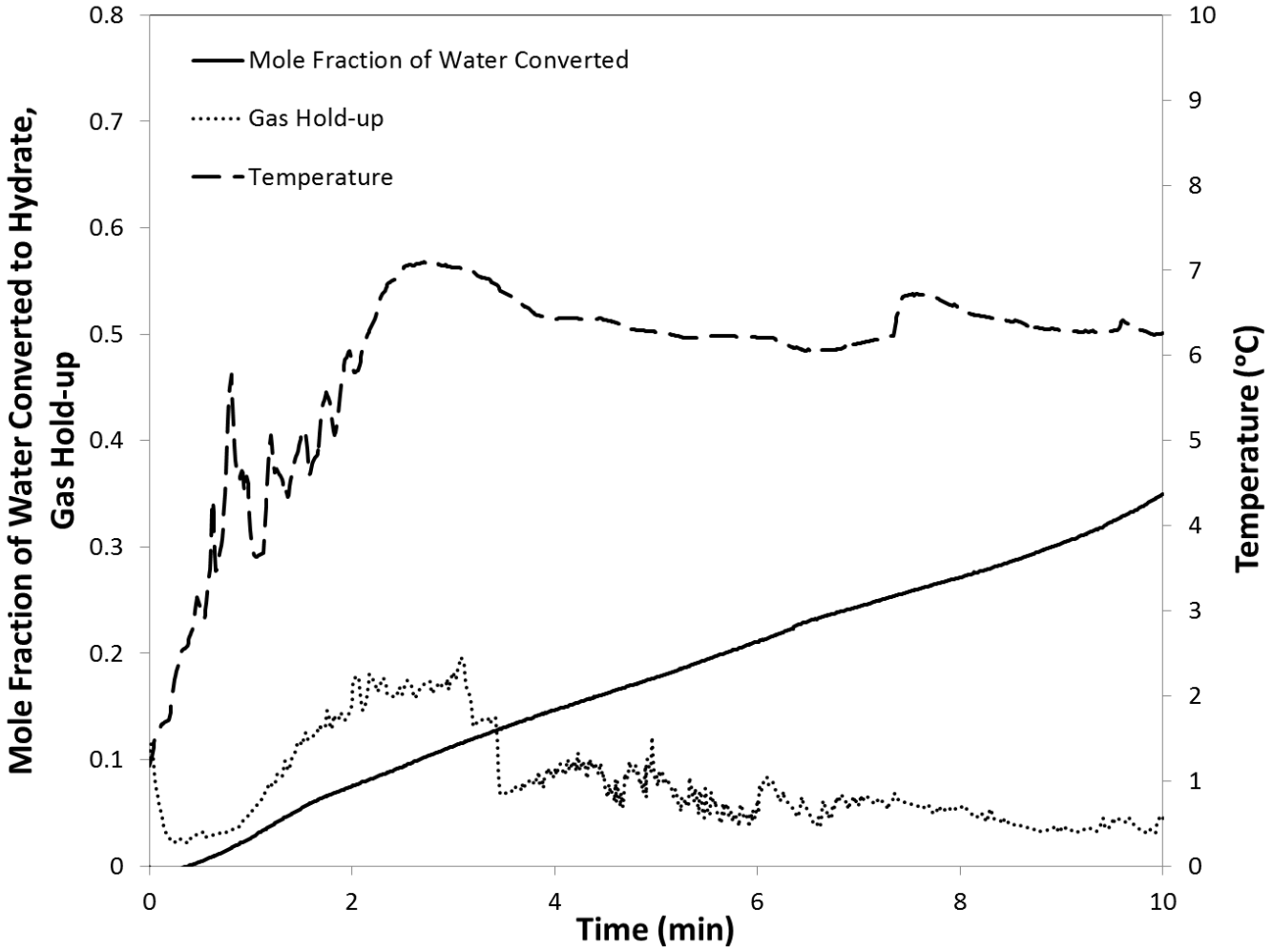

Figure 3.10: Temperature, hydrate formation and gas hold-up profiles for condition 6a, run 1.

In all runs where greater than 40% of the water was converted into hydrates by then end of the 10min run, a later stage of increased hydrate growth was observed. This later stage of increased growth is shown in Figure 3.6 and Figure 3.8 from around 8 minutes onward. The stage of increased hydrate formation started when 20-30% of the water had been converted into hydrates; however, as can be seen in Figure 3.10, converting more than 20% of the water into hydrates was not sufficient in and of itself to result in faster hydrate formation. The second stage was observed in only two runs with low gas flowrate, while it was observed in all high gas flowrate runs with the exception of those in condition 1. Therefore, a combination of the fraction of hydrates in reactor volume along with a higher gas flowrate produces this faster rate of formation. Furthermore, because hydrates were forming at faster rates during this second stage, considerably more of the entering gas was being consumed by hydrate formation. In the slower

initial growth rate between 10-30% of entering CO_2 was consumed by hydrate formation while in the second faster stage, more than 80% of the entering CO_2 was consumed by hydrate formation. Therefore, if a bubble column were used to produce gas hydrates on a continuous basis, there would be an optimal hydrate fraction for operation which would be above 20 mol% of water converted.

An interesting phenomenon was consistently visually observed in the first few minutes of hydrate growth in all runs. Buoyant bubble-hydrate clusters would form and rise to the top of the liquid. The clusters cumulated at the interface (akin to a foam head), retaining the gas bubbles below, until the operating temperature rose close to equilibrium. The cumulated bed would then slowly collapse, releasing the gas bubble, with the hydrate particles now evenly dispersed throughout the liquid volume. This bubble retention pattern is further supported by the gas hold-up data in Figure 3.6 to Figure 3.10. As hydrates continued to form, the bed was visually observed to become more static. Channeling of gas through the bed was observed in some cases. Based on these observations, the bed expansion is something that should be accounted for during start-up of a continuously operated bubble column and during the initial phases of operation of a semi-batch bubble column. The size of the hydrate clusters themselves varied considerably. Visible hydrate clusters ranged from 1-2mm in diameter at their smallest to up to 5cm in diameter at their largest. As more hydrates formed they tended to compress into a large mass of hydrates, ultimately being split into different sections by the gas channeling through the mass.

In order to compare reactor designs for industrial applications, two more pieces of information are required: the rate of hydrate formation per unit volume of reactor and the amount of power required for hydrate formation. Since the bubble column performance at the various operating conditions has already been compared in detail on the basis of fraction of water converted; only the maximum rates achieved will be discussed in relation to volume and power requirement. The rates are given in terms of the moles of gas consumed for hydrate growth. The average rate of formation was calculated at 2.5min intervals as well as for the overall 10min run. The maximum rate for each condition was selected as it is assumed that a continuous reactor could be designed to operate in that regime. In runs where a second faster stage of hydrate formation was observed, the maximum rate of formation occurred during this second stage. The

volume normalized maximum rates are shown in Figure 3.11 where the increased hydrate formation of the runs with particles is not sufficient to compensate for loss of reactor capacity to particles. Instead the performance of the runs with and without particles at the lower coolant temperature is the same. It should be noted that while condition 1 was able to achieve very fast rates of formation, it was unable to sustain hydrate formation or hydrate populations due to the corresponding increase in temperature.

The power and volume normalized rates are shown in Figure 3.12. It should be noted that the estimated power required does not take into account the small increase in liquid density associated with hydrate formation. At the low driving force for mass transfer conditions, where increasing gas flowrate increased hydrate formation, the extra energy required by the higher flowrate was compensated for by a sufficient increase in hydrate formation. On the other hand, at high mass transfer driving force conditions, this was not always the case. Based on these results, there is an optimal gas flowrate for hydrate formation. This optimal gas flowrate should be high enough to achieve the second faster stage of hydrate growth but beyond that it is not necessary to further accelerate the gas. Also of note in Figure 3.12, in the runs with particles, the extra energy required to move the gas through the particle slurry further decreases the normalized performance of the particle runs relative to the non-particle runs. Therefore, although particles could be useful in the start-up phase of a continuous bubble column reactor they do not show enough benefit to make their continued use after start-up beneficial.

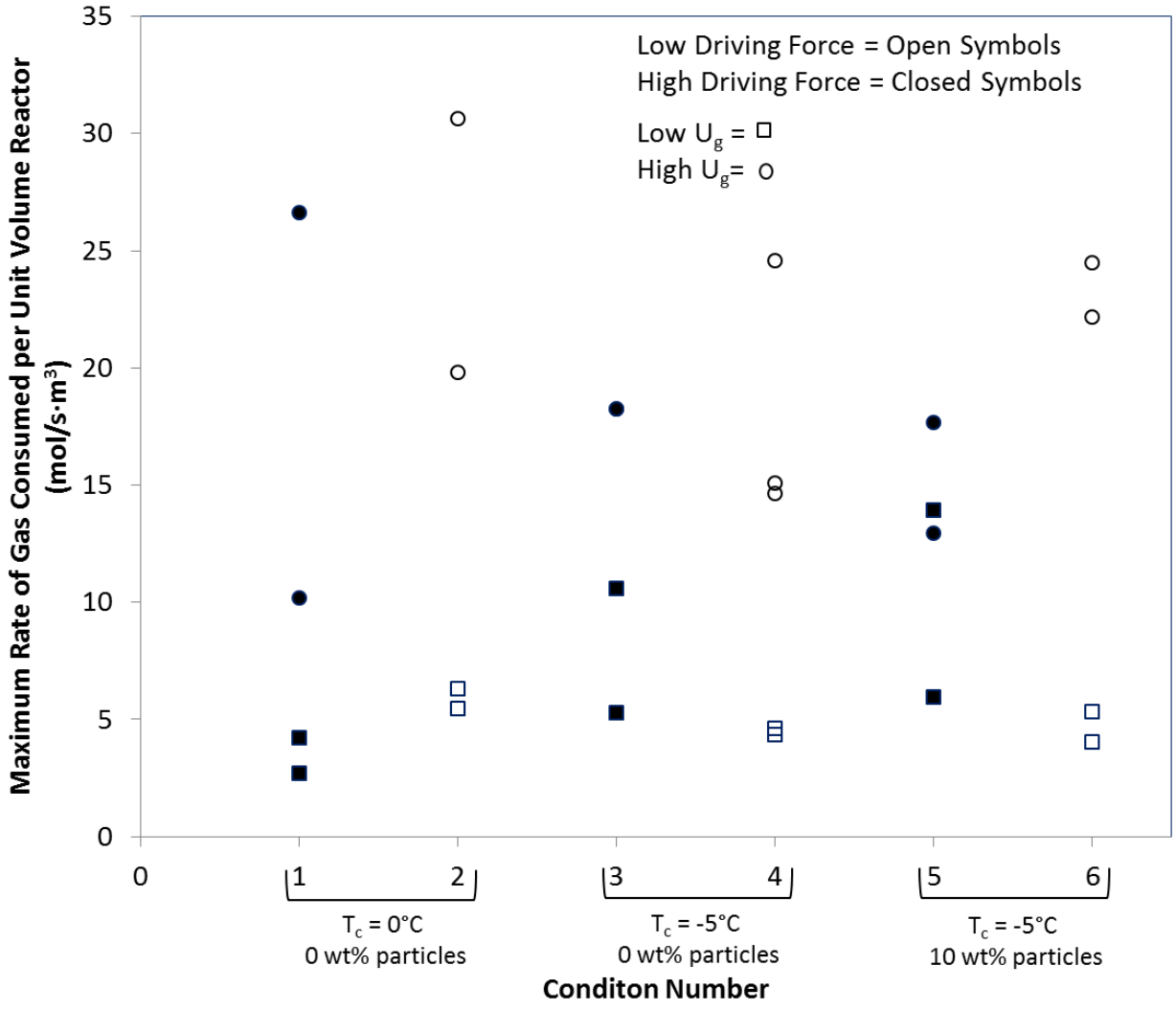

Figure 3.11: Maximum rate of gas consumption per unit volume of reactor.

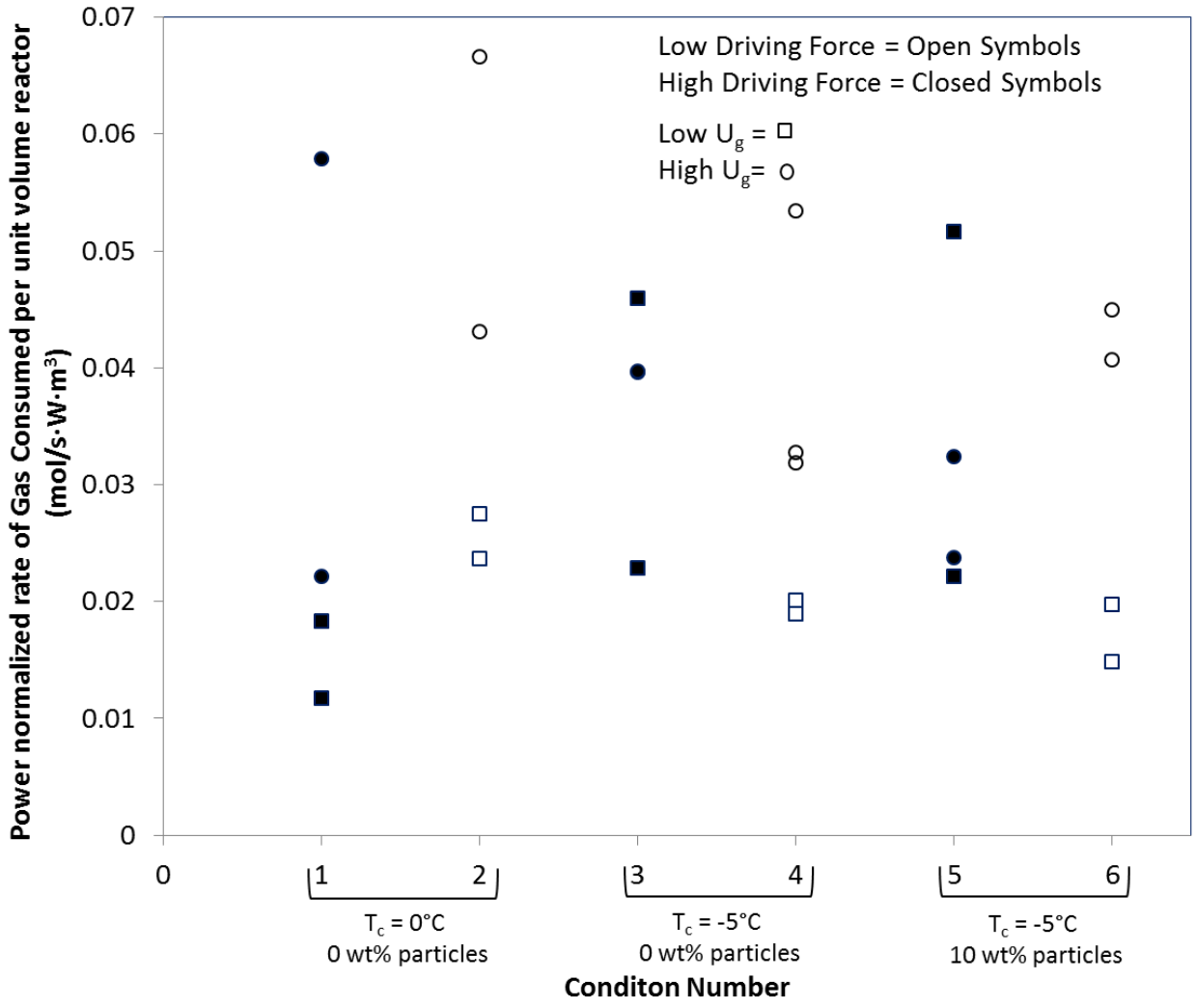

Figure 3.12: Maximum rate of gas consumption per unit volume of reactor, normalized for power consumption.

When the normalized rates are compared to those achieved in the semi-batch stirred tank from the previous work discussed in Chapter 2, the results strongly favour the bubble column. The volume normalized rate of hydrate formation in a bubble column is a factor of 10 greater than the rate achieved in the stirred tank. The power normalized rates are in the same range for the bubble column and semi-batch stirred tank, whose dimensions were smaller. The impeller power scales proportionally with impeller diameter to the exponent of 5, which scales linearly with tank diameter and Thus, the stirred tank scaled-up to the same volume as the bubble column would require significantly more power resulting in a much lower power normalized rate

of hydrate formation. The bubble column was also able to maintain the rate of hydrate formation as the hydrate volume fraction increased. The bubble column reactor was able to convert 77% of the available moles of water into hydrate in 10min, while the stirred tank struggled to convert more than 20% in 2 hours. Additionally, nucleation was consistently observed to occur almost instantaneously in the bubble column while it could take anywhere from a few minutes to a few hours to occur in the stirred tank. The bubble column reactor was able to achieve these improved results for two reasons. Firstly, a jacketed bubble column has more energy efficient heat transfer than a stirred tank and is therefore the heat of hydrate formation can be more efficiently removed and heat transfer limitations minimized. Secondly, because gas is bubbled up from the bottom of the bubble column rather than being mixed in from the top of the stirred tank, better contact can be achieved between the gas, water and hydrate phases. Particularly as hydrates form and the reactor contents become thicker, an impeller will struggle to mix gas into the combined water and hydrate phase. In the bubble column, however, the gas was still required to pass through the combined water and hydrate phase before exiting the reactor. This greatly increased the surface area of gas water hydrate contact and therefore more gas molecules were available to be enclathrated.

3.4 - Conclusions

Achieving a balance between mass transfer and heat removal is essential for optimal hydrate production. If the driving force for mass transfer is high, but there is insufficient heat removal, hydrate growth is severely limited to the point where previously formed hydrates can dissociate. Lowering the coolant temperature to increase heat removal rates increased hydrate production under conditions where growth was severely heat transfer limited; however, it had less of an effect on conditions with lower driving force for mass transfer. What was critical for high conversions of water and CO_2 and fast rates of production was the second, faster stage of hydrate formation. Therefore, there is an optimal hydrate fraction for continuously operated hydrate producing bubble columns. The second stage would start after 20-30% of water had been converted to gas hydrate, and occurred more frequently in higher gas flowrate runs than in lower gas flowrate runs. The increased energy associated with producing the higher gas

flowrate, is sufficiently compensated for with increased hydrate production (single pass gas conversion) and it is therefore recommended to operate at higher gas flowrates. The addition of 10wt% glass beads to the reactor promoted hydrate formation; however, it did not do so sufficiently enough to make up for the loss in reactor capacity or for the increased energy requirement. Therefore, they could be useful in continuous reactors in the start-up phase to help reach optimal hydrate fractions, but their continued use afterwards is not justified. A bed expansion was consistently observed during the first few minutes of hydrate production, as hydrate-bubble clusters accumulated at the liquid-gas interface. The bed would collapse and release the accumulated gas when the reactor temperature nearly reached the equilibrium temperature. This phenomenon should be taken into consideration during the start-up of a continuous bubble column and during the initial phases of a semi-batch bubble column. When compared to a stirred tank operated at the same thermodynamic conditions, the bubble column was able to achieve higher conversions of water to hydrate, with faster hydrate formation rates and with less energy required for operation. As a result, a bubble column would be better suited for hydrate production than a stirred tank.

3.5 – Nomenclature

D	Diameter
g	Acceleration due to gravity
MW	Molecular Mass
n	Number of moles
P	Pressure
p	Power
Q	Flowrate
R	Gas constant
T	Temperature
V	Volume
v	Velocity
X	Mole fraction in liquid phase
Z	Compressibility Factor
ε_g	Gas hold-up
ρ	Density

3.6 – Acknowledgements

The authors would like to acknowledge the Natural Sciences and Engineering Research Council of Canada, the Canadian Foundation for Innovation, the Ontario Innovation Trust and Ontario Graduate Scholarship Program for financial assistance.

3.7 – References

Anderson, G. K. (2003). "Enthalpy of dissociation and hydration number of carbon dioxide hydrate from the Clapeyron equation." Journal of Chemical Thermodynamics **35**(7): 1171-1183.

Anderson, G. K. (2004). "Enthalpy of dissociation and hydration number of methane hydrate from the Clapeyron equation." Journal of Chemical Thermodynamics **36**(12): 1119-1127.

Fujita, S., K. Watanabe and Y. H. Mori (2009). "Clathrate-Hydrate Formation by Water Spraying onto a Porous Metal Plate Exuding a Hydrophobic Liquid Coolant." AIChE Journal **55**(4): 1056-1064.

Gudmundsson, J. S., F. Hveding and A. Borrehaug (1995). Transport of Natural Gas as Frozen Hydrate. Fifth International Offshore & Polar Engineering Conference, The Hague.

Hashemi, S. M. R., A. Macchi and P. Servio (2009). "Dynamic simulation of gas hydrate formation in a three-phase slurry reactor." Industrial and Engineering Chemistry Research **48**(15): 6983-6991.

Kang, S.-P. and J.-W. Lee (2010). "Formation characteristics of synthesized natural gas hydrates in meso- and macroporous silica gels." Journal of Physical Chemistry B **144**: 6973-6978.

Li, G., D. Liu, Y. Xie and Y. Xiao (2010). "Study on effect factors for CO2 hydrate rapid formation in a water-spraying apparatus." Energy and Fuels **24**(8): 4590-4597.

Linga, P., R. Kumar, J. D. Lee, J. Ripmeester and P. Englezos (2010). "A new apparatus to enhance the rate of gas hydrate formation: Application to capture of carbon dioxide." International Journal of Greenhouse Gas Control **4**(4): 630-637.

Marinhas, S., A. Delahaye, L. Fournaison, D. Dalmazzone, W. Fürst and J. P. Petitet (2006). "Modelling of the available latent heat of a CO2 hydrate slurry in an experimental loop applied to secondary refrigeration." Chemical Engineering and Processing: Process Intensification **45**(3): 184-192.

Matsuda, S., H. Tsuda and Y. H. Mori (2006). "Hydrate formation using water spraying onto a cooled solid surface in a guest gas." AIChE Journal **52**(8): 2978-2987.

Mori, Y. H. (2003). "Recent Advances in Hydrate-Based Technologies for Natural Gas Storage - A Review." Journal of Chemical Industry and Engineering (China) **54**.

Myre, D., A. Macchi and P. Servio (2010). Sythesis of CO2 Hydrates in a Slurry Bubble Column. 7th International Conference for Gas Hydrates. Edinburg, Scotland.

Sloan, E. D. and C. A. Koh (2008). Clathrate Hydrates of Natural Gas. 3rd ed. Boca Raton, Florida, CRC Press.

Springman, H. G., A. Steiff and P. M. Weinspach (1991). "Feststoffeinfluß auf den Stofftransport in Suspensionblasensäulen." Chem. Ing. Tech. **63**: 512-513.

Vahakis, J. G., H.-S. Chen, M. S. Suwandi and A. J. Barduhn (1972). "Research and Development Report 830." Prepared for the US DOE of the Interior.

Yang, D., L. A. Le, R. J. Martinez, R. P. Currier and D. F. Spencer (2011). "Kinetics of CO2 hydrate formation in a continuous flow reactor." Chemical Engineering Journal **172**(1): 144-157.

Chapter 4 – Conclusions and Future Research

4.1 – Conclusions

The objective of this research was to compare the performance of different gas hydrate reactor configurations and conditions in order to determine their effectiveness for different applications. Since mass and heat transfer limitations frequently dominate over intrinsic formation kinetics, determining the optimal phase contacting patterns and mass and heat transfer driving forces for hydrate formation is particularly important. To achieve this objective, three main reactor configurations, a stirred tank, a fixed bed and a bubble column, were operated a varying phase-contacting patterns and at varying but similar driving force conditions. Their performance was then compared based on total water and single-pass gas conversion, as well as on volume and volume and power normalized rates of gas consumption.

Semi-batch stirred tank reactors are frequently used in literature due to their applicability for determining reaction intrinsic kinetics. Because gas was added to the head space through a pressure drop triggered control valve, a 100% single pass conversion of gas is possible. Increased agitation of the stirred tank intensified both heat and mass transfer within the reactor, but the initial rapid rate of hydrate formation leads to heat transfer limited conditions. As hydrates formed, impact of interphase mass transfer became significant as the thickening slurry became increasingly difficult to stir. Both a gas inducing impeller and a 10 wt% glass bead slurry were studied, to observe if they could increase the rate and quantity of hydrates produced. However, since both only affected mass transfer and not heat transfer, they did not significantly affect the performance of the reactor. The particle slurry did decrease the induction time and could be used to stimulate nucleation without otherwise affecting hydrate growth. The particles would also be easily recoverable from the process water after the hydrates have been dissociated, unlike chemical promoters. Additionally, increasing the mass transfer driving force by increasing the pressure of the experiment did not significantly change the performance, further indicating the heat transfer limitation of the stirred tank system. Increasing the stirring rates required increased

power input, but did not affect the maximum fraction of hydrates produced at the end of the 2 hour run. Therefore, if a stirred tank is used for hydrate production, an optimal stirring rate should be used to convert the desired fraction of hydrates with a minimal power input.

In contrast, a semi-batch fixed bed requires no power input for mixing because it is a completely static system within the reactor vessel. A 100% single pass conversion of gas was also possible in this system since gas was introduced through the same control valve. However, for the conditions investigated, fixed bed systems were mass transfer limited and show much slower rates of hydrate formation than the stirred systems. As a result, driving force had a significant effect on hydrate formation rates. Fixed bed systems will, therefore, require a much larger reactor volume to have a comparable performance, not just because of the slower rates of hydrate formation, but also because of the lower water fraction within the reactor.

The formation of gas hydrates in a bubble column is a potential avenue for large scale production. The energy requirements of bubble columns scale more favourably than stirred tanks and they are also able to remove heat more efficiently based on energy input. Achieving a balance between mass transfer and heat removal is essential for optimal hydrate production in a bubble column. If the driving force for mass transfer was high, but there was insufficient heat removal, hydrate growth was severely limited to the point where previously formed hydrates dissociated. While lowering the coolant temperature to increase the heat removal rate increased hydrate production in severely heat transfer limited conditions, it has less of an effect on conditions where mass transfer and heat removal were already better balanced. Instead, what was critical for high conversions of water and CO_2 and fast rates of production was a second, faster stage of hydrate formation observed after 20-30% of the water had been converted into hydrates. The second stage of hydrate formation was observed more frequently at higher gas flowrates. Therefore a continuously operated bubble column would have an optimal hydrate fraction for hydrate formation. Since the increased energy associated with producing the higher gas flowrate, was sufficiently compensated for with increased hydrate production and single pass gas conversion, it is therefore recommended to operate at higher gas flowrates. The addition of

10wt% glass beads to the reactor promoted hydrate formation; however, it did not do so sufficiently to make up for the loss in reactor capacity or for the increased energy requirement.

During bubble column operation, a bed expansion was consistently observed during the first few minutes of hydrate production as hydrate-bubble clusters accumulated at the liquid-gas interface. The bed would collapse and release the accumulated gas when the reactor temperature nearly reached the equilibrium temperature. Therefore, this phenomena should be considered during the initial phases of a semi-batch bubble column and the start-up of a continuous bubble column, and sufficient space be provided for the bed to expand.

When compared to a stirred tank or fixed bed operated at the same thermodynamic conditions, the bubble column was able to achieve higher conversions of water to hydrate, with faster hydrate formation rates and with less energy required for operation. As a result, a bubble column would be better suited for hydrate production than a stirred tank.

4.2 - Future Research

While the bubble column was able to achieve good hydrate formation, the temperature in the reactor would consistently rise to nearly equilibrium for the given pressure. Therefore the heat transfer capabilities of the system can still improve and yield greater rates of hydrate formation. Use of traditional heat exchanger technology must be done with care, as heat exchange surfaces can become quickly fouled with forming hydrates (Waycullis, Sirajuddin et al. 2011). The use of a four tube, shell and tube fluidized bed reactor has been investigated by Marathon Oil Corporation (Waycullis, Sirajuddin et al. 2011). This design used small particles to gently scour hydrates that form on the heat exchange surfaces (Waycullis, Sirajuddin et al. 2011). The research presented in this thesis indicated that the use of particles did not sufficiently increase hydrate production to justify the increased energy input and loss of reactor capacity; however, whether this holds true with increased heat transfer and longer run times merits investigating.

Run times in the bubble column were limited to 10min because the gas flowrate could not be maintained for longer in all conditions. As the run progressed, the pressure in the receiving gas cylinders increased while the pressure in the input cylinders decreased. The pressure in the input cylinders decreased because the rapid vaporization of carbon dioxide caused the temperature to drop. The drop in temperature then caused a decreased in the vapour pressure of the carbon dioxide in the cylinder. Run time could be increased by the following two system modifications. Installing additional reservoir cylinders would allow them to maintain a lower pressure for longer, resulting in an increase in the average driving force for gas flow. The driving force for gas flow could also be increased by installing extra input cylinders. As the temperature in one input cylinder dropped, another warmer cylinder could be switched into operation.

Given the importance that heat removal rates play in hydrate formation in the bubble column, a further useful system modification would be the ability to monitor the heat removal rates. This could be done through a combination of knowing the flow rate and temperature rise of the coolant through the cooling jacket.

4.3 – References

Waycullis, J., H. Sirajuddin, P. Rensing and Marathon Oil Corporation (2011). A Novel Approach to Production of Hydrate Slurries at High Process Intensity and Conceptual Applications. 7th International Conference on Gas Hydrates. Edinburgh, Scotland, United Kindom.